Arctic Report Card 2023

More frequent extreme weather and climate events are transforming the Arctic, yet resiliency and opportunity lie within diverse partnerships.

DOI: 10.25923/5vfa-k694

R. L. Thoman, T. A. Moon, and
M. L. Druckenmiller; Eds.

December 2023

Richard L. Thoman, Twila A. Moon, Matthew L. Druckenmiller; Editors
Sarah J. Tucker; NOAA Coordinating Editor

arctic.noaa.gov/report-card

How to Cite Arctic Report Card 2023
Citing the complete report or Executive Summary:
Thoman, R. L., T. A. Moon, and M. L., Druckenmiller, Eds., 2023: *Arctic Report Card 2023*, https://doi.org/10.25923/5vfa-k694.

Citing an essay (example):
Mudryk, L. R., A. Elias Chereque, C. Derksen, K. Luojus, and B. Decharme, 2023: Terrestrial Snow Cover. *Arctic Report Card 2023*, R. L. Thoman, T. A. Moon, and M. L. Druckenmiller, Eds., https://doi.org/10.25923/xqwa-h543.
(Note: Each essay has a unique DOI assigned)

Front cover photo credits
Center: Ilulissat, Greenland at sunset in August 2023–Twila Moon, USA
Bottom Right: Forest surrounding the Koita River in Finland–Snowchange Cooperative, Finland
Bottom Left: Sockeye salmon in the Russian River within the Kenai National Wildlife Refuge, Alaska–Ryan Hagerty, U.S. Fish and Wildlife Service, USA

Funding Acknowledgments for the Arctic Report Card
Financial support for Arctic Report Card 2023 was provided by NOAA's Global Ocean Monitoring & Observing Arctic Research Program, including content editing funded through the Cooperative Institute for Earth System Research and Data Science (CIESRDS) via NOAA Cooperative Agreement NA22OAR4320151 (Druckenmiller and Moon) and by the Cooperative Institute for Climate, Ocean, and Ecosystem Studies (CICOES) under NOAA Cooperative Agreement NA20OAR4320271 (Thoman). The editors thank AMAP for organizing the independent peer review and those who provided review comments. The editors also recognize the tremendous contribution of Sarah Tucker, John A. Knauss Marine Policy Fellow, and the Arctic Research Program in NOAA's Global Ocean, Monitoring, and Observing Program, who coordinated and managed the various elements of the ARC's production process; and the whole of the Arctic Report Card production team for the professionalism, dedication, and enthusiasm in producing each year's Report.

Table of Contents

2023 Headlines

More frequent extreme weather and climate events are transforming the Arctic, yet resiliency and opportunity lie within diverse partnerships

The Arctic is increasingly warmer, less frozen, and wetter, with regional extremes in weather, climate patterns, and ecosystem responses. Centering locally and internationally-focused partnerships, long-term observations, and equitable climate solutions provides Arctic communities and nations as well as society-at-large with information and mechanisms to cope with a rapidly changing Arctic.

Headlines

In the air

- Average **surface air temperatures** for the Arctic in the past year were the **sixth warmest since 1900**.
- **Summer surface air temperatures were the warmest on record.**
- Summer high-pressure systems brought **warm temperatures, widespread melting, and exceptional rainfall volumes across the Greenland Ice Sheet.**

In the ocean

- **Sea ice extent continues to decline**, with the last 17 September extents (2007-23) as the lowest on record. Sea ice extent was 6th lowest in the satellite record, since 1979.
- August mean **sea surface temperatures show continued warming trends** for 1982-2023 in almost all Arctic Ocean regions that are ice-free in August. Mean sea surface temperature over regions between 65° N and 80° N is increasing at a rate of ~0.9°F (~0.5°C) per decade.
- Arctic regions, except for the Chukchi Sea, Beaufort Sea, and Canadian Archipelago, continue to show **increased ocean phytoplankton blooms, or ocean primary productivity**, with the largest percent change in the Eurasian Arctic and Barents Sea.
- Since the end of the Last Glacial Maximum, rising sea levels have inundated terrestrial permafrost surrounding the Arctic Ocean, **resulting in nearly 1 million square miles (~2.5 million square km) of subsea permafrost that is at risk of thawing**. International research collaboration is needed to address critical questions regarding the extent and current state of subsea permafrost and to estimate the **potential release of greenhouse gasses** (carbon dioxide and methane) as it thaws.

On the land

- North American snow cover extent set a record low in May 2023, while **snow accumulation during the 2022/23 winter was above average** across both North America and Eurasia.
- **Heavy precipitation events broke existing records** at various locations across the Arctic and the **Pan-Arctic precipitation for 2022-23 was the sixth highest on record**.
- On 26 June 2023, **Summit Station, Greenland reached 32.7°F (0.4°C)** and experienced melt for only the fifth time in its 34-year observational history.

- The **Greenland Ice Sheet lost roughly 350 trillion pounds (156 ± 22 Gt) of mass** from 1 September 2022 to 31 August 2023 because discharge and melting exceeded accumulation.
- The 2023 circumpolar **average peak tundra greenness**, which is the overall vegetation, including plants, shrubs, and trees taking over grassland and tundra, as measured by satellite, **was the third highest in the 24-year record**.
- In Finland, **peatland restoration and rewilding demonstrate a globally relevant climate solution of carbon sinks** and point to a need for replication across impacted sites. Rewilding **requires partnership, recognition of Indigenous and community rights, and the use of Indigenous knowledge** alongside science to succeed and avoid replication of past inequities.

Nunaaqqit Savaqatigivlugich: Working with communities to observe the Arctic

- The Alaska Arctic Observatory and Knowledge Hub (AAOKH) works with a **network of coastal Indigenous observers to document long-term and holistic observations** of environmental change and impacts in northern Alaska.
- Recently, Indigenous observers have noted **sea ice loss, warmer air and ocean temperatures, changing wind patterns, and increased intensity and frequency of coastal storms** that contribute to flooding and erosion.
- Indigenous observers also document local-scale impacts of environmental changes to community and cultural **infrastructure, traditional harvests and activities, and travel safety across the land and sea**.
- Applying and centering Indigenous perspectives and observations of Arctic change in decision-making can lead to more **inclusive, equitable, and community-led responses**.

Divergent responses of western Alaska salmon to a changing climate

- **Western Alaska salmon abundance reached historic extremes during 2021-22**, with record lows for Chinook and chum salmon (81% and 92% below the 30-year mean, respectively) and record highs for sockeye salmon (98% above the 30-year mean).
- Salmon are maturing at smaller sizes. Since the 1970s, Yukon River Chinook salmon have **decreased an estimated 6% in mean adult body length and 15% in fecundity**, or ability to produce offspring, likely exacerbating population declines.
- Salmon population declines have led to **fishery closures, worsened user conflicts, and had profound cultural and food security impacts in Indigenous communities** that have been tied to salmon for millennia.
- Changes in salmon abundance and size are **associated with climatic changes in freshwater and marine ecosystems and competition in the ocean**. Changes in predators, food supply, and disease are also likely important drivers.

Executive Summary

https://doi.org/10.25923/5vfa-k694

R. L. Thoman[1,2], T. A. Moon[3], and M. L. Druckenmiller[3]

[1]Alaska Center for Climate Assessment and Policy, University of Alaska Fairbanks, Fairbanks, AK, USA
[2]International Arctic Research Center, University of Alaska Fairbanks, Fairbanks, AK, USA
[3]National Snow and Ice Data Center, Cooperative Institute for Research in Environmental Sciences, University of Colorado Boulder, Boulder, CO, USA

The Arctic continues to rapidly evolve, shaped by past and ongoing human activities that release greenhouse gases into the atmosphere and push the broader Earth system into uncharted territory. Now in its 18th edition, this year's Arctic Report Card (ARC2023) provides an updated annual view into the state of the Arctic by checking in on key Vital Signs—eight defining elements of the Arctic's climate and environmental system. ARC2023 also samples critical and emerging Arctic topics, bringing into focus diverse collections of observations that help to assess the trajectory and impacts of Arctic change. Figure 1 locates some of these events in the pan-Arctic perspective and Fig. 2 is provided as a convenient place name reference.

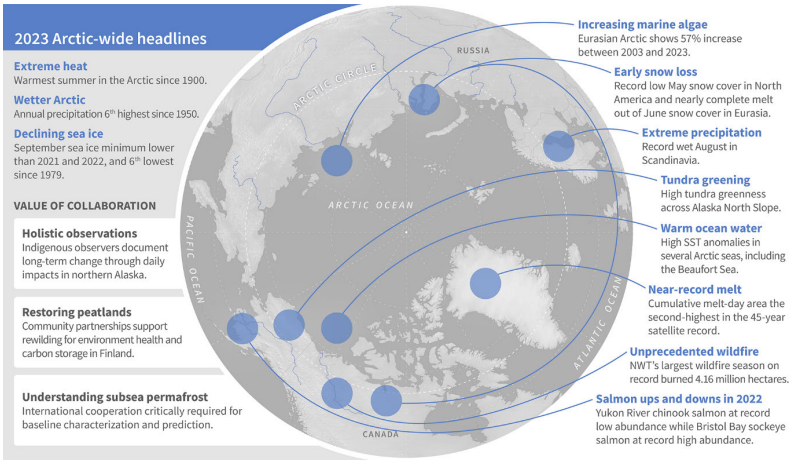

Fig. 1. A sample of notable events and important topics from across the Arctic.

Arctic Wildfire 2023

During late summer 2023, northern Canada experienced unprecedented and destructive wildfire. Because topics for the annual Arctic Report Card (ARC) are selected and finalized by early summer, the report was unable to include a full essay on this extraordinary wildfire season and associated impacts. This sidebar, however, provides a brief report on the Arctic summer wildfire season.

Based on government reporting, as of late October 2023, wildfire burned 4.61 million hectares (11.39 million acres) in high-latitude North America (Alaska, USA and Yukon Territory and Northwest Territories, Canada). More than 90 percent of the area burned was in the Northwest Territories, where about 300 separate fires burned 4.16 million

Fig. 2. The ARC2023 map provides a general geographic reference for many locations mentioned in this year's report.

This year's physical and biological Vital Sign observations are in line with trends reported in past Arctic Report Cards—warming sea surface and surface air temperatures, decreasing snow cover, diminishing sea ice, both in spatial extent and thickness, and continued mass loss from the Greenland Ice Sheet. Year-to-year variations, in addition to long-term trends, are significant and can be especially important at regional scales.

Extreme weather and climate events during the past year in the Arctic and elsewhere have brought unambiguous, climate change-supercharged impacts to people and ecosystems. Such events vary in scale across time and space. In the span of a few hours, individual storms may create hardships and damage that last for years. Longer-term extremes, such as drought or prolonged high temperatures, also have direct, distinct impacts, produce cascading effects in other parts of the environment, and may exacerbate (or mitigate) shorter time frame weather extremes.

Some high impact events are a clear signature of sustained climate change. For example, Canada experienced its worst national wildfire season on record. Multiple communities in the Northwest Territories were evacuated during August as a precaution, including more than hectares (10.28 million acres), the largest area burned in 44 years of record (Northwest Territories Department of Environment and Climate Change 2023, see Fig. SB1).

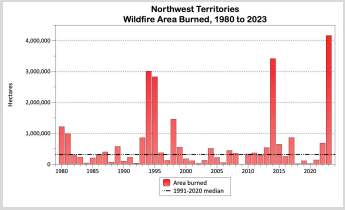

Fig. SB1. Annual area burned in the Northwest Territories, Canada. Updated from York et al. (2020) using data from Northwest Territories Department of Environment and Climate Change (2023).

A dozen communities both north and south of Great Slave Lake were evacuated due to the threat posed by wildfire. At some time during the summer, more than two-thirds of the Northwest Territories's 46,000 residents were displaced, in many cases for weeks at a time, with significant economic impacts from lost income, disrupted traditional activities, and infrastructure lost to the fires (Thompson 2023). The community of Enterprise, NWT was largely destroyed by a fast moving fire during 13-14 August 2023 (CBC News 2023). And like much of Canada, there was widespread prolonged poor air quality from dense smoke.

20,000 people from the capital city of Yellowknife (see *Arctic Wildfire Sidebar*). In August 2023 near Juneau, Alaska, a glacial lake on a tributary of the Mendenhall Glacier burst through its ice dam and caused unprecedented flooding and severe property damage on Mendenhall River, a direct result of dramatic glacial thinning over the past 20 years (see Wolkin et al. 2021 for additional examples).

Average surface air temperatures for the Arctic as a whole in the past year (October 2022-September 2023) ranked as the sixth warmest since 1900, and summer (July through September 2023) was the warmest on record. There were, however, important regional differences, including a colder-than-normal spring across Alaska that slowed snowpack and sea-ice melt, while parts of north-central Canada experienced the highest spring average temperatures on record. Prolonged warmth over Arctic lands can even impact summer sea ice extent and sea surface temperatures by warming waters in the major rivers draining the region, as noted this year near the ocean outlets of the Mackenzie River in North America and the Ob, Yenisei and Lena Rivers in Asia, draining areas that had significantly above-normal late spring and summer temperatures.

The presence or absence of sea ice and the timing of Arctic sea ice cover are major factors in modulating ecosystem and human activity. In spring 2023, the Arctic-wide sea ice volume was similar to spring 2022. Sea ice loss was slower than average at the start of the 2023 melt season but accelerated in July. By late August both the Northern Sea Route and Northwest Passage were open for non-ice hardened ship traffic. The September sea ice minimum extent of 4.23 million square kilometers (1.6 million square miles) was about 10 percent lower than the past two years, and overall the sixth lowest in the 45-year long satellite record. The 17 lowest minimum extents have all occurred in the 17 years since 2007.

Summer sea surface temperatures, tundra vegetation growth on land, and phytoplankton blooms or primary productivity in the sea are closely tied to the timing of sea ice loss and warm-season air temperatures. Spring and early summer loss of sea ice exposes the dark ocean surface and allows time for significant solar heating of the ocean. Linked to early sea ice loss, average sea surface temperatures for August 2023 were much higher than the 30-year average in the Barents, Kara, Laptev and Beaufort Seas. Anomalously cool August 2023 sea surface temperatures were observed in Baffin Bay, the Greenland Sea, and parts of the Chukchi Sea. The 2023 circumpolar average peak tundra greenness was the fifth highest in the 24-year MODIS satellite record, a slight decline from the previous year. Closely aligned with air temperatures and nearshore sea ice anomalies, peak vegetation greenness in 2023 was much higher than usual in the North American tundra, particularly in the Beaufort Sea region. In

In contrast to the Northwest Territories, the Yukon Territory's area burned was about 328,000 hectares (810,000 acres), which is slightly above the previous 30-year median. In Alaska, wildfires burned 119,500 hectares (295,000 acres), less than half of the 30-year median (Alaska Interagency Coordination Center 2023). Although not complete, preliminary remote sensing-derived estimates of Siberian (Sakha Republic) wildfire in 2023 indicates that the area burned was slightly higher than 2022, but much lower than the summers of 2018 to 2021 (A. Soja and E. Gargulinski, NASA Langley Research Center, 14 September 2022, personal communication).

Wildfire in the Arctic and sub-Arctic boreal forest is a natural part of the ecosystem, but the extent and intensity of fires has likely changed over time, in part due to changing human activity and recent variations in wildfire management practices. High latitude wildfire poses threats to human life, property and activities, including traditional food gathering. In recent years, extreme wildfire activity relative to the late 20th and early 21st centuries'

contrast, tundra greenness was relatively low in the Eurasian Arctic, particularly in northeastern Siberia. Both tundra greenness and primary productivity show multi-decade increasing trends but with significant regional and year-to-year variability.

The changing Arctic hydroclimate is documented through precipitation and snowfall (water equivalent) analyses. Precipitation in the past year was above normal in all seasons for the Arctic as a whole, but with important seasonal and regional variations. Unusually low precipitation and high temperatures produced severe drought and contributed to the record-breaking wildfire season in Canada's Northwest Territory (see *Arctic Wildfire Sidebar*). Snowpack in early spring 2023 was above normal for both North America and Eurasia, but then rapid snow loss in much of the Arctic resulted in record low average snow water equivalent for the North American Arctic in May and near-record low snow cover for the Eurasian Arctic in June.

averages has occurred in the North American or Eurasian sub-Arctic in most summers (York et al. 2020). Separate essays on high-latitude wildfires were published in the 2017 and 2020 ARC, and we expect to report more fully on recent wildfires in a future ARC.

Precipitation patterns also influence the Greenland Ice Sheet. Above-average snowfall over parts of the Greenland Ice Sheet between autumn 2022 and spring 2023 contributed to a relatively low (for the 21st century) total mass loss from the Greenland Ice Sheet in spite of extensive late June to September ice melt. So, while the Greenland Ice Sheet lost mass in the past year, as it has every year since 1998, the loss for September 2022 to August 2023 was much lower than the 22-year average and similar to 2020-21. However, the cumulative melt-day area during summer 2023 was the second-highest in the 45-year satellite observational record.

Since time immemorial the Arctic has been home to diverse peoples, and through hundreds of generations they have honed the skills needed to thrive in this environment. In recent years, Western science and societies are more strongly and equitably recognizing the value of the lived experiences and cultural expertises of Arctic Indigenous peoples, not just as a source of information but as experts. ARC2023 features a Frostbite on the yearslong work of the Alaska Arctic Observatory and Knowledge Hub, a collaborative effort wherein community experts in northern Alaska communities, including Indigenous Knowledge holders, share their expertise and observations, which are fundamentally important for tracking the scale and implications of Arctic change. The value of Indigenous Knowledge to address contemporary environmental problems is also highlighted in an essay on the restoration of peatlands in northern and eastern Finland.

The Arctic Report Card also aims to shed light on some of the least understood features of the Arctic environment. In ARC2023, we address the divergent trends of salmon in western Alaska, where Chinook and chum salmon returns are collapsing on the Yukon and Kuskokwim Rivers, while at the same time sockeye salmon in Bristol Bay are at near record high numbers. Both extremes are having severe economic and cultural impacts. Changing environmental conditions clearly are playing a role yet additional work incorporating both Indigenous Knowledge and Western science is needed to understand what is driving these observed trends. We also examine the state of observations of subsea permafrost. Subsea permafrost today exists in Arctic regions that were aerially exposed during the late Pleistocene but were subsequently submerged by rising sea levels. Detailed research exists for only small portions of the Kara and Beaufort Seas, but by far the largest area of subsea permafrost underlies the modern Laptev and East Siberian Seas. There is a lack of observations and research in these areas, significantly inhibiting our understanding of how and when the rapidly warming Arctic will affect the more than 2

million km^2 of subsea permafrost. This scientific gap highlights the urgent need for international cooperation to better understand this facet of the Arctic system.

ARC2023 includes 12 essays providing multiple perspectives on the rapidly transitioning Arctic. Long-term trends are reinforced by another year of observations, while the importance of year-to-year variability and regional differences across the Arctic are apparent. Extreme weather and climate events and their impacts to society and ecosystems are stark reminders that transition is not just about multi-decadal trends but about day-to-day living in and around the Arctic. The Arctic remains a varied, expansive, and expensive region to monitor. To understand and adapt to this transition, local to international partnerships, including with Arctic Peoples and Indigenous communities, are vital for collecting and using diverse observations and knowledge, as well as for identifying resilient actions to long-term climate impacts and abrupt disturbances.

References

Wolkin, G. J., and Coauthors, 2021: Glacier and permafrost hazards. *Arctic Report Card 2021*, T. A. Moon, M. L. Druckenmiller, and R. L. Thoman, Eds., https://doi.org/10.25923/v40r-0956.

Sidebar Wildfire References

Alaska Interagency Coordination Center, 2023: https://fire.ak.blm.gov/, accessed 31 October 2023.

CBC News, 2023: "Enterprise, N.W.T., '90 per cent gone' after wildfire ravages community" (15 August 2023). https://www.cbc.ca/news/canada/north/enterprise-damage-wildfire-1.6936652, accessed 15 September 2023.

Northwest Territories Department of Environment and Climate Change, 2023: https://www.gov.nt.ca/ecc/en/services/wildfire-update, accessed 31 October 2023.

Thompson, Shane, Northwest Territories Minister of Environment and Natural Resources, Ministers' Statements and Speeches, 2023: Remarks on 28 September 2023, https://www.gov.nt.ca/en/newsroom/shane-thompson-historic-2023-wildfire-season, accessed 29 October 2023.

York, A., U. S. Bhatt, E. Gargulinski, Z. Grabinski, P. Jain, A. Soja, R. L. Thoman, and R. Ziel, 2020: Wildland fire in high northern latitudes. *Arctic Report Card 2020*, R. L. Thoman, J. Richter-Menge, and M. L. Druckenmiller, Eds., https://doi.org/10.25923/2gef-3964.

Yukon Wildfire Services, 2023: https://wildfires.service.yukon.ca/, accessed 31 October 2023.

November 21, 2023

Surface Air Temperature

https://doi.org/10.25923/x3ta-6e63

T. J. Ballinger[1], S. Bigaalke[2], J. E. Walsh[1,3], B. Brettschneider[4], R. L. Thoman[1,3], U. S. Bhatt[5], E. Hanna[6], I. Hanssen-Bauer[7], S. -J. Kim[8], J. E. Overland[9], and M. Wang[9,10]

[1]International Arctic Research Center, University of Alaska Fairbanks, Fairbanks, AK, USA
[2]Department of Geography, Portland State University, Portland, OR, USA
[3]Alaska Center for Climate Assessment and Policy, University of Alaska Fairbanks, Fairbanks, AK, USA
[4]National Weather Service Alaska Region, NOAA, Anchorage, AK, USA
[5]Geophysical Institute, University of Alaska Fairbanks, Fairbanks, AK, USA
[6]Department of Geography and Lincoln Climate Research Group, University of Lincoln, Lincoln, UK
[7]Norwegian Meteorological Institute, Oslo, Norway
[8]Korea Polar Research Institute, Incheon, Republic of Korea
[9]Pacific Marine Environmental Laboratory, NOAA, Seattle, WA, USA
[10]Cooperative Institute for Climate, Ocean, and Ecosystem Studies, University of Washington, Seattle, WA, USA

Headlines

- Above-average pan-Arctic (60-90° N) annual surface air temperatures continued in 2023, ranking 6th warmest since 1900.
- The Barents Sea region exhibited above-average surface air temperatures in all seasons, punctuated by large anomalies in autumn 2022 and winter 2023.
- The warmest summer (July-September mean) on record was observed in 2023.

Introduction

Warming near-surface air and upper-ocean temperatures in the Arctic represent an ongoing signature of Arctic change (Ballinger et al. 2022). This regional warming rate exceeds that of the global mean temperature, a phenomenon known as Arctic Amplification (e.g., Serreze and Barry 2011). Air temperature warming is associated with changes in the Arctic hydrologic cycle, including increased seasonal precipitation totals and short-term extremes (see essay *Precipitation*), as well as declines in terrestrial snow, land ice, and sea ice coverage (Box et al. 2021; see essays *Terrestrial Snow Cover*, *Greenland Ice Sheet*, and *Sea Ice*). The increase in Arctic air temperatures is congruent with more frequent extreme air temperature events, which can have detrimental, rapid, and direct biophysical impacts within the Arctic (e.g., thaw-driven coastal erosion; Walsh et al. 2020) with indirect effects that permeate globally (e.g., as land ice mass losses contribute to sea-level rise; Moon et al. 2019). Thus, Arctic warming has far-reaching long-term consequences beyond the region.

Consistent with previous Arctic Report Card Surface Air Temperature essays, we provide the historical context of this past year's Arctic (60-90° N) air temperatures followed by a seasonal synopsis of air temperature patterns.

Arctic annual air temperatures

Long-term Arctic and Global surface air temperature anomalies from NASA's GISTEMP (version 4) and the ERA5 reanalysis (see *Methods and data* for details) are shown for their respective full periods of record in Fig. 1 following the water year (i.e., October-September mean). Considering the GISTEMP and ERA5 records, the 2023 annual anomaly was 0.76°C and 0.77°C, respectively, for the Arctic, ranking as the 6th warmest since 1900. For the GISTEMP record, this year marks the 14th consecutive year where Arctic temperatures have exceeded the 1991-2020 mean, while the eight warmest years in the Arctic have all occurred since 2016. Within this past year, autumn, winter, and spring Arctic air temperatures saw >90th percentile warmth with summer air temperatures emerging as the record warmest in over 120 years.

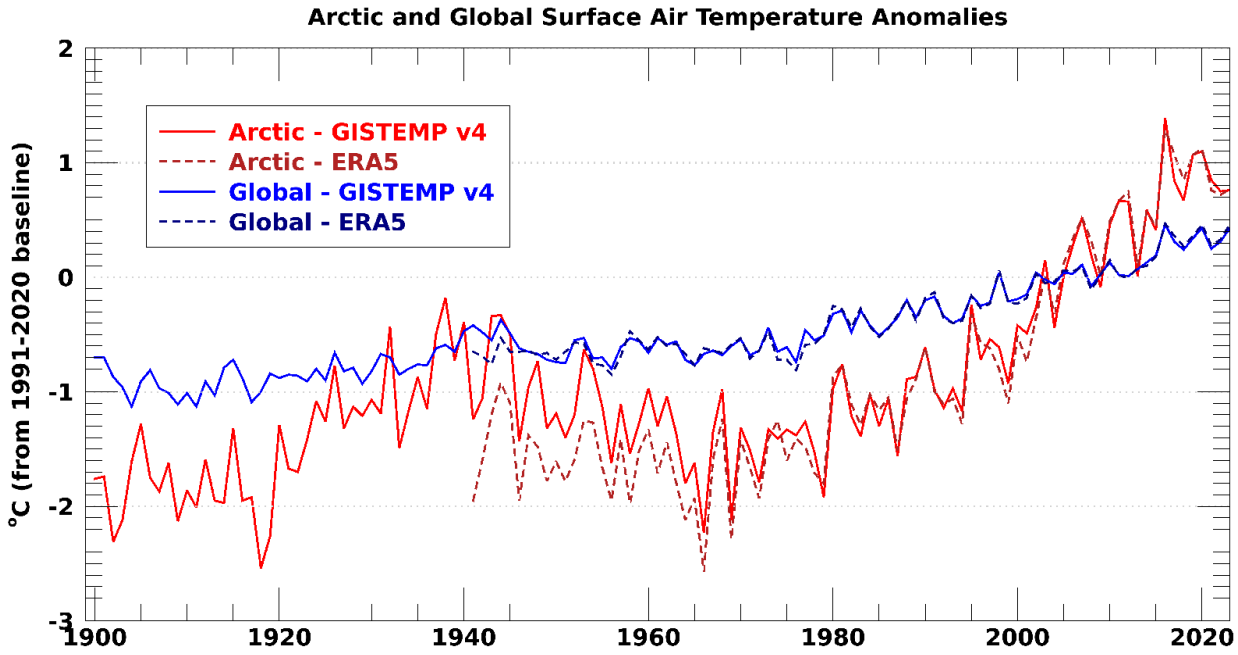

Fig. 1. Arctic (60-90° N) and Global (90° S-90° N) surface air temperature anomalies (in °C) averaged across land and ocean areas. Each year's air temperature reflects the water year average (e.g., October 2022-September 2023 represents the 2023 SAT value). Source: NASA GISTEMP v4 data are obtained from the NASA Goddard Institute for Space Studies and ERA5 data are retrieved from the Copernicus Climate Change Service.

The Arctic Amplification signal is clear and persistent at the annual scale as shown by warmer Arctic surface air temperature anomalies relative to those measured for the whole of planet Earth (Fig. 1). Diverse, complex, and interrelated mechanisms and feedbacks underlie accelerated Arctic warming. For example, less extensive and thinner sea ice tends (see essay *Sea Ice*) to melt out earlier in the year. Longer periods of open water and sparse ice during summer result in more direct and prolonged transfer of atmospheric energy into the Arctic Ocean. As a result, the upper-ocean cools more slowly, delaying sea ice formation as upper-ocean heat is released to the atmosphere, warming the surface air temperatures in autumn and early winter (Serreze and Barry 2011). In today's Arctic, these interactions affect the marginal ice zones and adjacent coastal areas, most notably in the Chukchi and Beaufort Seas (Ballinger et al. 2023) and Barents Sea (Isaksen et al. 2022). These examples are further touched upon in the following section.

Seasonal air temperature patterns

Arctic surface air temperature anomaly patterns are further discussed at the seasonal scale as follows: autumn 2022 (October-December [OND]), winter (January-March [JFM]), spring (April-June [AMJ]), and summer (July-September [JAS]) 2023 (Fig. 2). The seasons are defined to span the water year (October-September) and coincide with annual cycles of variables consistently referenced in Arctic Report Card essays. For example, Arctic sea-ice melt begins in spring, while late summer (i.e., September) tends to mark the annual sea ice cover minimum.

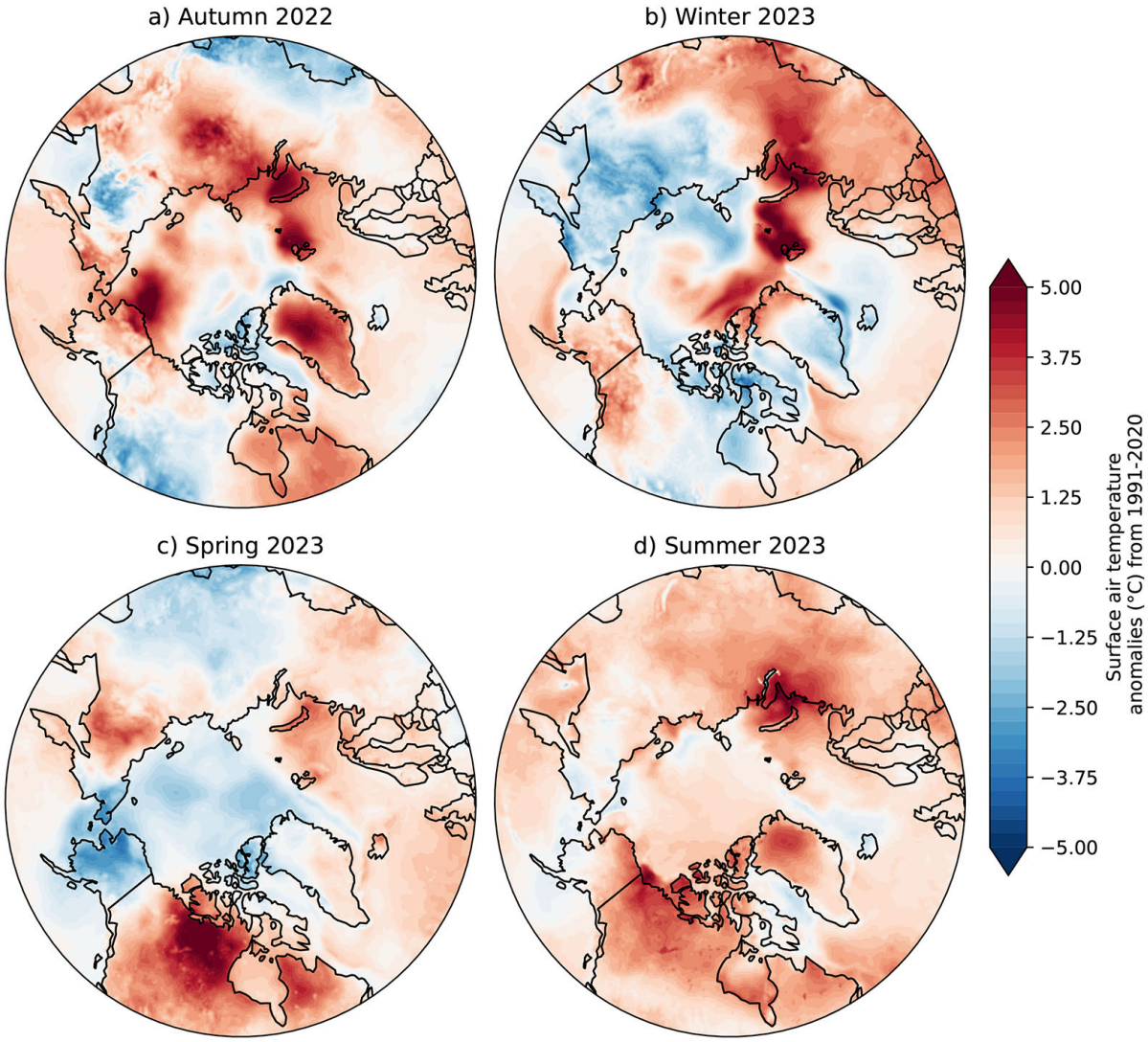

Fig. 2. Seasonal surface air temperature anomalies (in °C) for (a) autumn 2022, (b) winter 2023, (c) spring 2023, and (d) summer 2023. Temperature anomalies are shown relative to their 1991-2020 means. Source: ERA5 reanalysis air temperature data are obtained from the Copernicus Climate Change Service.

During *autumn 2022*, the largest warm anomalies (~5°C) were found over the Arctic marginal seas and nearby coastal zones, including eastern Chukchi and western Beaufort Seas and North Slope of Alaska, the interior of the Greenland Ice Sheet, atop Svalbard, and over the westernmost Barents Sea (Fig. 2a). Of note, a high temperature extreme at Utqiaġvik on 5 December 2022 (4.4°C) set a daily maximum

temperature record for *any date* between 30 October and 22 April (Rick Thoman, personal communication). Warm anomalies were also apparent over north-central Eurasia, Chukotka, and northern Quebec. A negative sea-level pressure anomaly over the Laptev and East Siberian Seas transported warm air poleward into the Pacific Arctic from the Eurasian continent (Fig. 3a). The summer sea ice loss and delayed ice formation in autumn (see essay *Sea Ice*), combined with the large-scale atmospheric pressure pattern, may have contributed to the warm anomalies over Chukotka and the Chukchi and Beaufort areas.

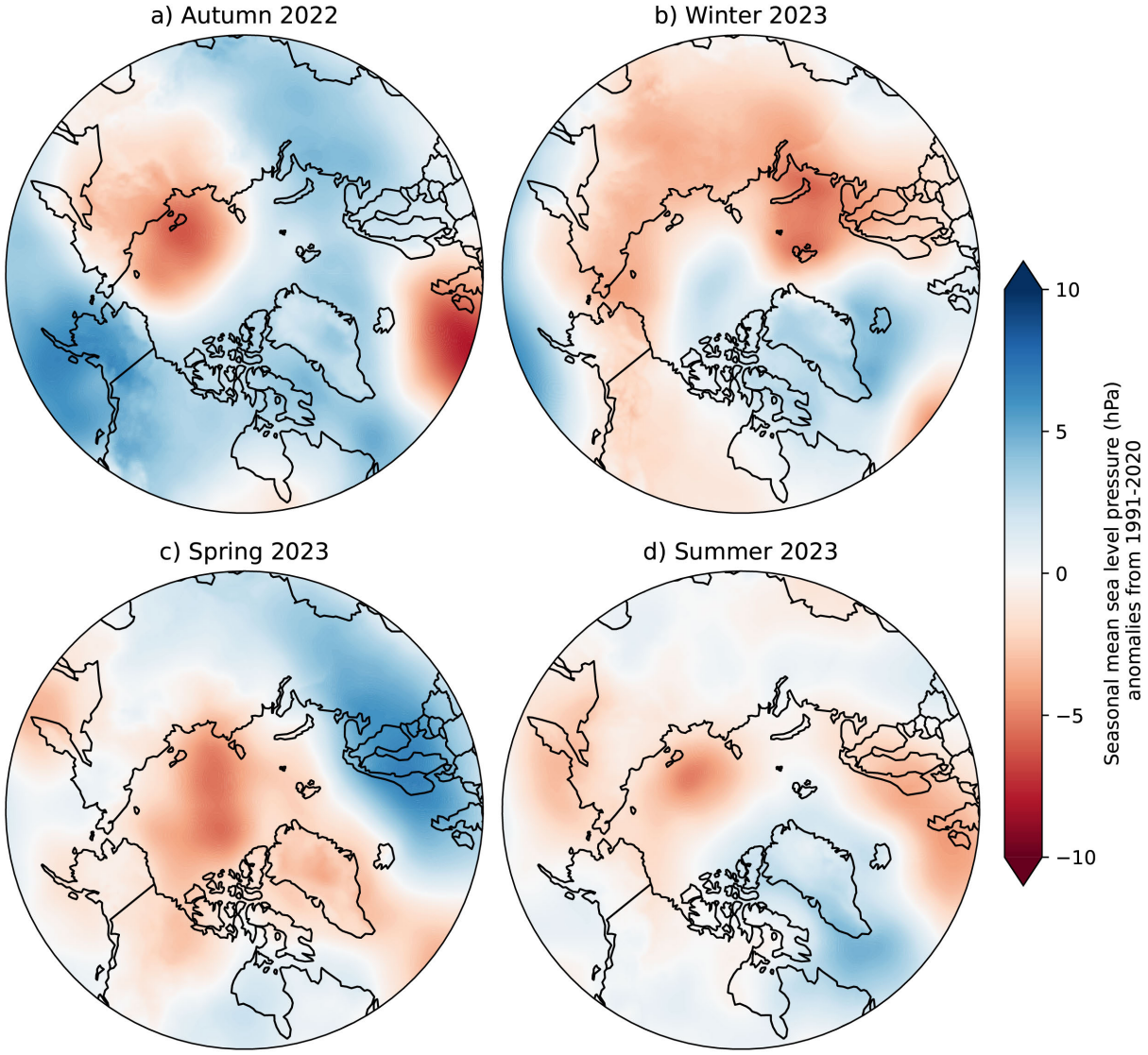

Fig. 3. Seasonal sea-level pressure (SLP) anomalies (in hPa) for (a) autumn 2022, (b) winter 2023, (c) spring 2023, and (d) summer 2023. SLP anomalies are shown relative to their 1991-2020 means. Source: ERA5 reanalysis SLP data are obtained from the Copernicus Climate Change Service.

The warmest anomalies in *winter 2023* were noted over the northern and southern Barents Sea and northwestern Eurasia (~5°C) (Fig. 2b). Additional positive temperature anomalies are shown over the Lincoln Sea and just north of the Canadian Arctic Archipelago. Much of central and eastern Siberia, Hudson Bay, the southern Canadian Arctic Archipelago, and Greenland Sea were characterized by cold anomalies. Negative surface pressure anomalies were found across much of the Arctic landscape and

over the Barents Sea (Fig. 3b), suggestive of an active high-latitude winter storm track linked with the observed mild temperatures.

Spring 2023 showed notable warming over the Northwest Territories and Nunavut (~5°C anomalies; Fig. 2c) associated with reduced snow cover and a shorter snow cover duration (see essay *Snow Cover*). The north Atlantic Arctic, from central Greenland stretching to the Barents Sea and eastern Eurasia, also exhibited warmer-than-average conditions. In contrast, below-average air temperatures (~-2-3°C) were found across Alaska, the northern Bering and southern Chukchi Seas, and Chukotka. Much of the Arctic Ocean air temperatures were also near or slightly below average, associated with a low-pressure anomaly across the Central Arctic Ocean (Fig 3c).

Summer 2023, the warmest captured by NASA GISTEMP v4 since at least 1900 and ERA5 since 1941, was punctuated by warm air temperatures over most of the northern Canadian provincial areas and southern Barents Sea and Kara Sea (Fig. 2d). Regionally, the anomalous warmth atop the Northwest Territories, Nunavut, and the Canadian Arctic Archipelago coincided with below-normal precipitation over these areas (see essay *Precipitation*) and contributed to Northern Canada's extreme wildfire season (see *Arctic Wildfire Sidebar*). Warm anomalies in northern and central Greenland were associated with near-record cumulative melt-day area across the ice sheet (see essay *Greenland Ice Sheet*). Warm air temperatures were also found in conjunction with low pressure anomaly patterns atop much of northern Europe, over the Laptev Sea, western Bering Sea, Kamchatka, and Sea of Okhotsk (Fig. 3d).

Methods and data

The NASA Goddard Institute for Space Studies surface temperature analysis version 4 (GISTEMP v4) is used to describe long-term Arctic (60-90° N) and Global (90° S-90° N) surface air temperatures since 1900 (Fig. 1). GISTEMP v4 air temperatures over lands are obtained from the NOAA Global Historical Climatology Network version 4 (GHCN v4) dataset and ocean surface temperatures are taken from the NOAA Extended Reconstructed Sea Surface Temperature version 5 (ERSST v5) dataset. The creation of the GISTEMP product is described in Hansen et al. (2010) and Lenssen et al. (2019).

We supplement the GISTEMP v4 data with an Arctic two-meter (i.e., surface) air temperature time series from ERA5 reanalysis (Hersbach et al. 2020). Comparison of these respective Arctic and Global time series shows good agreement with minimal differences during the last four decades (Fig. 1). We use both surface air temperature and sea-level pressure fields from ERA5 in Figs. 2 and 3, respectively. All values and fields are presented as anomalies with respect to the 1991-2020 mean.

References

Ballinger, T. J., and Coauthors, 2022: Surface air temperature. *Arctic Report Card 2021*, M. L. Druckenmiller, R. L. Thoman, and T. A. Moon, Eds., https://doi.org/10.25923/13qm-2576.

Ballinger, T. J., and Coauthors, 2023: Alaska terrestrial and marine climate trends, 1957-2021. *J. Climate*, **36**, 4375-4391, https://doi.org/10.1175/JCLI-D-22-0434.1.

Box, J. E., and Coauthors, 2021: Recent developments in Arctic climate observational indicators. *AMAP Arctic Climate Change Update 2021: Key Trends and Impact*s. Arctic Monitoring and Assessment Programme (AMAP), Tromso, Norway, pp. 7-29.

Hansen, J., R. Ruedy, M. Sato, and K. Lo, 2010: Global surface temperature change. *Rev. Geophys.*, **48**, RG4004, https://doi.org/10.1029/2010RG000345.

Hersbach, H., and Coauthors, 2020: The ERA5 global reanalysis. *Quart. J. Roy. Meteor. Soc.*, **146**, 1999-2049, https://doi.org/10.1002/qj.3803.

Isaksen, K., and Coauthors, 2022: Exceptional warming over the Barents area. *Sci. Rep.*, **12**, 9371, https://doi.org/10.1038/s41598-022-13568-5.

Lenssen, N. J. L., G. A. Schmidt, J. E. Hansen, M. J. Menne, A. Persin, R. Ruedy, and D. Zyss, 2019: Improvements in the GISTEMP uncertainty model. *J. Geophys. Res.-Atmos.*, **124**, 6307-6326, https://doi.org/10.1029/2018JD029522.

Moon, T. A., and Coauthors, 2019: The expanding footprint of rapid Arctic change. *Earth's Future*, **7**, 212-218, https://doi.org/10.1029/2018EF001088.

Serreze, M. C., and R. G. Barry, 2011: Processes and impacts of Arctic amplification: A research synthesis. *Global Planet. Change*, **77**, 85-96, https://doi.org/10.1016/j.gloplacha.2011.03.004.

Walsh, J. E., T. J. Ballinger, E. S. Euskirchen, E. Hanna, J. Mård, J. E. Overland, H. Tangen, and T. Vihma, 2020: Extreme weather and climate events in northern areas: A review. *Earth-Sci. Rev.*, **209**, 103324, https://doi.org/10.1016/j.earscirev.2020.103324.

November 17, 2023

Terrestrial Snow Cover

https://doi.org/10.25923/xqwa-h543

L. R. Mudryk[1], A. Elias Chereque[2], C. Derksen[1], K. Luojus[3], and B. Decharme[4]

[1]Climate Research Division, Environment and Climate Change Canada, Toronto, ON, Canada
[2]Department of Physics, University of Toronto, Toronto, ON, Canada
[3]Arctic Research Centre, Finnish Meteorological Institute, Helsinki, Finland
[4]Centre National de Recherches Météorologiques, Météo-France, Toulouse, France

Headlines

- North American May snow cover extent set a record low in 2023 (lowest in the 57-year record) associated with high spring temperatures across the Northwest Territories and Nunavut.
- Snow accumulation during the 2022/23 winter was above average across both continents, particularly Eurasia.
- Since 2010, there was a near-complete absence of snow cover in June in Eurasia (except for residual amounts at higher elevations) for 11 of the 14 years; this lack of June snow cover did not occur at all between 1967 and 2009.

Introduction

Many Arctic land surface processes are directly influenced by snow cover from fall through spring, including the surface energy budget, ground thermal regime, permafrost, and terrestrial and freshwater ecosystems (Brown et al. 2017; Meredith et al. 2019). Even following the snow cover season, the influence of spring snow melt timing persists through impacts on river discharge timing and magnitude, surface water, soil moisture, vegetation phenology, and fire risk (Meredith et al. 2019).

Multiple datasets derived from satellite observations and snowpack models driven by atmospheric reanalyses are used to assess Arctic seasonal snow cover. Collectively, this approach provides a reliable picture of Arctic snow cover variability over the last five decades. We characterize snow conditions across the Arctic land surface using three quantities: how much total land area is covered by snow (snow cover extent – SCE), how much of the year snow covers the land surface (snow cover duration – SCD), and how much total water is stored in solid form by the snowpack (snow water equivalent – SWE; the product of snow depth and density). We examine each of these quantities in turn for the 2022/23 Arctic snow season.

Snow cover extent and duration

SCE anomalies (relative to the 1991-2020 baseline) in spring 2023 are shown separately for the North American and Eurasian sectors of the Arctic in Fig. 1. North American May SCE set a record low in 2023 (lowest SCE in the 57-year record) associated with spring temperatures up to 5°C above normal across the region (see essay *Surface Air Temperature*) but rebounded slightly by June (ranked 4th lowest). In the Eurasian sector, May anomalies were close to the 1991-2020 average but were well below normal by June (ranked 9th lowest in the 57-year record).

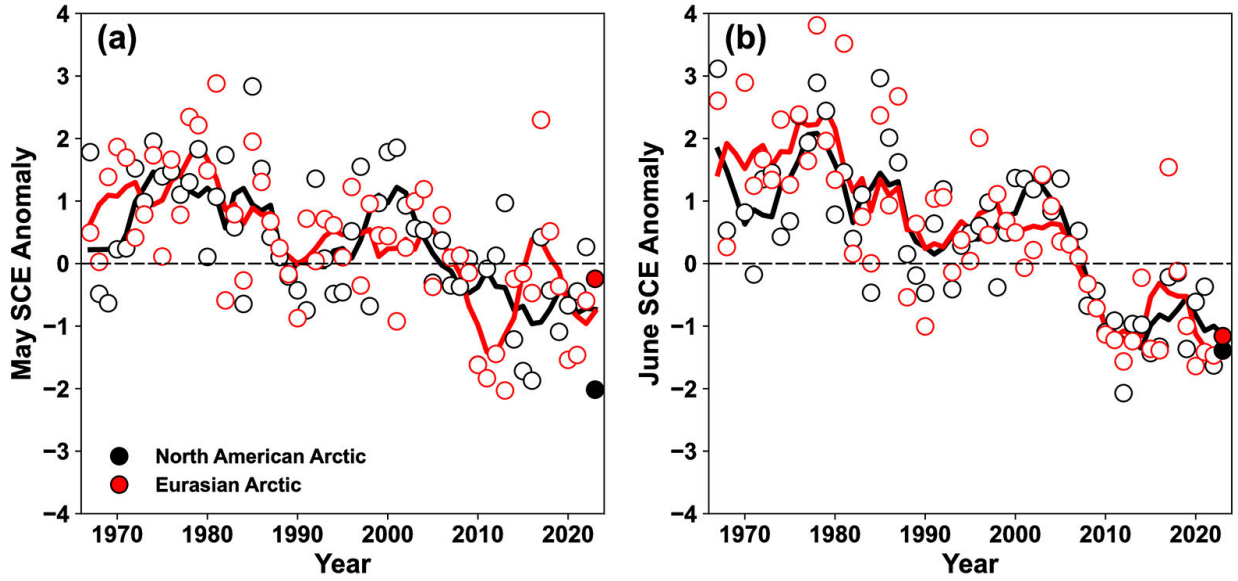

Fig. 1. Standardized monthly snow cover extent anomalies relative to the 1991-2020 climatology for Arctic land areas (>60° N) for (a) May, and (b) June from 1967 to 2023. Solid black and red lines depict 5-year running means for North America and Eurasia, respectively. Filled circles are used to highlight 2023 anomalies. Source: NOAA snow chart Climate Data Record (CDR).

SCD anomalies (Fig. 2a) during the 2022/23 snow season had a combination of early and late snow onset (relative to a 1998/99 to 2017/18 baseline) with an especially variable pattern across the North American Arctic. Across central and eastern Eurasia Arctic snow onset occurred earlier than normal while across western Eurasia there was a modest delay. The signal of extensive snow melt across North America in May SCE is also apparent in the signal of spring SCD anomalies (Fig. 2b) where a broad swath of mainland Nunavut and Northwest Territories in Canada saw a more than 50% increase in the number of snow-free days in spring. While spring snow melt across Eurasia was not as extensive as in the previous two years, far northern coastal regions across the continent still had above-normal numbers of snow-free days indicative of earlier snow melt.

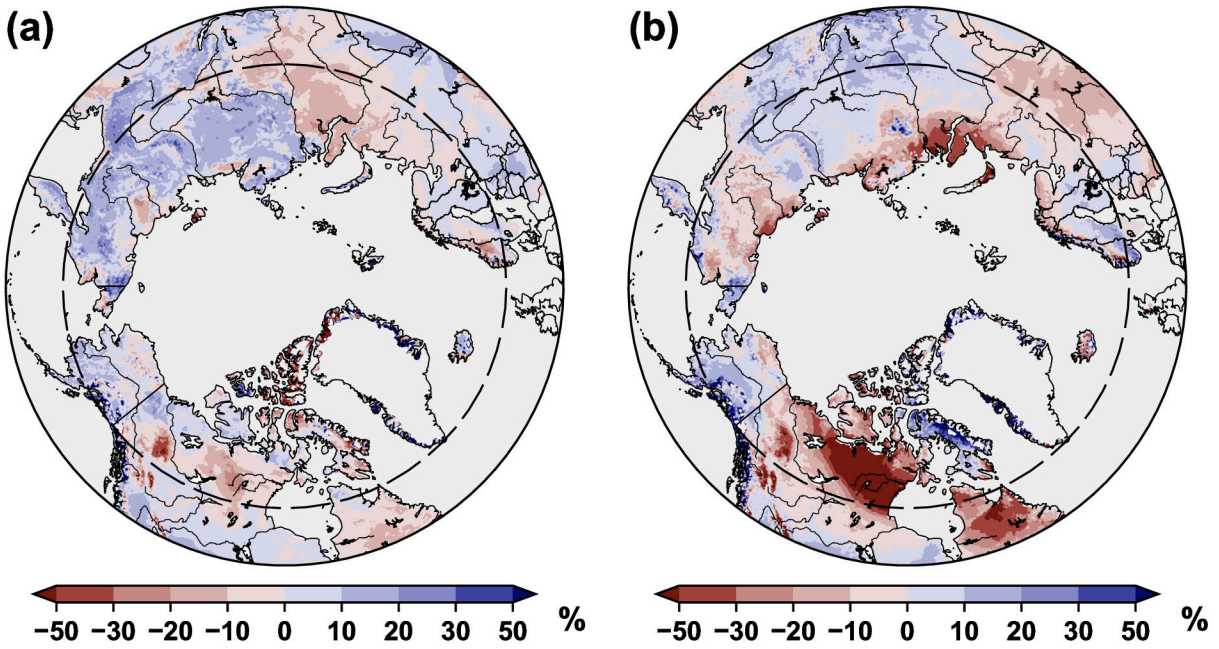

Fig. 2. Snow cover duration anomalies (% difference relative to average number of snow-free days) for the 2022/23 snow year: (a) snow onset (Aug-Jan); and (b) snow melt (Feb-Jul). Red (blue) indicates increased (decreased) snow-free days compared to the 1998/99 through 2017/18 mean, aligning with later (earlier) onset (a) or earlier (later) melt (b). The dashed circle marks the latitude 60° N; Arctic land areas north of this are considered in this study. Source: NOAA IMS data record.

Snow mass and snow water equivalent

Snow mass across the Arctic tends to peak annually during April, when snowfall has accumulated since the preceding autumn but before increasing temperatures during May and June lead to snow melt. Snow mass anomalies for April 2023 (Fig. 3; calculated by aggregating SWE across the Arctic land surface to measure the total mass of water stored by snow across the region) indicate snow accumulation was above the 1991-2020 baseline across both continents (consistent with the wet autumn and winter reported in the *Precipitation* essay), but especially Eurasia where it was the fifth highest accumulation in the record. The spatial patterns of monthly mean SWE (Fig. 4) illustrate how this accumulation varied regionally from just before peak (March) through to the end of the melt period (June). Regions with positive SWE anomalies in March had even stronger positive anomalies by May (most of Alaska, large parts of central and eastern Siberia), which suggests that snow in these regions took longer to melt compared to the historical baseline. Mainland Arctic Canada was an exception. This region experienced extensive reductions in SWE during May which extended northward into the southern Canadian Arctic Archipelago during June. By June snow was mostly melted across both continents except for Baffin and the Queen Elizabeth Islands in the Canadian Arctic Archipelago. Early snow melt across mainland Arctic Canada (and boreal regions to the south) during spring 2023 and summer precipitation deficits (see essay *Precipitation*) may both have contributed to the extensive summer 2023 wildfire season, which forced the complete evacuation of communities in the western Canadian Arctic (see *Arctic Wildfire Sidebar*).

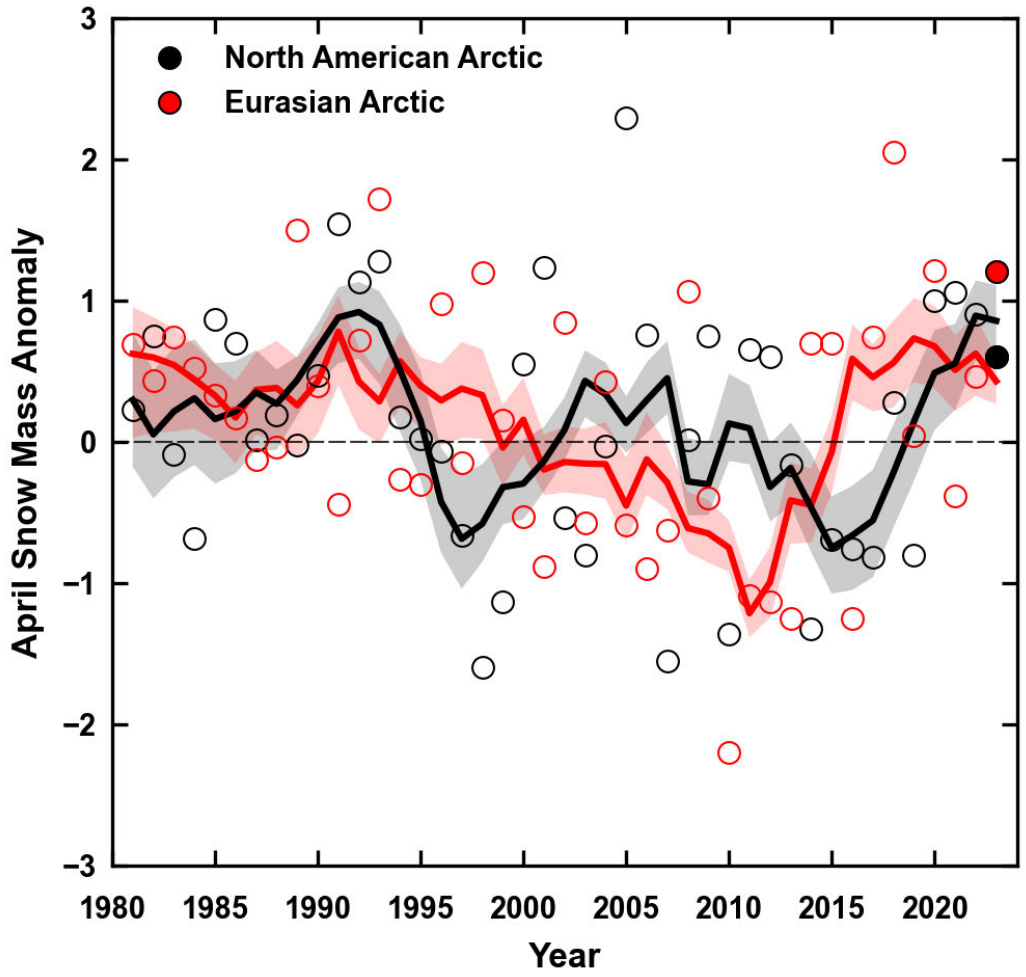

Fig. 3. Standardized April snow mass anomalies for Arctic land areas across the North American (black) and Eurasian (red) sectors. Anomalies (relative to the 1991-2020 average) represent the ensemble mean from a suite of four independent snow analyses. Filled circles are used to highlight 2023 anomalies. Solid black and red lines depict 5-yr running means; shading depicts the spread amongst individual dataset running means. Source: snow analyses as described in *Methods and data*.

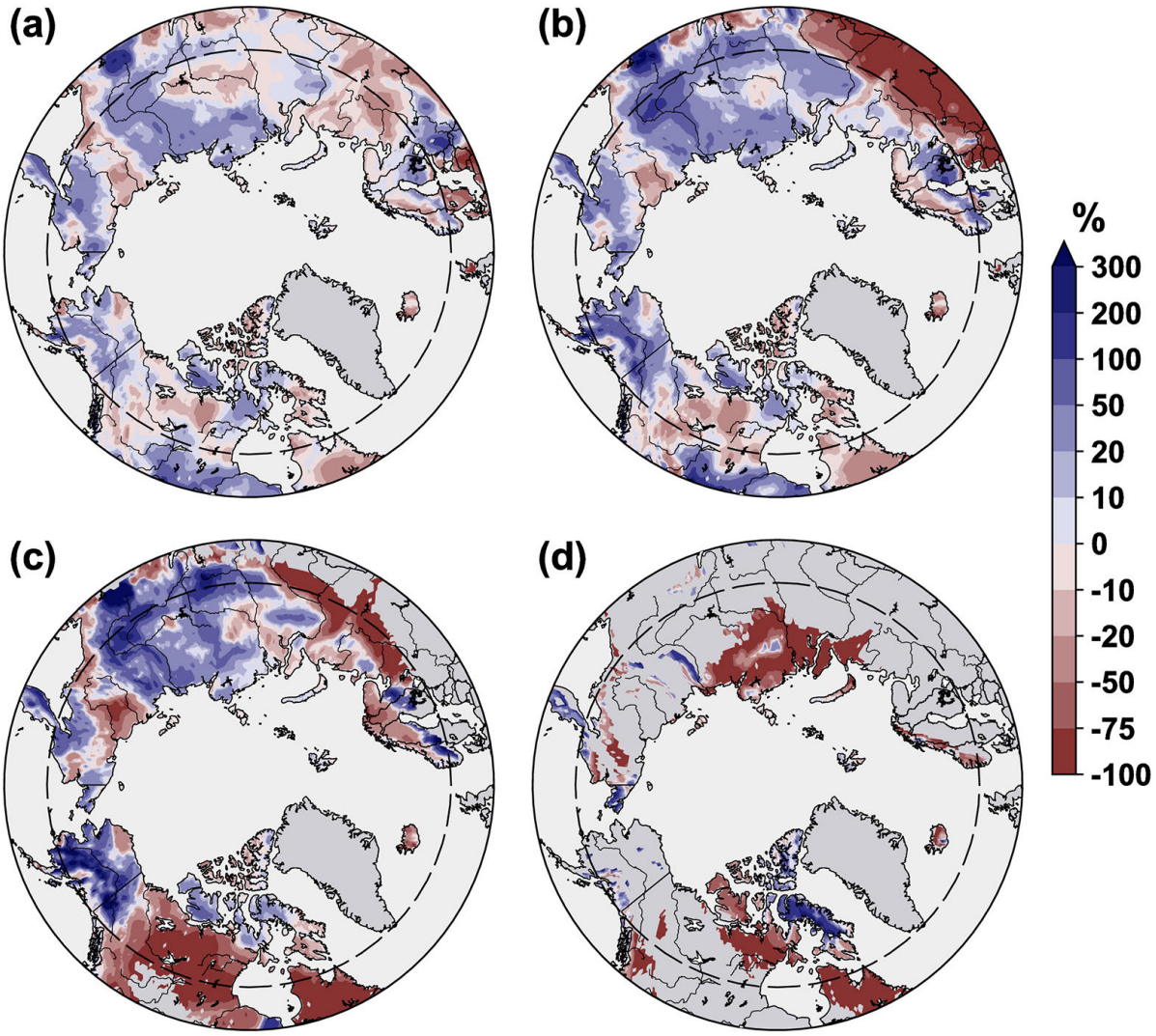

Fig. 4. Snow water equivalent (SWE) anomalies (% difference from the 1991-2020 average) in 2023 for (a) March, (b) April, (c) May, and (d) June. Anomalies represent the ensemble mean from a suite of four independent snow analyses (see *Methods and data*). The dashed circle marks the latitude 60° N. SWE over Greenland is not represented consistently among the data products and has been masked out.

Summary and long-term trends

Snow accumulation during the 2022/23 winter was above average across both continents, especially Eurasia. This allowed above normal SWE in some regions to persist into May (e.g., central Siberia and Alaska). However, intensive melt during spring across Arctic Canada resulted in a new record low May snow extent for the North American Arctic. Looking historically across Eurasia, the June snow extent values for 11 of the past 14 years represent near complete absence of snow cover across the continent except for residual amounts in higher elevation locations. Compared to historical conditions, this results in approximately two additional weeks of snow-free conditions before July. The more northernly location of the Canadian Arctic Archipelago prevents complete loss of snow extent until after June across the North American sector of the Arctic.

Methods and data

SCE anomalies are derived from the NOAA snow chart climate data record, which extends from 1967 to present (Estilow et al. 2015; Robinson et al. 2012). Monthly anomalies of total areal snow cover over land for a given Arctic sector (North America or Eurasia, > 60° N) are computed and standardized relative to the 1991-2020 period (each observation differenced from the mean and divided by the standard deviation and thus unitless).

SCD fields are derived from the NOAA daily Interactive Multisensor Snow and Ice Mapping System (IMS) snow cover product (U.S. National Ice Center 2008). Anomalies in the total number of days with snow cover were computed separately for each half of the snow season: August 2022 to January 2023, referred to as "onset period," and February 2023 to July 2023, referred to as "melt period." IMS availability starts in 1998, so a 1998/99 to 2017/18 climatological period is used (including information from August-December 1998 for snow onset). Anomalies for each season are presented as percent differences from the climatological number of snow-free days. In the Arctic, this varies from approximately three months near 60° N, to approximately two months at 70° N, and decreases to less than a month over the Canadian Arctic Archipelago. Because the Arctic is generally always snow covered between November and April, Arctic region snow onset anomalies are indicative of conditions during September and October, while Arctic region snow melt anomalies are indicative of conditions during May and June.

Four SWE data sets were used to generate multi-dataset SWE fields from March-June (inclusive) for the 1981-2023 period: (1) the European Space Agency Snow Climate Change Initiative (CCI) SWE version 2 product derived through a combination of satellite passive microwave brightness temperatures and climate station snow depth observations (Luojus et al. 2022); (2) the Modern-Era Retrospective Analysis for Research and Applications version 2 (MERRA-2, GMAO 2015; Gelaro et al. 2017) daily SWE fields; (3) SWE output from the ERA5-Land analysis (Muñoz Sabater 2019); and (4) the physical snowpack model Crocus (Brun et al. 2013) driven by ERA5 meteorological forcing. Limited availability of climate station snow data during May and June lowers the accuracy of the Snow CCI SWE product during these months; therefore, we only use it during March and April. An approach using gridded products is required because in situ observations alone are too sparse to capture snow conditions across the Arctic. We consider multiple datasets because averaging multiple SWE products has been shown to be more accurate than individual datasets when validated with in situ observations (Mortimer et al. 2020). The ensemble-mean SWE field is used to calculate monthly SWE anomalies relative to the 1991-2020 period, which are presented as percent differences. For April, the SWE fields for each product are also aggregated across Arctic land regions (> 60° N) for both North American and Eurasian sectors to produce multiple estimates of April snow mass. These monthly snow mass values are used to calculate standardized anomalies relative to the 1991-2020 period for each data product. The standardized anomalies are then averaged to produce an ensemble-mean time series.

Acknowledgments

ERA5-Land data (Muñoz Sabater 2019) was downloaded from the Copernicus Climate Change Service (C3S) Climate Data Store (2023). Neither the European Commission nor ECMWF is responsible for any use that may be made of the Copernicus information or data it contains.

References

Brown, R., and Coauthors, 2017: Arctic terrestrial snow cover. In: Snow, Water, Ice and Permafrost in the Arctic (SWIPA) 2017. pp. 25-64, Arctic Monitoring and Assessment Programme (AMAP), Oslo, Norway.

Brun, E., V. Vionnet, A. Boone, B. Decharme, Y. Peings, R. Valette, F. Karbou, and S. Morin, 2013: Simulation of Northern Eurasian local snow depth, mass, and density using a detailed snowpack model and meteorological reanalyses. *J. Hydrometeor.*, **14**, 203-219, https://doi.org/10.1175/JHM-D-12-012.1.

Estilow, T. W., A. H. Young, and D. A. Robinson, 2015: A long-term Northern Hemisphere snow cover extent data record for climate studies and monitoring. *Earth Syst. Sci. Data*, **7**, 137-142, https://doi.org/10.5194/essd-7-137-2015.

Gelaro, R., and Coauthors, 2017: The Modern-era retrospective analysis for research and applications, Version 2 (MERRA-2). *J. Climate*, **30**, 5419-5454, https://doi.org/10.1175/JCLI-D-16-0758.1.

GMAO (Global Modeling and Assimilation Office), 2015: MERRA-2tavg1_2d_lnd_Nx:2d, 1-Hourly, Time-Averaged, Single-Level, Assimilation, Land Surface Diagnostics V5.12.4, Goddard Earth Sciences Data and Information Services Center (GESDISC), accessed: 3 August 2023, https://doi.org/10.5067/RKPHT8KC1Y1T.

Luojus, K., and Coauthors, 2022: ESA Snow Climate Change Initiative (Snow_cci): Snow Water Equivalent (SWE) level 3C daily global climate research data package (CRDP) (1979 – 2020), version 2.0. NERC EDS Centre for Environmental Data Analysis, accessed: 27 August 2023, https://doi.org/10.5285/4647cc9ad3c044439d6c643208d3c494.

Meredith, M., and Coauthors, 2019: Polar Regions. IPCC Special Report on the Ocean and Cryosphere in a Changing Climate, H. -O. Pörtner, and co-editors, Cambridge University Press, Cambridge, UK and New York, NY, USA, 203-320, https://doi.org/10.1017/9781009157964.005.

Mortimer, C., L. Mudryk, C. Derksen, K. Luojus, R. Brown, R. Kelly, and M. Tedesco, 2020: Evaluation of long-term Northern Hemisphere snow water equivalent products. *Cryosphere*, **14**, 1579-1594, https://doi.org/10.5194/tc-14-1579-2020.

Muñoz Sabater, J., 2019: ERA5-Land hourly data from 1950 to present. Copernicus Climate Change Service (C3S) Climate Data Store (CDS), accessed: 3 October 2023, https://doi.org/10.24381/cds.e2161bac.

Robinson, D. A., T. W. Estilow, and NOAA CDR Program, 2012: NOAA Climate Data Record (CDR) of Northern Hemisphere (NH) Snow Cover Extent (SCE), Version 1 [r01]. NOAA National Centers for Environmental Information, accessed: 30 August 2023, https://doi.org/10.7289/V5N014G9.

U.S. National Ice Center, 2008: IMS Daily Northern Hemisphere Snow and Ice Analysis at 1 km, 4 km, and 24 km Resolutions, Version 1. Boulder, Colorado, USA. NSIDC: National Snow and Ice Data Center, accessed: 18 August 2023, https://doi.org/10.7265/N52R3PMC.

November 27, 2023

Precipitation

https://doi.org/10.25923/hcm7-az41

J. E. Walsh[1,2], S. Bigalke[3], S. A. McAfee[4], R. Lader[2], M. C. Serreze[5], and T. J. Ballinger[2]

[1]Alaska Center for Climate Assessment and Policy, University of Alaska Fairbanks, Fairbanks, AK, USA
[2]International Arctic Research Center, University of Alaska Fairbanks, Fairbanks, AK, USA
[3]Department of Geography, Portland State University, Portland, OR, USA
[4]Department of Geography, University of Nevada Reno, Reno, NV, USA
[5]National Snow and Ice Data Center, Cooperative Institute for Research in Environmental Sciences, University of Colorado Boulder, Boulder, CO, USA

Headlines

- Pan-Arctic mean precipitation from ERA5 for the 2022/23 water year ranked as sixth highest on record and was modestly above the 1991-2020 average in all seasons.
- Heavy precipitation events broke existing records at various locations across the Arctic.
- Notable regional anomalies during the 2022/23 water year included a wet winter over parts of Alaska, a dry spring over western Eurasia, a dry summer over northern Canada, and record rains in Scandinavia during August.

Introduction

Consistent with Arctic warming (see essay *Surface Air Temperature*), precipitation in the Arctic is increasing (Box et al. 2021). As shown in the 2022 Arctic Report Card and updated here (Fig. 1), the increase of pan-Arctic mean precipitation is apparent in all seasons (Walsh et al. 2022). However, trends in Arctic precipitation vary regionally (Ye et al. 2021; Yu and Zhong 2021) and interannual variability is large. These variations have important implications for wildfire season severity and for river and lake levels. Warming is also leading to a transition from solid to liquid precipitation in the warmer parts of the Arctic (Box et al. 2021), although the coldest areas of the Arctic are expected to see snowfall increases in the future (McCrystall et al. 2021; Bigalke and Walsh 2022).

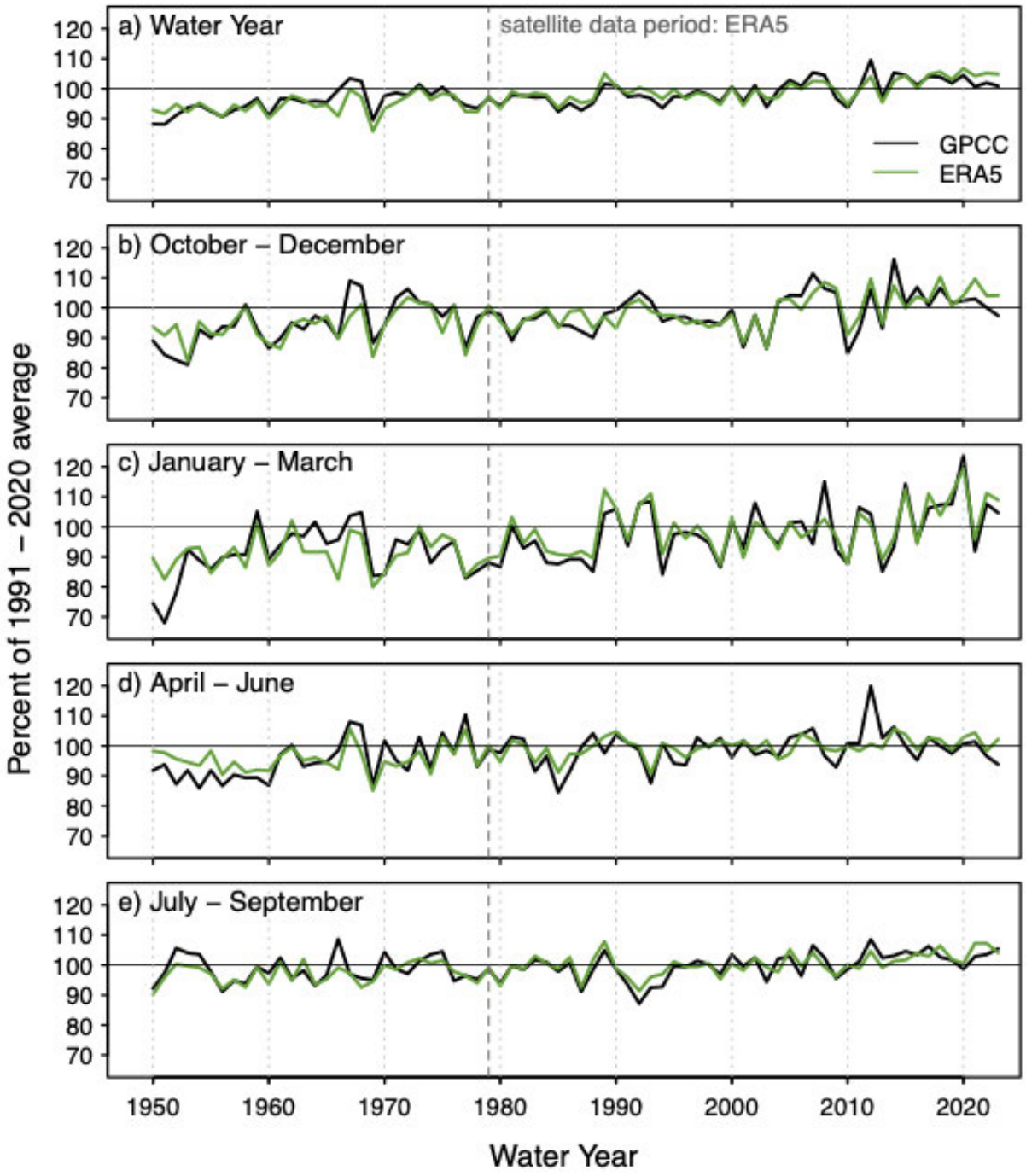

Fig. 1. Time series of Arctic (60-90° N) precipitation for water-years from 1951 through 2023 expressed as a percentage of the 1991-2020 average (the average, which is 100%, is shown by the horizontal black lines). Results are from ERA5 (green lines) and GPCC 1.0° data (black lines). GPCC values are for land only; ERA5 values are for land plus ocean. Seasonal time series are for (a) OND, (b) JFM, (c) AMJ, and (d) JAS. The GPCC full data product is used through 2020. The ERA5 monitoring product is used for January 2021-September 2023.

2022/23 water year precipitation at a glance

The Arctic experienced notable precipitation anomalies in the 2022/23 water year. The prominent features were (1) a continuation of the trend towards wetter conditions on the pan-Arctic scale, (2) large seasonal anomalies, including a wet winter in parts of Alaska, a dry spring in much of western Eurasia and over the northern North Atlantic, and a dry summer over much of northern Canada, (3) shorter-duration heavy precipitation that broke existing records at various locations within the Arctic (which is not necessarily surprising in a statistical sense given the large area being considered).

Overall, pan-Arctic (north of 60° N) precipitation for the 2022/23 water year in the ERA5 reanalysis was the sixth highest in the 74-year period that began in 1950. The Arctic autumn (October-December), winter (January-March), spring (April-June), and summer (July-September) all ranked among the 12 wettest of their corresponding seasons in the post-1950 period.

Figure 2 shows the ERA5-derived seasonal departures of precipitation during the 2022/23 water year from the 1991-2020 means. For the October-December (OND) period, a dipole pattern is apparent over the North Atlantic subarctic, with positive precipitation anomalies from the U.K. to southern Norway and negative anomalies from Iceland southwest to the Canadian maritime provinces. This pattern coincides with strong positive sea level pressure anomalies over Greenland and northeastern Canada, with negative pressure anomalies west of the U.K. (see essay *Surface Air Temperature*, Fig. 3a). Positive precipitation anomalies over the Bering Sea are supported by southwesterly gradient wind anomalies associated with strong low-pressure anomalies over eastern Siberia. According to the NOAA National Centers for Environmental Centers (NCEI) (NOAA 2023a, 2023b) analysis, Alaska's North Slope region experienced its fourth wettest autumn of the past 98 years, consistent with the gradient wind anomaly and the late-season persistence of open water over the Chukchi Sea. However, this regional precipitation feature is not captured in the ERA5 reanalysis.

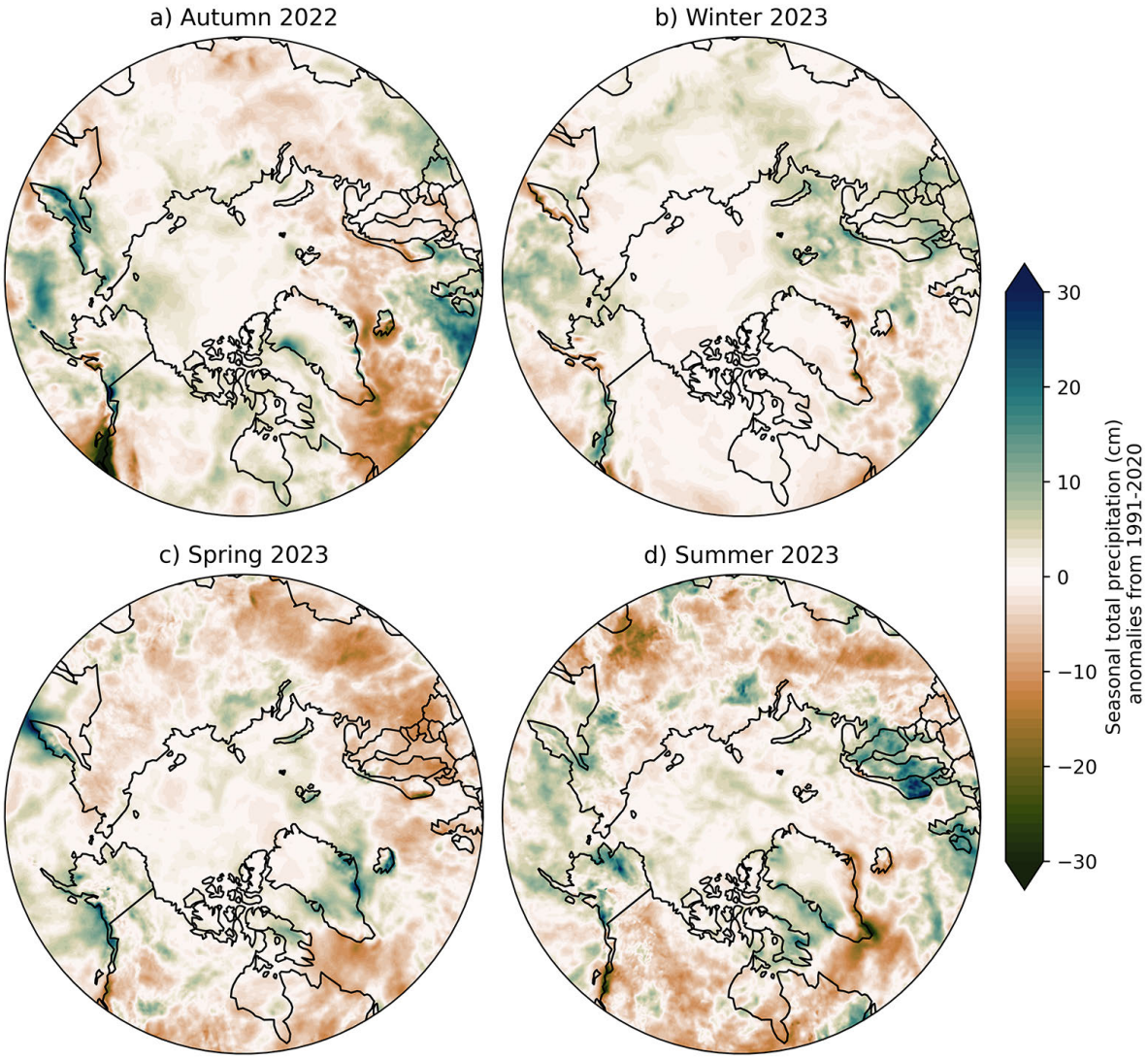

Fig. 2. Seasonal departures of precipitation from the 1991-2020 climatological means for (a) autumn (OND) 2022, (b) winter (JFM) 2023, (c) spring (AMJ) 2023, and (d) summer 2023 (JAS). Green shades denote above-normal precipitation, brown shades denote below-normal precipitation. Data source: ERA5 reanalysis.

Winter (JFM) precipitation anomalies were generally weak, except for above-normal precipitation in the Bering Sea, the Svalbard region, and south of Iceland. As in the OND season, the wetter-than-normal conditions in the Bering Sea were a consequence of abnormally low pressure north and west of the Bering Sea (see essay *Surface Air Temperature*, Fig. 3b). According to the NOAA NCEI analysis, Alaska's West Coast climate region had its second wettest winter in its 99-year period of record. Negative pressure anomalies also extended from Svalbard southeastward to northern Europe during the month of March. During this time, station data showed much above-average precipitation, including some record amounts for March, in a broad east-west band from northern Europe across to northeastern Asia.

A notable feature of the April-June (AMJ) period was a precipitation deficit over northern land areas, including much of Canada and a broad Eurasian region extending from Scandinavia to eastern Russia. The dry conditions were especially prevalent during May in both northern Europe and Canada, setting

the stage for the severe wildfire season in Canada. High pressure anomalies over western Eurasia drove the precipitation deficit in Europe, while high temperatures driven by warm advection contributed to the dry conditions in regions of Canada (see essay *Surface Air Temperature*, Fig. 3c). Meanwhile, Alaska was generally wetter than normal with below-normal temperatures (see essay *Surface Air Temperature*, Fig. 2c). Parts of the Greenland Ice Sheet saw high precipitation in the form of snow in June (see essay *Greenland Ice Sheet*).

Finally, July-September (JAS) 2023 was notable for above-average precipitation over northern Europe, including flood-producing rains in early August. Most of Alaska saw above-average precipitation, as did western Greenland and southern Baffin Island. By contrast, precipitation was well below average southeast of Greenland, over southeastern Russia and along the panhandle of Alaska. Below-average precipitation was widespread over much of Eurasia and Canada. Portions of Northwest Territories, Canada were analyzed in severe to extreme drought during August and September (NOAA North American Drought Monitor), and this contributed to wildfires that continued through late summer in the Northwest Territories (see *Arctic Wildfire Sidebar*).

Historical perspective

The time series in Fig. 1 introduced earlier compares seasonal precipitation from ERA5 and the station-based dataset of the Global Precipitation Climatology Center (GPCC) during 1950-2023. The GPCC dataset is for land only, while ERA5 covers ocean areas as well as land. The seasonal and annual values are plotted as percentages of the corresponding 1991-2020 averages. In all four seasons of the 2022/23 water year the ERA5 values are greater than the 1991-2020 averages. GPCC indicates slightly below-average precipitation in OND and AMJ, and slightly above normal precipitation in JFM and JAS. While the JFM value is less than the previous year's value, it is still 9% higher than the 1991-2020 average, consistent with the positive trend in cold season Arctic precipitation discussed in the 2022 Arctic Report Card (Walsh et al. 2022). Of particular note is that the water-year total has exceeded the 1991-2020 mean in 15 of the past 20 years, including 2022/23.

Heavy precipitation events

Heavy precipitation events continued in 2022/23. In addition to the extreme seasonal totals noted earlier for several Alaska climate regions from NCEI, based on station data Anchorage set a new record for December precipitation, including the most December snowfall in more than 60 years. Elsewhere, the above-normal summer precipitation in northern Europe included heavy rains in early August. The heaviest rains in 25 years occurred in southern Norway, where water levels and pressure caused a dam to break along Norway's largest river. Extensive flooding was also reported in Sweden, and the impacts of the heavy rain event extended southward to Denmark and Lithuania. It appears that a rare weather pattern involving two cyclones was responsible for the event.

Figure 3 provides a pan-Arctic perspective on the heavy precipitation events of 2022/23 from ERA5 by showing the ranks (relative to the 1950-2022 historical period) of the maximum 5-day precipitation events (Rx5) in each season of the 2022/23 water year. During autumn (OND), record or near record (2nd or 3rd highest) events occurred in parts of the North American Arctic and the Beaufort and Chukchi Seas. That the known record December precipitation and snowfall in Anchorage does not reveal itself in the OND plot may reflect the local nature of the event. The winter (JFM) distribution shows a broad swath of heavy events across northern Europe and north-central Russia. However, this later feature

does not show up in the winter seasonal anomaly plot (Fig. 2); this is also true of the heavy precipitation feature over the Arctic Ocean in winter. The spring (AMJ) pattern shows only small isolated areas of heavy precipitation, most notable over Greenland. While heavy precipitation for summer (JAS) as a whole was also spotty in coverage, the August pattern from ERA5 (not shown) features a prominent area over Northern Europe where heavy precipitation and damaging flooding were observed; this is readily seen in the summer anomaly map of total precipitation (Fig. 2).

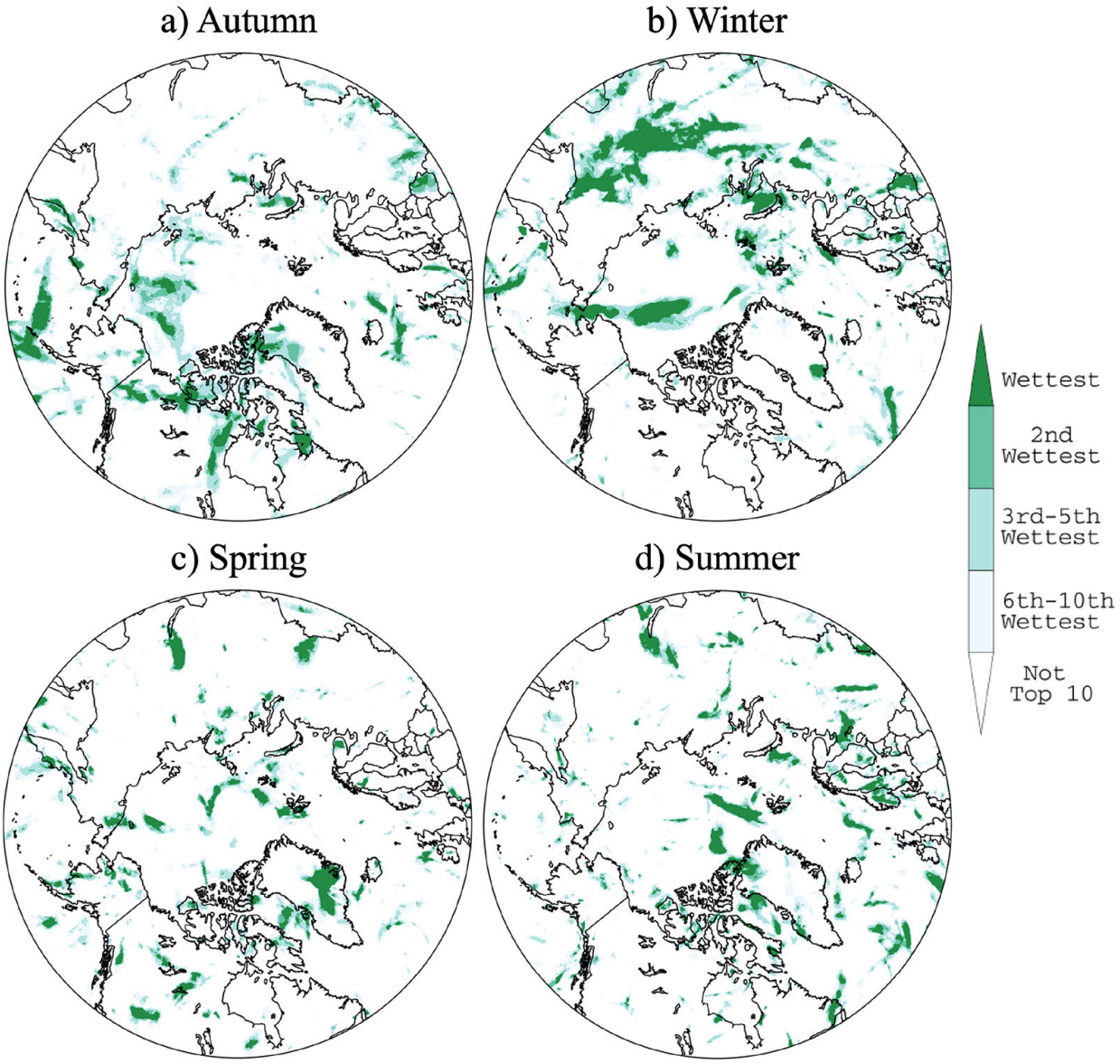

Fig. 3. Ranks of maximum 5-day precipitation for each season during water year 2022/23: (a) autumn (OND), (b) winter (JFM), (c) spring (AMJ), and (d) summer (JAS). Data source: ERA5 reanalysis, 1950-present.

Methods and data

Because of the challenges of gauge measurements in the Arctic, we make use of gridded precipitation fields from both the ERA5 atmospheric reanalysis of the European Centre for Medium Range Weather Forecasts (ECMWF) (Hersbach at al. 2020) and the Global Precipitation Climatology Centre's GPCC V.

2022 (Becker et al. 2013). ERA5 data are available from January 1940 onwards, but the quality of the output is more reliable starting in 1979 (Hersbach et al. 2020), after which modern satellite data are assimilated into the analysis and forecast system. ERA5 is the latest atmospheric reanalysis effort, and performs slightly better than other atmospheric reanalyses at matching observed precipitation totals from extreme events in the Arctic (Loeb et al. 2022). Given the model-derived nature of ERA5, comparisons are made with the GPCC's Full Data Product, a monthly gridded gauge-based product available from 1891 onwards (Schneider et al. 2022). Our comparisons of the time series of pan-Arctic precipitation computed from these two sources is limited to the post-1950 period because both products were impacted by missing data during the World War II period. We also use records from the NOAA NCEI analysis (NOAA 2023a, 2023b).

References

Becker, A., P. Finger, A. Meyer-Christoffer, B. Rudolf , K. Schamm, U. Schneider, and M. Ziese, 2013: A description of the global land-surface precipitation data products of the Global Precipitation Climatology Centre with sample applications including centennial (trend) analysis from 1901-present. *Earth Sys. Sci. Data*, **5**(1), 71-99, https://doi.org/10.5194/essd-5-71-2013.

Bigalke, S., and J. E. Walsh, 2022: Future changes of snow in Alaska and the Arctic under stabilized global warming scenarios. *Atmosphere*, **13**, 541, https://doi.org/10.3390/atmos13040541.

Box, J. E, and Coauthors, 2021: Recent developments in Arctic climate observation indicators. In AMAP Arctic Climate Change Update 2021: Key Trends and Impacts. Arctic Monitoring and Assessment Programme (AMAP), Tromso, Norway, 7-29 pp.

Hersbach, H, B., and Coauthors, 2020: The ERA5 global reanalysis. *Quart. J. Roy. Meteor. Soc.*, **146**, 1999-2049, https://doi.org/10.1002/qj.3803.

Loeb N.A., A. Crawford, J. C. Stroeve, and J. Hanesiak, 2022: Extreme precipitation in the eastern Canadian Arctic and Greenland: An evaluation of atmospheric reanalyses. *Front. Env. Sci.*, **10**, 866929, https://doi.org/10.3389/fenvs.2022.866929.

McCrystall, M. R., J. Stroeve, M. C. Serreze, B. C. Forbes, and J. A. Screen, 2021: New climate models reveal faster and larger increases in Arctic precipitation than previously projected. *Nat. Commun.*, **12**(1), 6765, https://doi.org/10.1038/s41467-021-27031-y.

NOAA National Centers for Environmental Information, 2023a: Climate at a Glance: Divisional Rankings, published September 2023, retrieved on 4 October 2023, https://www.ncei.noaa.gov/access/monitoring/climate-at-a-glance/divisional/rankings.

NOAA National Centers for Environmental Information, 2023b: North American Drought Monitor, retrieved 13 November 2023, https://www.ncei.noaa.gov/access/monitoring/nadm/maps.

Schneider, U., P. Finger, E. Rustemeier, M. Ziese, and S. Hänsel, 2022: Global precipitation analysis products of the GPCC, https://opendata.dwd.de/climate_environment/GPCC/PDF/GPCC_intro_products_v2022.pdf.

Walsh, J. E., S. Bigalke, S. A. McAfee, R. Lader, M. C. Serreze, and T. J. Ballinger, 2022: Precipitation. *Arctic Report Card 2022,* M. L. Druckenmiller, R. L. Thoman, and T. A. Moon, Eds., https://doi.org/10.25923/yxs5-6c72.

Ye, H., D. Yang, A. Behrangi, S. L. Stuefer, X. Pan, E. Mekis, Y. Dibike, and J. E. Walsh, 2021: Precipitation Characteristics and Changes. Chapter 2 in Arctic Hydrology, Permafrost and Ecosystems (D. Yang and D. L. Kane, Eds.), Springer Nature Switzerland, 25-59, https://doi.org/10.1007/978-3-030-50930-9.

Yu, L., and S. Zhong, 2021: Trends in Arctic seasonal and extreme precipitation in recent decades. *Theor. Appl. Climatol.*, **145**, 1541-1559, https://doi.org/10.1007/s00704-021-03717-7.

November 17, 2023

Greenland Ice Sheet

https://doi.org/10.25923/yetx-rs76

K. Poinar[1], K. D. Mankoff[2,3], R. S. Fausto[4], X. Fettweis[5], B. D. Loomis[6], A. Wehrlé[7], C. D. Jensen[8], M. Tedesco[9], J. E. Box[4], and T. L. Mote[10]

[1]University at Buffalo, Buffalo, NY, USA
[2]Goddard Institute of Space Studies, NASA, New York, NY, USA
[3]Autonomic Integra, New York, NY, USA
[4]Geological Survey of Denmark and Greenland, Copenhagen, Denmark
[5]SPHERES Research Unit, University of Liège, Liège, Belgium
[6]Goddard Space Flight Center, NASA, Greenbelt, MD, USA
[7]Department of Geography, University of Zurich, Zurich, Switzerland
[8]Danish Meteorological Institute, Copenhagen, Denmark
[9]Lamont-Doherty Earth Observatory, Columbia Climate School, Columbia University, Palisades, NY, USA
[10]Department of Geography, University of Georgia, Athens, GA, USA

Headlines

- Winter snow accumulation was above average this year, but the Greenland Ice Sheet still lost 156 ± 22 Gt of mass from 1 September 2022 to 31 August 2023 because discharge and melting exceeded accumulation.
- Summer high-pressure systems brought warm temperatures, widespread melting, and exceptional rainfall volumes.
- On 26 June 2023, Summit Station reached a temperature of 0.4°C and experienced melt for only the fifth time in its 34-year observational history.

Introduction

The Greenland Ice Sheet (GrIS) is the second-largest contributor of sea-level rise (SLR), after thermal expansion (Zemp et al. 2019). Ice mass loss from the GrIS affects environments and societies worldwide through coastal erosion, saltwater intrusion, habitat loss, increased flooding, and, in some locations, permanent inundation. In every year since 1998, the GrIS has lost mass overall. In the one-year period from 1 September 2022 to 31 August 2023, the GRACE-FO (Gravity Recovery and Climate Experiment Follow-on) satellite mission measured a total GrIS mass balance of -156 ± 22 Gt (mean ± 1 st. dev.), the equivalent of ~0.4 mm SLR (Fig. 1). This loss was 60 Gt (28%) less than the 2002-23 GrIS yearly average of -216 ± 8 Gt measured by GRACE/GRACE-FO.

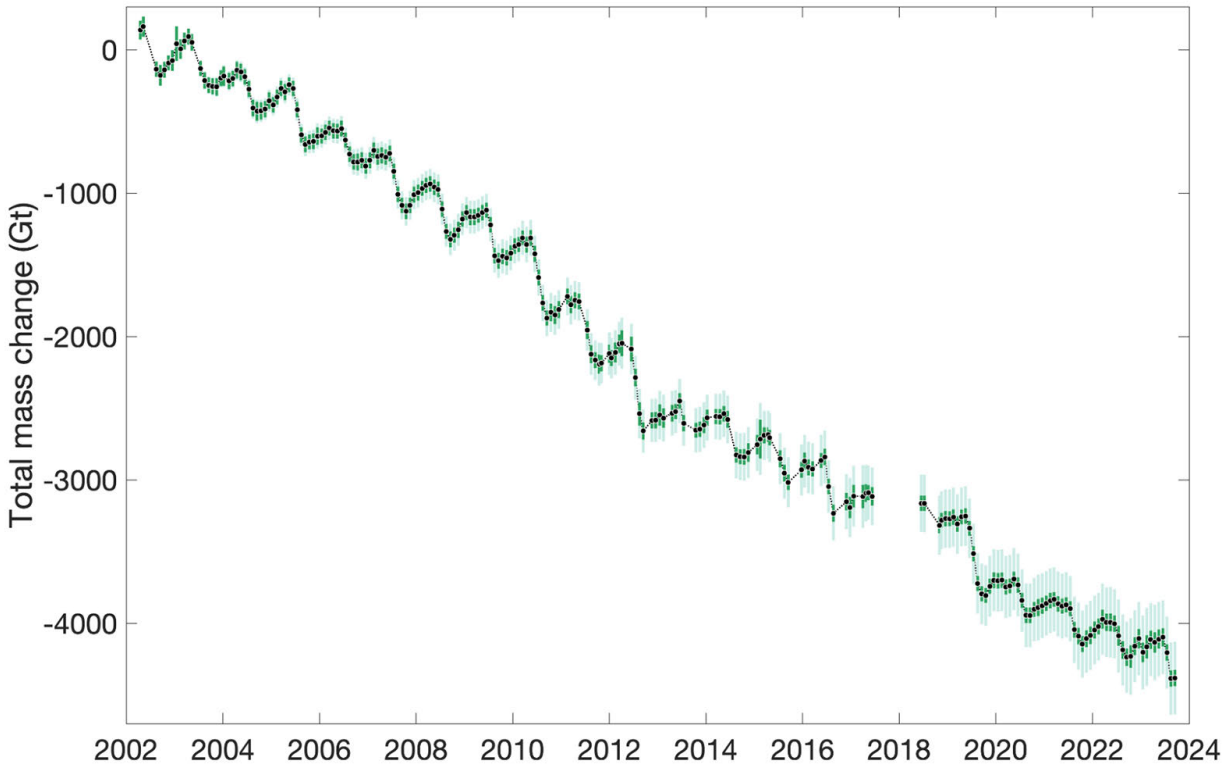

Fig. 1. GRACE-based mass balance. Total mass change, in gigatons (Gt), of the GrIS from April 2002 through September 2023 determined from the satellite gravimetry missions GRACE (2002-17) and GRACE-FO (2018-present) (Tapley et al. 2019). Black circles show monthly estimates, with 2-st. dev. uncertainties shown with (light green) and without (dark green) errors due to leakage of external signals (i.e., mass changes near Greenland but not associated with the GrIS). The time series has been scaled by 0.84 to remove the peripheral glaciers and ice caps from the GRACE-based estimates.

Surface mass balance

Ice sheets gain mass from net snow accumulation and lose mass through meltwater runoff and solid ice discharge. The sum of accumulation and runoff is termed surface mass balance (SMB) and is primarily responsive to air temperature, snow cover, albedo, and bare-ice area. We summarize in-situ and satellite observations that influenced SMB over the 2023 mass balance year, 1 September 2022 through 31 August 2023, and report them relative to the 1991-2020 climatology unless otherwise stated.

We report monthly mean air temperatures measured at up to 32 weather stations in Greenland (see *Methods and data*). During autumn (SON 2022), temperatures were predominantly higher than average. At Summit Station, the autumn average was a record high of -23.2°C, a +7.4°C anomaly. Record-high temperatures were observed at seven stations along the west coast and Summit Station in September, and at three stations in southeast Greenland in November. Winter 2022/23 (DJF) and spring 2023 (MAM) had less remarkable temperature patterns. Most stations recorded temperatures close to or slightly below average during winter, and close to or slightly above average during spring. At Summit Station, the air temperature was slightly below average in winter (-0.9°C anomaly) and average in spring. There was generally above-average snow accumulation, but this was regionally variable. Accumulation near the coasts in southern and northeastern Greenland was slightly below average.

Cooler-than-average conditions characterized the beginning of the melt season at most weather stations. In the last week of June, however, a high-pressure system associated with the negative phase of the North Atlantic Oscillation arrived abruptly and persisted for four weeks. Its warm air incited multiple melt events across the ice sheet: the mean July temperature reached a record high of -7.3°C, which was a +4.4°C anomaly and was almost 2°C warmer than the previous record from 2012.

The total number of melt days across the GrIS (Fig. 2a) was above average virtually everywhere, and especially in northwest, northeast, and South Greenland, which experienced >20 more melt days than average. The cumulative melt-day area (Fig. 2b) was the second largest on record, at ~70% of the value from the 2012 record melt year and 5.7 times greater than the 1981-2010 average.

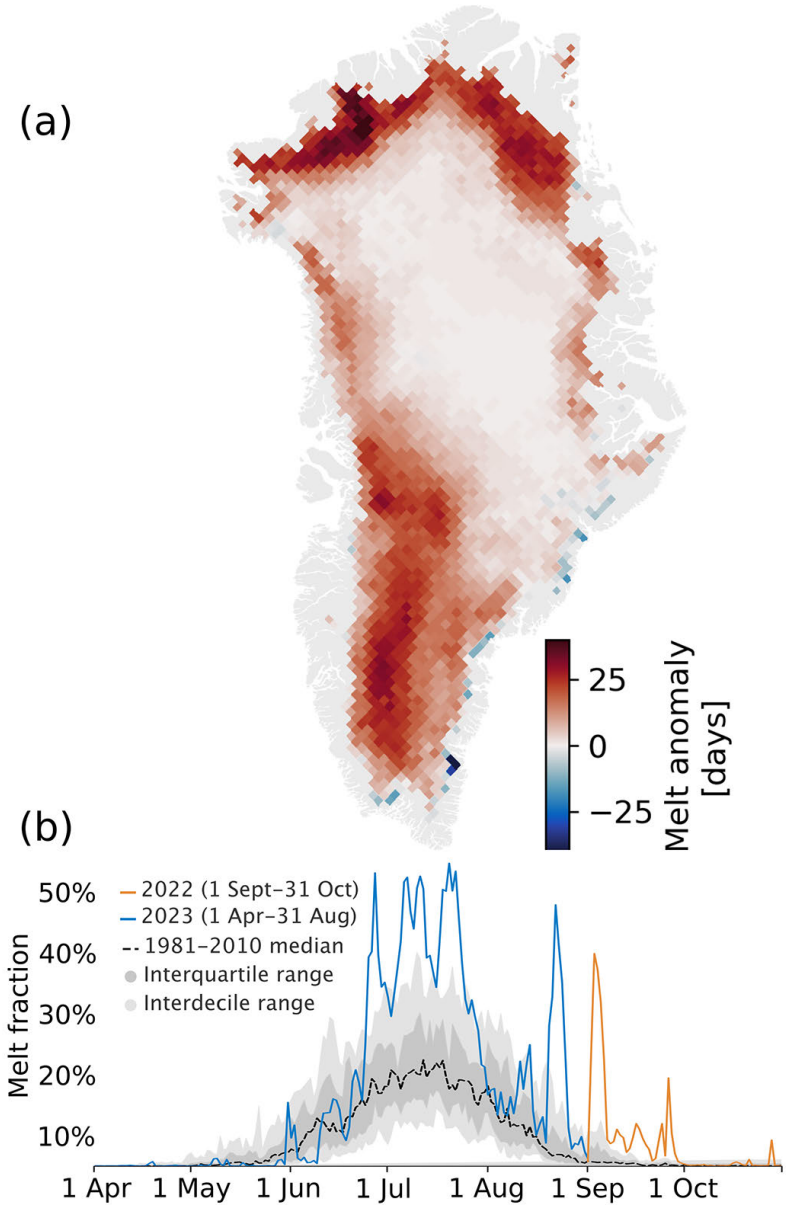

Fig. 2. (a) Number of surface melt days in 2023 from 1 April to 31 August, expressed as an anomaly with respect to the 1991-2020 period from daily Special Sensor Microwave Imager/Sounder (SSMIS) 37 GHz horizontally polarized passive microwave radiometer satellite data (Mote 2007). (b) Surface melt extent as a percentage of the ice sheet area during 2023 (blue) and autumn 2022 (orange) derived from SSMIS.

The generally mild winter conditions paired with the late-summer warmth yielded low melt-season (JJA) albedo, or broad-spectrum brightness (Fig. 3a), and high bare-ice area, especially in the lower accumulation zone and across southern and northeastern Greenland. The 2023 spatially averaged albedo ranked fifth lowest over the 2000-23 period covered by MODIS (Fig. 3b). The seasonal evolution of the albedo and bare-ice area proceeded similarly to the surface temperatures and melt. The ice sheet emerged from winter conditions later than average; early June showed the lowest bare-ice area measured in the 7-year Sentinel-3 observational record (Fig. 3c). For illustration, the bare-ice area measured on 15 June 2023 was only one tenth of that observed on 15 June 2019, a high-melt year. With the onset of high air pressures at the end of June, the bare-ice area increased rapidly, peaked on 23 July, and decreased through 8 August, when a large-areal melt event occurred (see *Notable melt episodes*). This pushed the bare-ice area to its seasonal maximum on 26 August. The summer albedo anomaly (Fig. 3a) was low (dark) across North and South Greenland, reaching -0.14 on the Qassimiut lobe. Across much of western Greenland, the albedo was higher (brighter) than normal at low elevations and lower (darker) than normal at higher elevations, over snow. This pattern coincided with a negative (cool) anomaly in summer 2-meter air temperature at low elevations and a positive (warm) anomaly at higher elevations.

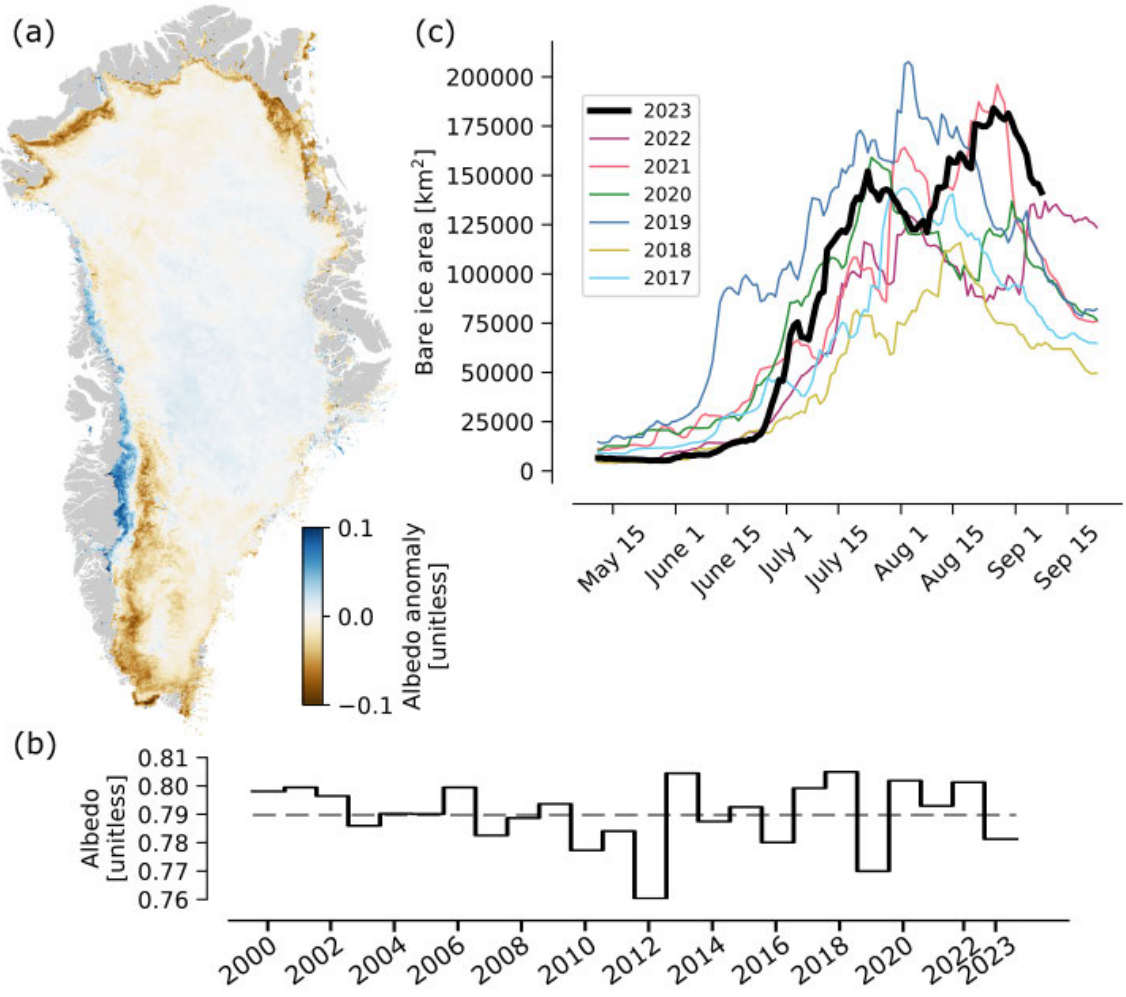

Fig. 3. (a) Albedo anomaly for summer (JJA) 2023 measured from Sentinel-3 data, relative to summers 2017-22 (Wehrlé et al. 2021). (b) Time series for average GrIS summer albedo since 2000, from MODIS, with dashed gray line showing mean of 0.79. (c) Bare ice area measured from Sentinel-3 observations, with 2023 in bold black (Wehrlé et al. 2021).

Overall, the 2023 melt season ablation (ice melt) measured across eight Programme for Monitoring of the Greenland Ice Sheet (PROMICE) weather transects on the ice sheet (Fig. 4) was within 20% of the average at most stations. Exceptions occurred in the northwestern sector, where 2.2 meters of net ablation (87% more than average) was measured at Thule, and at Upernavik, where 1.6 meters (32% less than average) was measured. These full-summer values point to the combined effects of the cooler June and warmer July and August yielding overall near-average ablation at coastal locations.

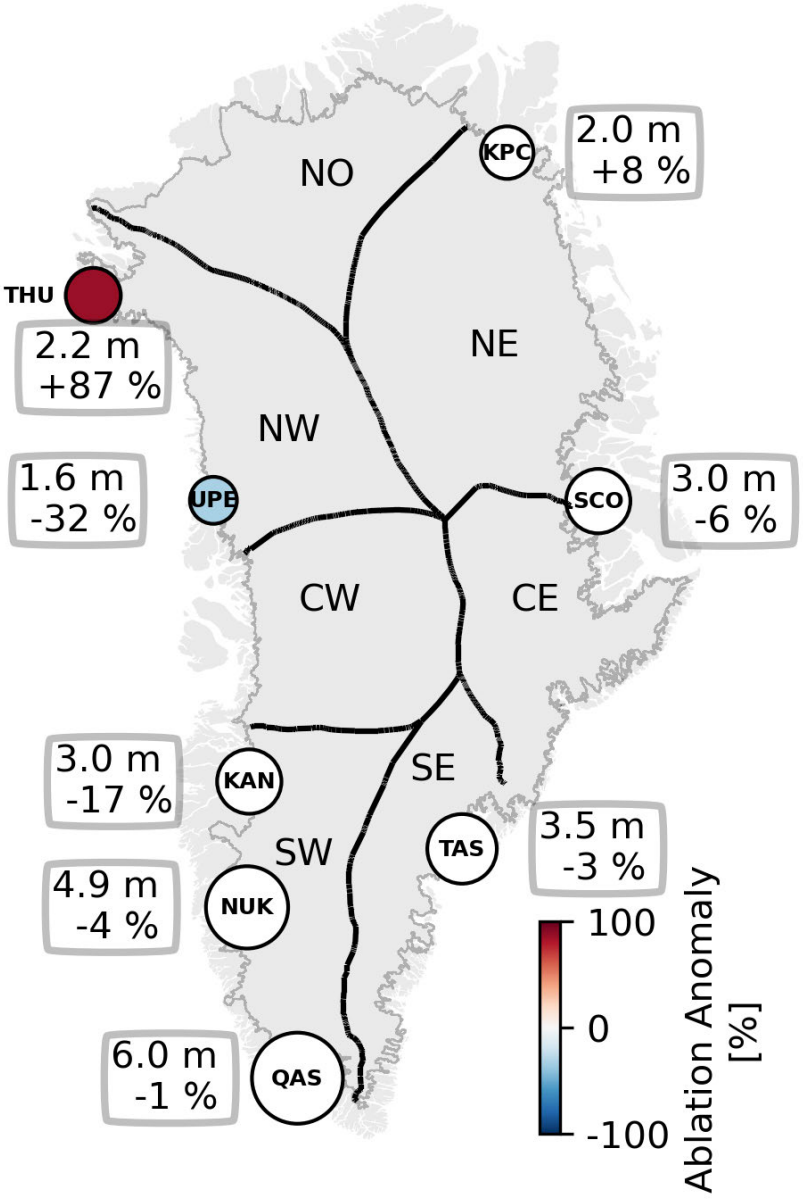

Fig. 4. Net ice ablation for 2023 (top number) measured by PROMICE weather transects and referenced to the 1991-2020 period (bottom percent). Circle sizes are scaled to net ablation and colored according to the anomaly value. White circles indicate anomaly values within methodological and measurement uncertainty. Transects: Thule (THU), Upernavik (UPE), Kangerlussuaq (KAN), Nuuk (NUK), Qassimiut (QAS), Tasiliiq (TAS), Scoresby Sund (SCO), and Kronprins Christians Land (KPC). Ice sheet regions: North (NO), Northeast (NE), Northwest (NW), Central East (CE), Central West (CW), Southeast (SE), and Southwest (SW) are referenced in Fig. 5.

Rainfall over the GrIS during the 2023 mass balance year was exceptional, more than 4 standard deviations above the mean. This was largely due to very high rainfall volumes in September 2022 and above-average rainfall in summer (JJA) 2023. As an example, the PROMICE weather station NUK_U, at 1100 m a.s.l., recorded 44 summer days with rainfall, totaling 140 mm.

In summary, ice discharge (see below) and basal mass balance for the 2023 hydrologic year from 1 September 2022 through 31 August 2023 were -504 ± 47 Gt and -27 ± 6 Gt, respectively (Mankoff et al. 2021). The total mass balance measured by GRACE/GRACE-FO was -156 ± 22 Gt, which yields a SMB of 375 ± 52 Gt. This derived SMB is slightly above regional climate model estimates of 240-395 Gt for the 2023 hydrologic year and is above the SMB climatology of 325 ± 29 Gt (mean ± 1 st. dev.) derived from daily regional climate model output summed annually and averaged over 1991-2020 (Fettweis et al. 2020; Mankoff et al. 2021).

Solid ice discharge

Discharge of solid ice decreases the overall mass balance of the ice sheet. This discharge occurs from the hundreds of marine-terminating glaciers that ring the GrIS and drain ice into the ocean. These glaciers are grouped by sector (see Fig. 4), each with several dozen glaciers, for regional pattern identification. In the 2023 calendar year, the glaciers in southeast (SE) Greenland discharged ice at the highest rate (145 ± 15 Gt/yr), although this has been slowing since the 2020 peak of 155 ± 17 Gt/yr (Fig. 5). The slowing trend since 2020 is fairly consistent across the SE region. Though this may seem to conflict with the above-average sea surface temperatures in the region (see essay *Sea Surface Temperature*), it is subsurface water temperatures that primarily affect glacier discharge (e.g., Wood et al. 2018).

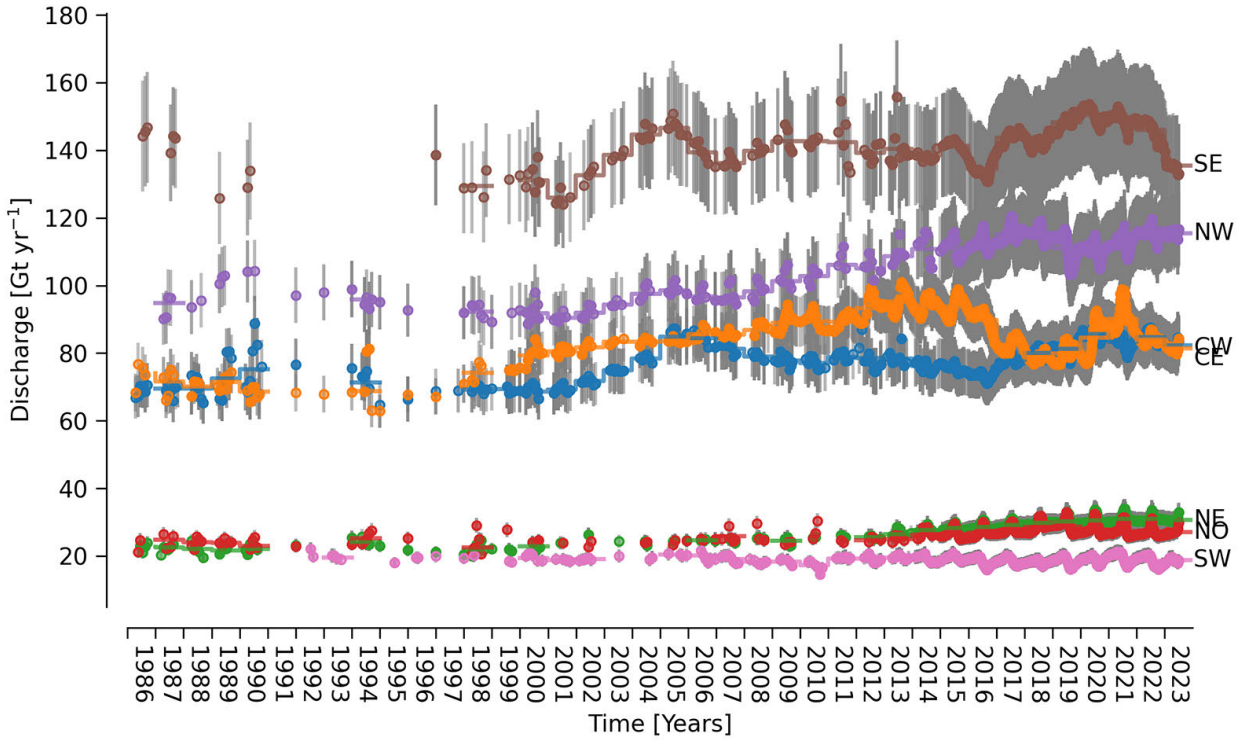

Fig. 5. Solid ice discharge (Gt yr^{-1}; gray bars show ±10% uncertainty range) by region (see Fig. 4). Source: PROMICE (Mankoff et al. 2020).

The SE discharge decrease was partially offset by increases in the northwest (NW), Central East (CE), and northeast (NE). Across the entire GrIS, glaciers discharged ice at 489 ± 47 Gt/yr in 2023, which is within measurement uncertainties of the recent average of 497 ± 47 Gt/yr since 2013, but is likely below the 2020 peak of 513 ± 48 Gt/yr. The 2023 discharge rate falls below, but is within measurement uncertainties of, the recent trend of increasing discharge at +2.4 Gt/yr per year (1991-2020).

Notable melt episodes

The 2023 mass balance year began with a high-pressure system over southern Greenland. On 3 September 2022, SSMIS satellite sensors (see *Methods and data*) observed melt conditions on 36% of the ice-sheet surface (592,000 km^2), an unprecedented extent for September. A second late-season melt event occurred later in the month when warm air associated with the aftermath of Hurricane Fiona reached Greenland: on 26 September 2022, the melt area peaked at 15% of the ice-sheet surface (245,000 km^2). Both melt episodes coincided with significant rainfall events.

Another notable melt event occurred during an extended period of high pressure in August 2023. The high-pressure dome pulled southerly winds up the west coast to the northern ice divide, from where the air flowed back south and descended along the ice-sheet surface to the east coast. The compression induced by the descent caused warm, dry conditions along the north and east coasts; PROMICE stations there recorded temperatures as high as 16°C above the seasonal average.

Record melt rates and high temperatures across the upper elevations

In a single week in July, ablation lowered the ice-sheet surface at South Dome (elevation 2893 m a.s.l.) by 40 cm, a record pace of melt at that inland location. Summit Station (3216 m a.s.l.) reached a temperature of 0.4°C on 26 June; this was only the fifth time in the 34-year observational record that the air temperature at Summit has surpassed 0°C. (The fourth time occurred on 3 September 2022, described above.) On 22 August 2023, during the high-pressure period described above, the temperature at Summit Station reached -0.6°C.

Methods and data

The GRACE (Gravity Recovery and Climate Experiment, 2002-17) and GRACE-FO (Follow On, 2018-present) satellite missions detect gravity anomalies to measure changes in total ice mass (technical notes: podaac-tools.jpl.nasa.gov/drive/files/allData). The GRACE/GRACE-FO source data include ice-sheet-peripheral glaciers and ice masses that are not part of the GrIS. We scale these numbers by 0.84 to approximate changes only on the GrIS (Colgan et al. 2015).

Weather data are directly obtained from 20 Danish Meteorological Institute (DMI) land-based weather stations with records starting from 1784 (Nuuk), 11 stations owned by Mittarfeqarfiit A/S, which operates airports and helipads, and data from Summit Station. NOAA GEOSummit has supplied data from Summit since 2019; we extend this to 1991 using the DMI station at Summit. Eight automatic weather station transects from the Programme for Monitoring of the Greenland Ice Sheet (PROMICE) at the Geological Survey of Greenland and Denmark (GEUS) provide temperatures and surface ablation measurements, following van As et al. (2016).

Surface melt duration and extent are derived from daily Special Sensor Microwave Imager/Sounder (SSMIS) 37 GHz, horizontally polarized passive microwave radiometer satellite data (Mote 2007).

Albedo monitoring since 2000 is from NASA MODIS satellite data (Box et al. 2017). The bare ice area is monitored using the Sentinel-3 SICE product (Kokhanovsky et al. 2020; Wehrlé et al. 2021).

PROMICE combines ice thickness estimates with ice velocity measurements based on Sentinel-1 satellite data to create a Greenland-wide, time-evolving solid-ice discharge product integrated over Greenland (Mankoff et al. 2020).

Acknowledgments

K. Mankoff was supported by the NASA Modeling Analysis and Prediction program. M. Tedesco was supported by National Science Foundation OPP 1713072, OPP 2136938, and PLR-1603331, National Aeronautics and Space Administration (NASA) 80NSSC20K1254, and Heising-Simons Foundation 2019-1160. T. Mote was supported by National Science Foundation #1900324. Data from the Programme for Monitoring of the Greenland Ice Sheet (PROMICE) were provided by the Geological Survey of Denmark and Greenland (GEUS) at www.promice.dk. Sentinel-3 SICE data processing via PolarView.org was enabled by the European Space Agency (ESA) Network of Resources Initiative. Summit Station is owned and operated by the National Science Foundation Office of Polar Programs with permission from the Government of Greenland.

References

Box, J. E., D. van As, and K. Steffen, 2017: Greenland, Canadian and Icelandic land-ice albedo grids (2000-2016). *GEUS Bull.*, **38**, 53-56, https://doi.org/10.34194/geusb.v38.4414.

Colgan, W., and Coauthors, 2015: Hybrid glacier Inventory, Gravimetry and Altimetry (HIGA) mass balance product for Greenland and the Canadian Arctic. *Remote Sens. Environ.*, **168**, 24-39, https://doi.org/10.1016/j.rse.2015.06.016.

Fettweis, X., and Coauthors, 2020: GrSMBMIP: intercomparison of the modelled 1980-2012 surface mass balance over the Greenland Ice Sheet. *Cryosphere*, **14**, 3935-3958, https://doi.org/10.5194/tc-14-3935-2020.

Kokhanovsky, A., J. E. Box, B. Vandecrux, K. D. Mankoff, M. Lamare, A. Smirnov, and M. Kern, 2020: The determination of snow albedo from satellite measurements using fast atmospheric correction technique. *Remote Sens.*, **12**, 234, https://doi.org/10.3390/rs12020234.

Mankoff, K. D., A. Solgaard, W. Colgan, A. P. Ahlstrøm, S. A. Khan, and R. S. Fausto, 2020: Greenland ice sheet solid ice discharge from 1986 through March 2020. *Earth Syst. Sci. Data*, **12**, 1367-1383, https://doi.org/10.5194/essd-12-1367-2020.

Mankoff, K. D., and Coauthors, 2021: Greenland ice sheet mass balance from 1840 through next week. *Earth Syst. Sci. Data*, **13**, 5001-5025, https://doi.org/10.5194/essd-13-5001-2021.

Mote, T. L., 2007: Greenland surface melt trends 1973-2007: Evidence of a large increase in 2007. *Geophys. Res. Lett.*, **34**, L22507, https://doi.org/10.1029/2007GL031976.

Tapley, B. D., and Coauthors, 2019: Contributions of GRACE to understanding climate change. *Nat. Climate Change*, **9**, 358-369, https://doi.org/10.1038/s41558-019-0456-2.

van As, D., R. S. Fausto, J. Cappelen, R. S. van de Wal, R. J. Braithwaite, H. Machguth, and PROMICE project team, 2016: Placing Greenland ice sheet ablation measurements in a multi-decadal context. *GEUS Bull.*, **35**, 71-74, https://doi.org/10.34194/geusb.v35.4942.

Wehrlé, A., J. E. Box, M. Niwano, A. M. Anesio, and R. S. Fausto, 2021: Greenland bare-ice albedo from PROMICE automatic weather station measurements and Sentinel-3 satellite observations. *GEUS Bull.*, **47**, 5284, https://doi.org/10.34194/geusb.v47.5284.

Wood, M., E. Rignot, I. Fenty, D. Menemenlis, R. Millan, M. Morlighem, J. Mouginot, and H. Seroussi, 2018: Ocean-induced melt triggers glacier retreat in Northwest Greenland. *Geophys. Res. Lett.*, **45**, 16, 8334-8342, https://doi.org/10.1029/2018GL078024.

Zemp, M., and Coauthors, 2019: Global glacier mass changes and their contributions to sea-level rise from 1961 to 2016. *Nature*, **568**, 382-386, https://doi.org/10.1038/s41586-019-1071-0.

November 21, 2023

Sea Ice

https://doi.org/10.25923/f5t4-b865

W. N. Meier[1], A. Petty[2], S. Hendricks[3], L. Kaleschke[3], D. Divine[4], S. Farrell[5], S. Gerland[4], D. Perovich[6], R. Ricker[7], X. Tian-Kunze[3], and M. Webster[8]

[1]National Snow and Ice Data Center, Cooperative Institute for Research in Environmental Sciences, University of Colorado Boulder, Boulder, CO, USA
[2]Earth System Science Interdisciplinary Center, University of Maryland, College Park, MD, USA
[3]Alfred Wegener Institute, Helmholtz Centre for Polar and Marine Research, Bremerhaven, Germany
[4]Norwegian Polar Institute, Fram Centre, Tromsø, Norway
[5]Department of Geographical Sciences, University of Maryland, College Park, MD, USA
[6]Thayer School of Engineering, Dartmouth College, Hanover, NH, USA
[7]NORCE Norwegian Research Centre, Tromsø, Norway
[8]Polar Science Center, Applied Physics Laboratory, University of Washington, Seattle, WA, USA

Headlines

- Sea ice extent was 6th lowest in the satellite record (1979 to present) and downward trends continue; the last 17 September extents (2007-23) are the 17 lowest in the record.
- The amount of multiyear ice was largely unchanged from 2022, as multiyear extent remained far lower than in the 1980s, with minimal old ice (>4 years old).
- Average sea ice thickness for the 2022/23 winter was lower than the previous winter, near the 2011-23 average; volume at the end of the 2022/23 winter was the same as the previous year.

Introduction

Arctic sea ice is the frozen interface between the ocean and the atmosphere. It reduces the absorption of solar energy because of its high albedo relative to the darker open ocean surface. In addition, as a physical barrier, it modifies the heat and moisture transfer between the atmosphere and ocean. Sea ice plays a key role in the ecosystem, providing an essential habitat for marine life and modulating the biogeochemical balance of the Arctic. The sea ice cover has long played a practical and cultural role in Indigenous communities of the north. Sea ice historically limited national and corporate activities in the Arctic, but decreased ice cover is influencing commercial transportation, resource extraction, and national security.

The winter 2022/23 freeze-up was typical of recent years with sea ice growth rates near average while the areal coverage remained in the lowest 10% extent (below the lower interdecile range) through the year. Ice growth was particularly slow in the Barents and Kara Seas as well as in the Chukchi Sea, but near normal in other regions. Winter near-surface air temperatures were higher than the 1991-2020 average over most of the Arctic Ocean, particularly in the Barents Sea and portions of the Beaufort Sea (see essay *Surface Air Temperature*). However, lower temperatures prevailed over much of the Eurasian side of the Arctic during spring. Summer temperatures were mixed, with higher-than-average temperatures over the Barents, Kara, Beaufort, and Chukchi Seas and average or slightly below average temperatures elsewhere.

Sea ice extent

One of the most commonly used indicators of long-term Arctic sea ice conditions is sea ice extent, which is defined as the total area covered by ice of at least 15% concentration. The primary source of extent observations is the 45-year record (starting in 1979) derived from satellite-borne passive microwave sensors.

This satellite record tracks long-term trends, variability, and seasonal changes from the annual extent maximum in late February or March and the annual extent minimum in September. Extents in recent years are ~50% lower than values in the 1980s. In 2023, March and September extents were lower than other recent years (Fig. 1), and though not a new record low, they continue the long-term downward trends (Table 1). March 2023 was marked by low sea ice extent around most of the perimeter of the sea ice edge, with the exception of the East Greenland Sea where extent was near normal (Fig. 2). At the beginning of the melt season, ice retreat was initially fairly slow through April. In May and June, retreat increased to a near-average rate, and then accelerated further through July and August. By mid-July, the ice had retreated from much of the Alaskan and eastern Siberian coast and Hudson Bay had nearly melted out completely. In August, sea ice retreat was particularly pronounced on the Pacific side, opening up vast areas of the Beaufort, Chukchi, and East Siberian Seas. Summer extent remained closer to average on the Atlantic side, in the Laptev, Kara, and Barents Seas (Fig. 2).

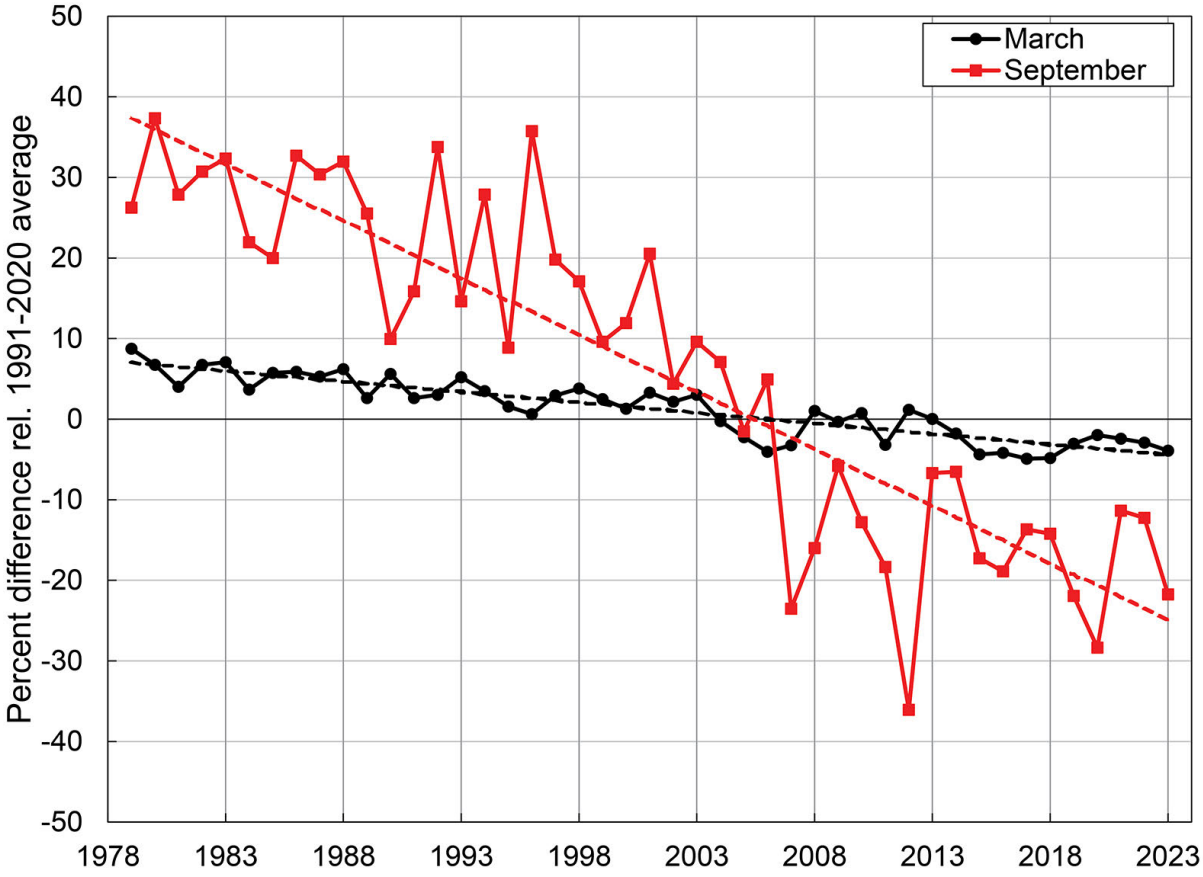

Fig. 1. Monthly sea ice extent anomalies (solid lines) and linear trend lines (dashed lines) for March (black) and September (red) 1979 to 2023. The anomalies are relative to the 1991-2020 average for each month (see Table 1).

Table 1. March and September monthly averages and annual daily maximum and minimum extent for 2023 and related statistics. The rank is from least sea ice to most sea ice of the 45-year record (starting in 1979) (1 = least, 45 = most).

Values	**March** Monthly Average	**March** Daily Maximum	**September** Monthly Average	**September** Daily Minimum
Extent (10^6 km^2)	14.44	14.62	4.37	4.23
Rank (out of 45 years)	6	5	5	6
1991-2020 average (10^6 km^2)	15.03	15.26	5.58	5.37
Anomaly rel. **1991-2020** average (10^6 km^2)	-0.59	-0.64	-1.21	-1.14
Trend, 1979-2022 (km^2/yr)	-39,100	-41,200	-78,500	-77,600
% change from 1979 linear trend value	-10.2	-10.7	-43.0	-43.1

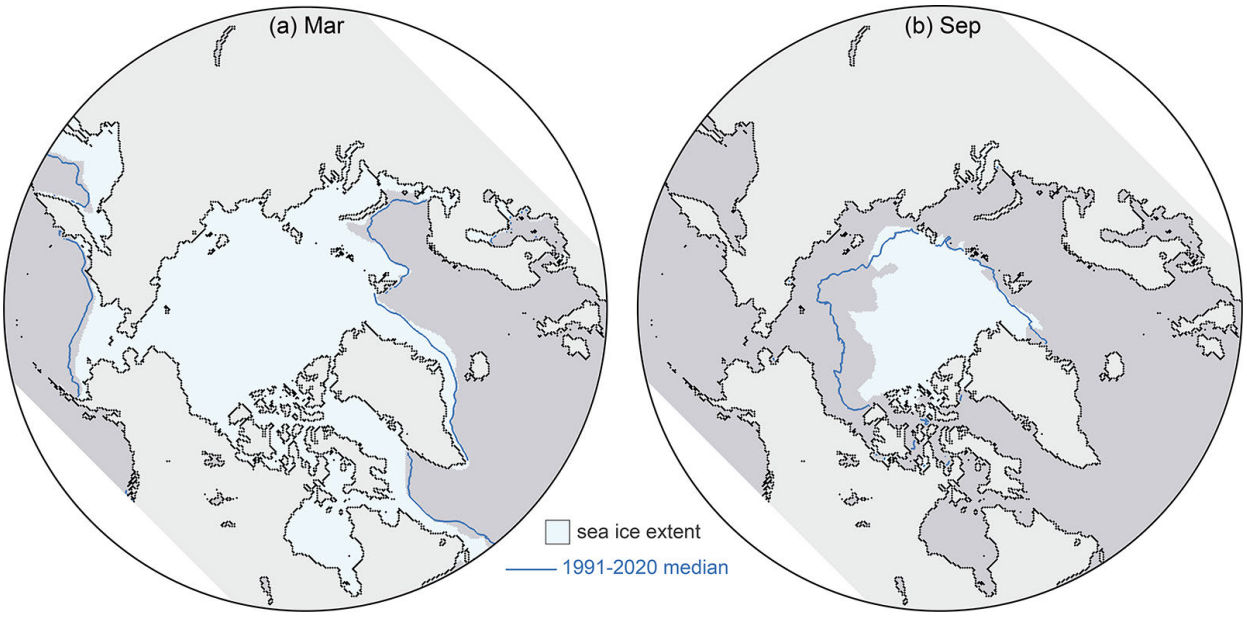

Fig. 2. Monthly average sea ice extent (light blue) for (a) March 2023, and (b) September 2023. The median extent for 1991-2020 is shown by the dark blue contour.

The Northern Sea Route, along the northern Russian coast, was relatively slow to open as sea ice extended to the coast in the eastern Kara Sea and the East Siberian Sea, but by late August, open water was found along the coast through the entire route. The Northwest Passage through the Canadian Archipelago became relatively clear of ice, though ice continued to largely block the western end of the northern route through M'Clure Strait through the melt season. Nonetheless, summer 2023 extent in the Passage was among the lowest observed in the satellite record, based on Canadian Ice Service ice charts (ASINA 2023).

Sea ice age

Tracking the motion of ice in passive microwave imagery using feature tracking algorithms can be used to infer sea ice age. Age is a proxy for ice thickness because multiyear ice generally grows thicker through successive winter periods. Multiyear ice extent has shown interannual oscillations but no clear trend since 2007, reflecting variability in the summer sea ice melt and export out of the Arctic. After a year when substantial multiyear ice is lost, a much larger area of first-year ice generally takes its place. Some of this first-year ice can persist through the following summer, contributing to the replenishment of the multiyear ice extent. However, old ice (here defined as >4 years old) has remained consistently low since 2012. Thus, unlike in earlier decades, multiyear ice does not remain in the Arctic for many years. At the end of the summer 2023 melt season, multiyear ice extent was similar to 2022 values (Fig. 3), far below multiyear extents in the 1980s and 1990s.

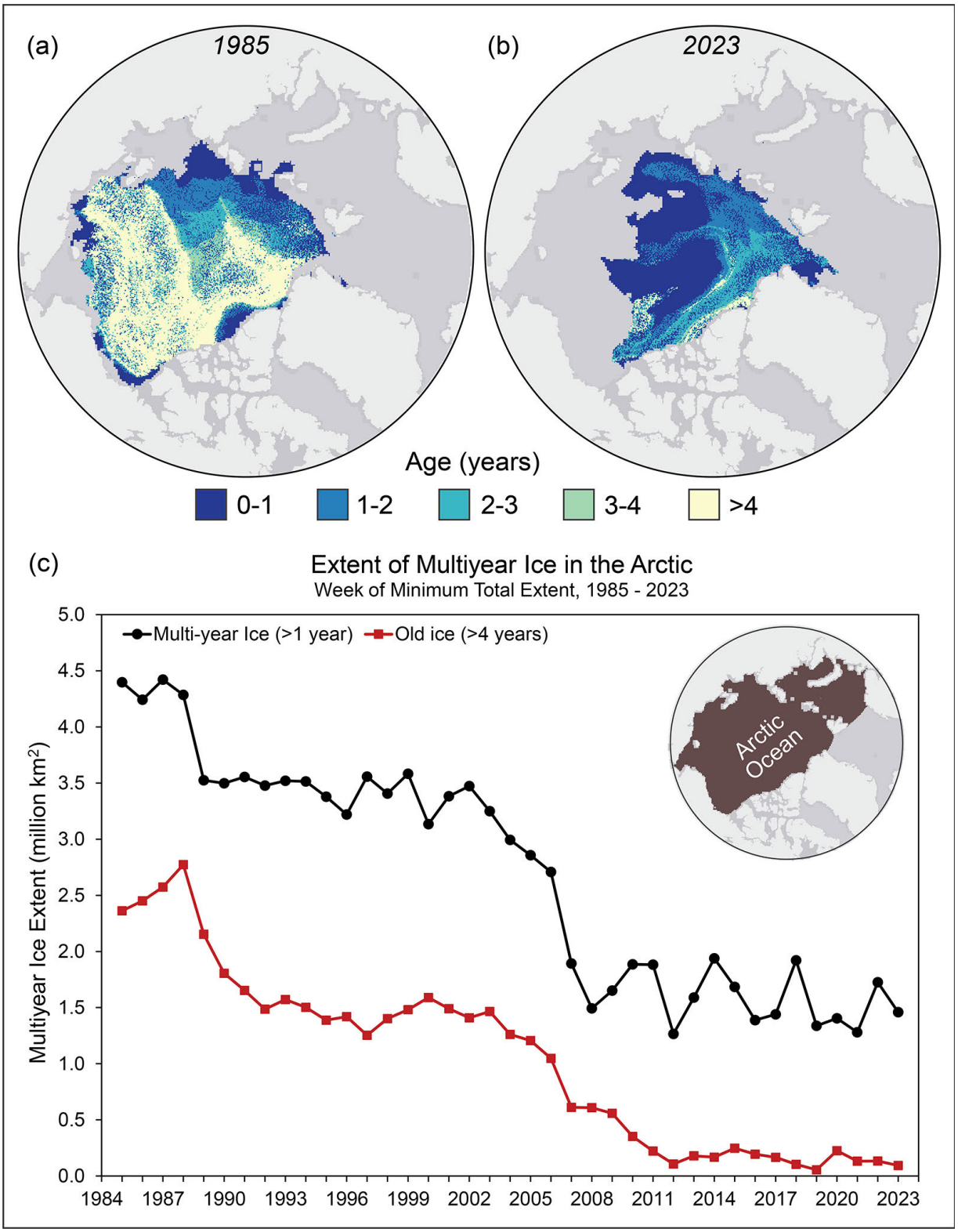

Fig. 3. Sea ice age coverage map for the week before minimum total extent (when age values are incremented to one year older) in (a) 1985, and (b) 2023; (c) extent of multiyear ice (black) and ice >4 years old (red) within the Arctic Ocean region (inset) for the week of the minimum total extent.

Sea ice thickness and volume

Estimates of sea ice thickness from satellite altimetry can be used to more directly track this important metric of sea ice conditions, although the data record is shorter than for extent and ice age. Data from ICESat-2 and CryoSat-2/SMOS satellite products tracking the seasonal October to April winter ice growth over the past four years (when all missions have been in operation) show a mean thickness generally thinner than the 2021/22 winter but with seasonal growth typical of recent winters (Fig. 4a). April 2023 thickness (Fig. 4b) from CryoSat-2/SMOS relative to the 2011-22 April mean (Fig. 4c) shows that the eastern Beaufort Sea and the East Siberian Sea had relatively thinner sea ice than the 2011-22 mean, particularly near the Canadian Archipelago. Thickness was higher than average in much of the Laptev and Kara Seas and along the west and northwest coast of Alaska, extending northward toward the pole. The East Greenland Sea had a mixture of thicker and thinner than average ice.

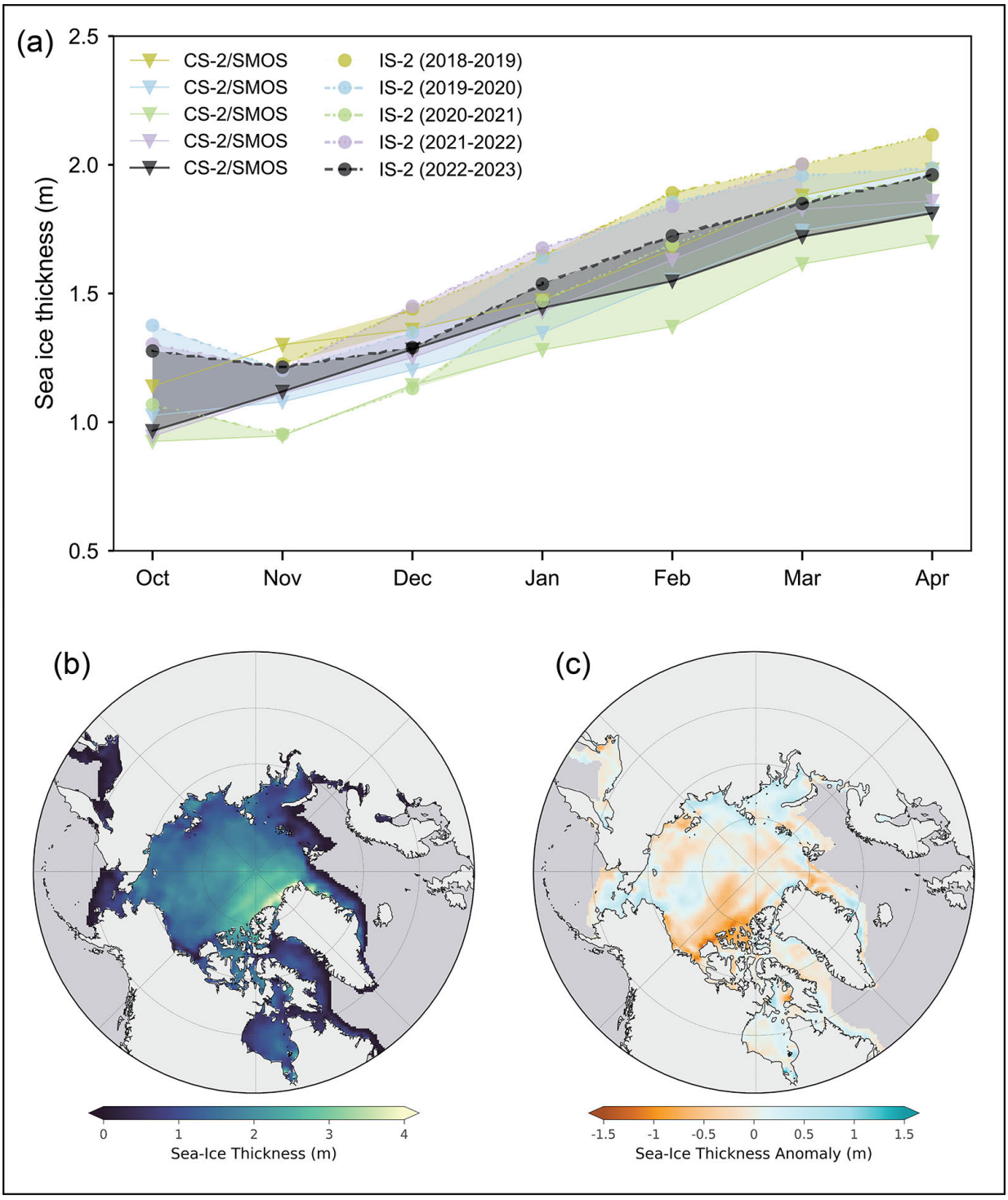

Fig. 4. (a) October through April monthly average sea ice thickness, calculated over an Inner Arctic Ocean Domain (Central Arctic, Beaufort, Chukchi, Laptev, East Siberian Seas), from ICESat-2 (circles) and CryoSat-2/SMOS (triangles) for 2018-19 (olive), 2019-20 (blue), 2020-21 (green), 2021-22 (lilac), and 2022-23 (black); (b) average April 2023 sea ice thickness map from CryoSat-2/SMOS; (c) CryoSat-2/SMOS thickness anomaly map (relative to the 2010-22 average).

Sea ice thickness estimates from moored instruments monitoring the sea ice continuously from below the ocean surface complement the satellite-derived products and give unique insights on the long-term

development of sea ice. Data from Norwegian Polar Institute upward looking sonars, installed in Fram Strait since the early 1990s, revealed that a regime shift of sea ice drifting out of the Arctic Ocean occurred in 2007; the region transitioned from thicker deformed ice to thinner, more uniform sea ice; this shift can be explained by more rapid export of ice from the Arctic Ocean (Sumata et al. 2023).

Sea ice thickness is integrated with ice concentration to provide winter volume estimates for the CryoSat-2/SMOS measurement time period. Seasonal change, from winter maximum to summer minimum and back, shows the strong seasonal cycle and interannual variability (Fig. 5). There is little indication of a trend through the relatively short 12-year time series. Volume gain through the 2022/23 growth season of 12,900 km^3 was within the range of earlier years in the record and balanced the volume loss during the summer 2022 melt season.

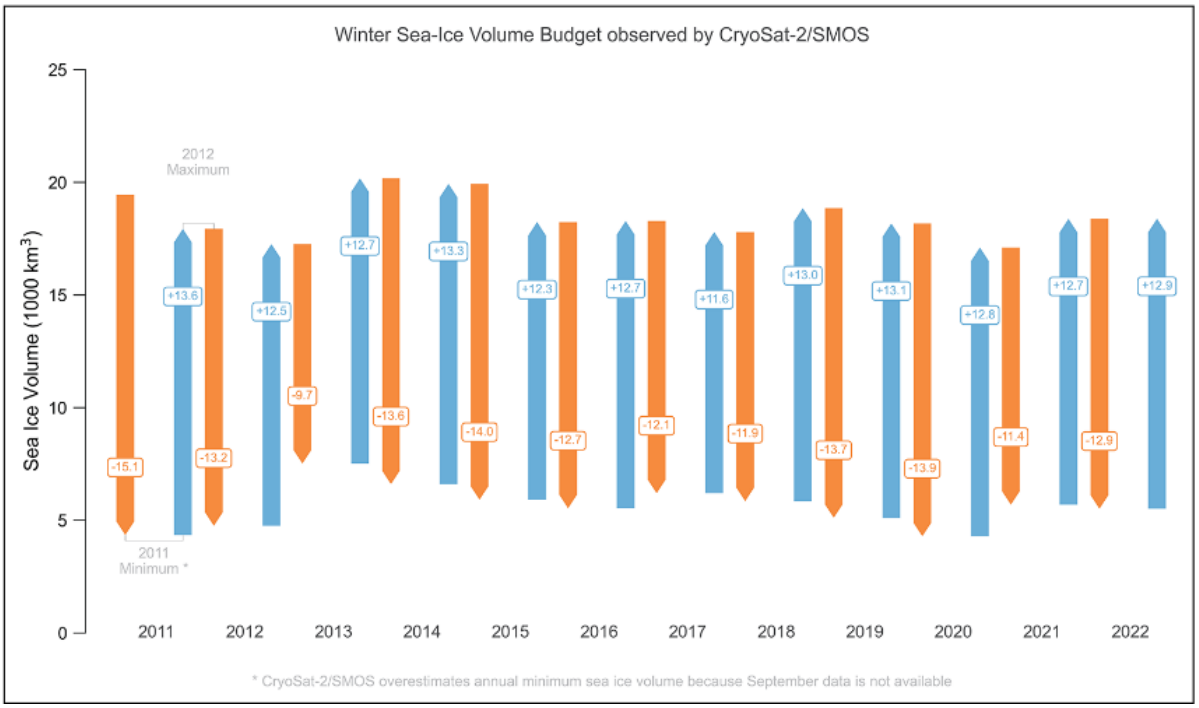

Fig. 5. Annual sea ice volume loss (orange) and gain (blue) between annual maximum and minimum from CrySat-2/SMOS. Numbers in orange and blue indicate the total volume change (gain or loss) in smaller font with signed values.

Methods and data

Sea ice extent values are from the NSIDC Sea Ice Index (Fetterer et al. 2017), based on passive microwave derived sea ice concentrations from the NASA Team algorithm (Cavalieri et al. 1996; Maslanik and Stroeve 1999), though other quality products exist (e.g., Lavergne et al. 2019).

Sea ice age data are from the EASE-Grid Sea Ice Age, Version 4 (Tschudi et al. 2019b) and Quicklook Arctic Weekly EASE-Grid Sea Ice Age, Version 1 (Tschudi et al. 2019a) archived at the NASA Snow and Ice Distributed Active Archive Center (DAAC) at NSIDC. Age is calculated via Lagrangian tracking of ice parcels using weekly sea ice motion vectors. Age is generally a proxy for thickness because older ice is typically thicker, via thermodynamic growth and potential dynamic thickening (i.e., ridging and rafting). Only the oldest age category is preserved for each grid cell.

Satellite altimetry has enabled the continuous retrieval of sea ice thickness and volume estimates over the entire Arctic basin during the freezing season, starting with the ESA CryoSat-2 radar altimeter, launched in 2010. This was followed in September 2018 by the launch of the NASA Ice, Cloud, and land Elevation 2 (ICESat-2) laser altimeter. Thus, there are now two independent altimetry-based thickness and volume estimates.

Weekly CryoSat-2 estimates have been combined with thin ice (<1 m) estimates from the ESA Soil Moisture Ocean Salinity (SMOS) instrument, launched in 2009, to obtain an optimal estimate across thin and thick ice regimes (Ricker et al. 2017) on a 25 km resolution EASE2 grid. Optimal interpolation is used to fill in data gaps in the weekly CryoSat-2 fields and to merge the CryoSat-2 and SMOS estimates. The results here are from Version 205. When combined with sea ice concentration, the CryoSat-2/SMOS record of ice thickness is used to compute sea ice volume; data are available at ftp://ftp.awi.de/sea_ice/product/cryosat2_smos/.

The ICESat-2 thickness data (Petty et al. 2022) used here are the gridded 25 km x 25 km monthly data originally presented in Petty et al. (2020), now using Version 5 ATL10 freeboards from the three strong beams of ICESat-2 and v1.1 NESOSIM snow loading (depth and density) as described in Petty et al. (2023).

Acknowledgments

W. Meier thanks the NSIDC DAAC and the NASA ESDIS project for support. Northwest Passage image and analysis from Stephen Howell, Environment and Climate Change Canada.

References

ASINA (Arctic Sea Ice News & Analysis), 2023: “Late summer heat wave avoids central Arctic”, National Snow and Ice Data Center, accessed 6 September 2023, https://nsidc.org/arcticseaicenews/2023/09/late-summer-heat-wave-arctic/.

Cavalieri, D. J., C. L. Parkinson, P. Gloersen, and H. J. Zwally, 1996 (updated yearly): Sea Ice Concentrations from Nimbus-7 SMMR and DMSP SSM/I-SSMIS Passive Microwave Data, Version 1. NASA National Snow and Ice Data Center Distributed Active Archive Center, Boulder, CO, USA, accessed 12 September 2023, https://doi.org/10.5067/8GQ8LZQVL0VL.

Fetterer, F., K. Knowles, W. N. Meier, M. Savoie, and A. K. Windnagel, 2017 (updated daily): Sea Ice Index, Version 3. NSIDC: National Snow and Ice Data Center, Boulder, CO, USA, accessed 12 September 2023, https://doi.org/10.7265/N5K072F8.

Lavergne, T., and Coauthors, 2019: Version 2 of the EUMETSAT OSI SAF and ESA CCI sea-ice concentration climate data records. *Cryosphere*, **13**, 49-78, https://doi.org/10.5194/tc-13-49-2019.

Maslanik, J., and J. Stroeve, 1999: Near-Real-Time DMSP SSMIS Daily Polar Gridded Sea Ice Concentrations, Version 1. NASA National Snow and Ice Data Center Distributed Active Archive Center, Boulder, CO, USA, accessed 12 September 2023, https://doi.org/10.5067/U8C09DWVX9LM.

Petty, A. A., N. T. Kurtz, R. Kwok, T. Markus, and T. A. Neumann, 2020: Winter Arctic sea ice thickness from ICESat-2 freeboards. *J. Geophys. Res.-Oceans*, **125**, e2019JC015764, https://doi.org/10.1029/2019JC015764.

Petty, A. A., N. Kurtz, R. Kwok, T. Markus, T. A. Neumann, and N. Keeney, 2022: ICESat-2 L4 Monthly Gridded Sea Ice Thickness, Version 2 [Data Set]. NASA National Snow and Ice Data Center Distributed Active Archive Center, Boulder, CO, USA, accessed 13 August 2023, https://doi.org/10.5067/OE8BDP5KU30Q.

Petty A. A., N. Keeney, A. Cabaj, P. Kushner, and M. Bagnardi, 2023: Winter Arctic sea ice thickness from ICESat-2: upgrades to freeboard and snow loading estimates and an assessment of the first three winters of data collection. *Cryosphere*, **17**, 127-156, https://doi.org10.5194/tc-17-127-2023.

Ricker, R., S. Hendricks, L. Kaleschke, X. Tian-Kunze, J. King, and C. Haas, 2017: A weekly Arctic sea-ice thickness data record from merged CryoSat-2 and SMOS satellite data. *Cryosphere*, **11**, 1607-1623, https://doi.org/10.5194/tc-11-1607-2017.

Sumata, H., L. de Steur, D. V. Divine, M. A. Granskog, and S. Gerland, 2023: Regime shift in Arctic Ocean sea ice thickness. *Nature*, **615**, 442-449, https://doi.org/10.1038/s41586-022-05686-x.

Tschudi, M., W. N. Meier, and J. S. Stewart, 2019a: Quicklook Arctic Weekly EASE-Grid Sea Ice Age, Version 1. [September, 2023]. NASA National Snow and Ice Data Center Distributed Active Archive Center, Boulder, CO, USA, accessed 5 September 2023, https://doi.org/10.5067/2XXGZY3DUGNQ.

Tschudi, M., W. N. Meier, J. S. Stewart, C. Fowler, and J. Maslanik, 2019b: EASE-Grid Sea Ice Age, Version 4. [September, 1984-2022]. NASA National Snow and Ice Data Center Distributed Active Archive Center, Boulder, CO, USA, accessed 5 September 2023, https://doi.org/10.5067/UTAV7490FEPB.

November 9, 2023

Sea Surface Temperature

https://doi.org/10.25923/e8jc-f342

M. -L. Timmermans[1] and Z. Labe[2]

[1]Yale University, New Haven, CT, USA
[2]Atmospheric and Oceanic Sciences Program, Princeton University, Princeton, NJ, USA

Headlines

- August 2023 mean sea surface temperatures (SSTs) were ~5-7°C warmer than 1991-2020 August mean values in the Barents, Kara, Laptev and Beaufort Seas.
- Anomalously cool August 2023 SSTs (~1-3°C cooler) were observed in Baffin Bay, the Greenland Sea and parts of the Chukchi Sea.
- August mean SSTs show warming trends for 1982-2023 in almost all Arctic Ocean regions that are ice-free in August, with mean SST increases over regions between 65° N and 80° N of ~0.5°C per decade.

Arctic Ocean sea surface temperatures (SSTs) in the summer (June-August) are driven by the amount of incoming solar radiation absorbed by the sea surface and by the flow of warm waters into the Arctic from the North Atlantic and North Pacific Oceans. Solar warming of the Arctic Ocean surface is influenced by sea ice distribution (with greater warming occurring in ice-free regions), cloud cover, and upper-ocean stratification. Discharge of relatively warm Arctic river waters can provide an additional heat source to the surface of marginal seas.

Arctic SST is an essential indicator of the role of the ice-albedo feedback cycle in any given summer sea ice melt season. As the sea ice cover decreases, more incoming solar radiation is absorbed by the darker ocean surface and, in turn, the warmer ocean melts more sea ice. In addition, higher SSTs are associated with delayed autumn freeze-up and increased ocean heat storage throughout the year. Marine ecosystems are also influenced by SSTs, which affect primary production and available habitat.

Here we present August 2023 mean SSTs in context with the climatological record. The SST data analyzed are monthly mean values for August (1982-2023) (see Reynolds et al. 2002, 2007; Huang et al. 2021), and comparisons are made to the 1991-2020 baseline period (see *Methods and data*). August mean SSTs provide the most appropriate representation of Arctic Ocean summer SSTs because sea-ice extent is near a seasonal low at this time of year, and there is not the influence of surface cooling and subsequent sea-ice growth that takes place in the latter half of September.

August 2023 mean SSTs were as warm as ~11°C in the Barents, Kara, and Beaufort Seas and reached values as warm as ~8°C in other Arctic basin marginal regions (eastern Chukchi Sea and Laptev Sea, Fig. 1a,b). August 2023 mean SSTs were anomalously warm compared to the 1991-2020 August mean (around 5-7°C warmer) in the Barents, Kara, Laptev, and Beaufort Seas, and anomalously cool in Baffin Bay and parts of the Greenland and Chukchi Seas (around 1-3°C cooler than the 1991-2020 mean; Fig. 1c). These regional variations vary significantly from year-to-year. For example, there were considerably warmer SSTs in the Beaufort Sea in August 2023 compared to August 2022, with differences of up to 7°C (Fig. 1d).

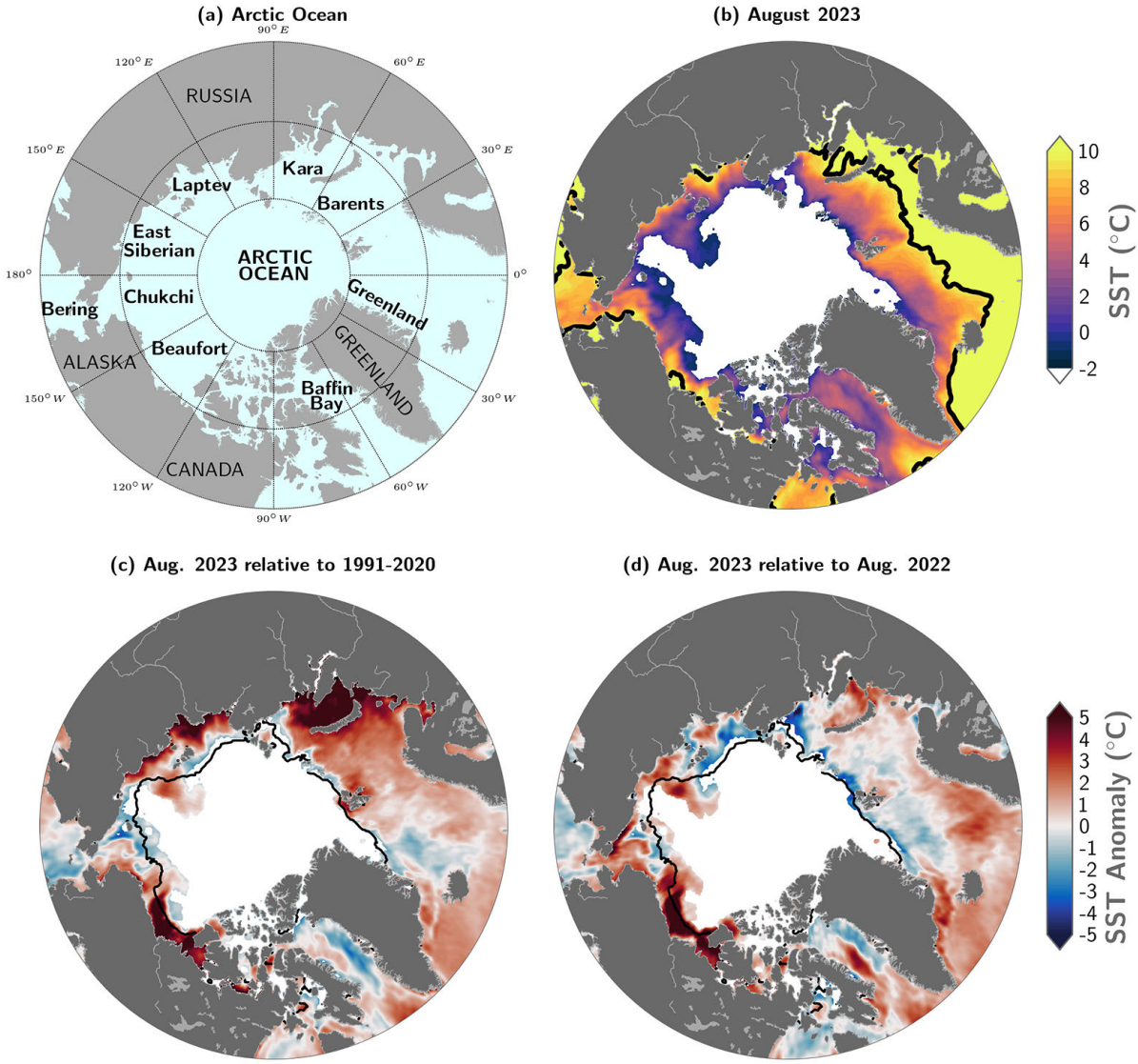

Fig. 1. (a) Arctic Ocean map showing marginal sea locations. (b) Mean sea surface temperature (SST; °C) in August 2023. Black contours indicate the 10°C SST isotherm. (c) SST anomalies (°C) in August 2023 relative to the Aug 1991-2020 mean. (d) Difference between August 2023 SSTs and August 2022 SSTs (negative values indicate where 2023 was cooler). White shading in all panels is the August 2023 mean sea ice extent. Black lines in (c) and (d) indicate the August 1991-2020 median ice edge. See *Methods and data* for data-source information.

Warm river inflows may have influenced marginal sea SSTs with anomalously warm August 2023 SSTs in the Beaufort Sea where the Mackenzie River enters, in the Kara Sea in the vicinity of the Ob and Yenisei River outflows, and in the Laptev Sea where the Lena River enters (Fig. 1c). This corresponds with anomalously warm surface air temperatures in June-August 2023 over northern North America and Siberia (see essay *Surface Air Temperature*).

The above normal August 2023 SSTs in the Beaufort Sea, which were also observed in July (Fig. 2b), relate to relatively low August 2023 sea-ice concentrations in the region (second only to the record low August 2012 conditions for the area extending from the Beaufort to East Siberian Seas; see essay *Sea*

Ice). The timing of seasonal sea-ice retreat from the Beaufort Sea, where sea ice was almost entirely absent by July 2023 (Fig. 2), also links to warm SSTs via the ice-albedo feedback (see essay *Sea Ice*).

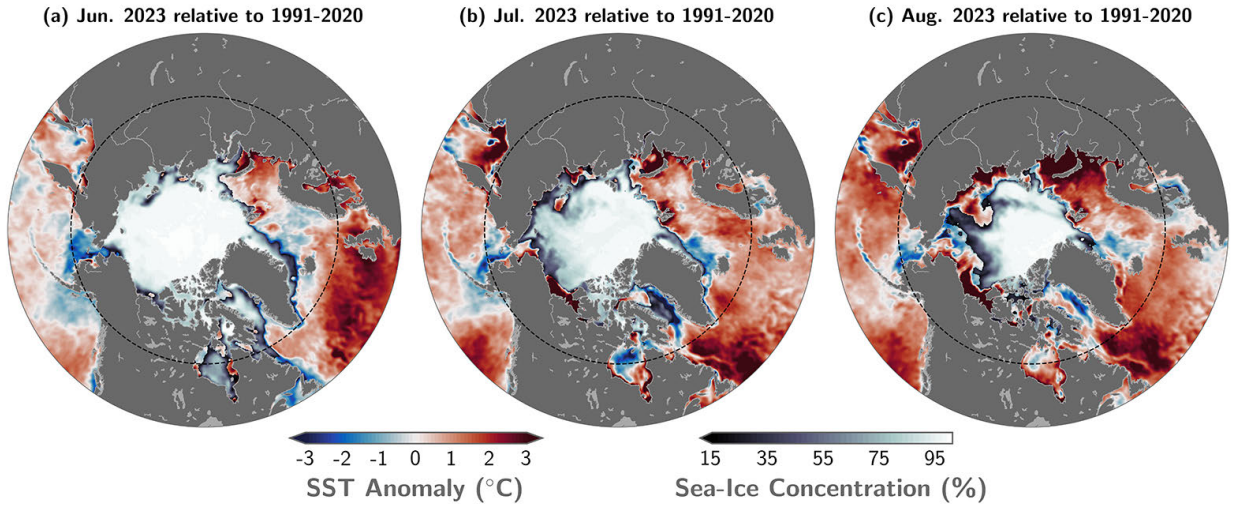

Fig. 2. SST anomalies (°C) for (a) June 2023, (b) July 2023, and (c) August 2023 relative to the 1991-2020 mean for the respective months. The sea-ice concentration for the corresponding month is also shown. The evolution of sea-ice concentration over the months of June to August illustrates why it is not appropriate to evaluate long-term SST trends in June and July over most of the Arctic marginal seas, which still have significant sea-ice cover in those months. The dashed circle indicates the latitudinal bound of Figs. 1 and 3 map images. See *Methods and data* for data-source information.

The cooler-than-normal August 2023 SSTs in Baffin Bay are commensurate with below normal surface air temperatures in the region in June-August 2023 (see essay *Surface Air Temperature*). Early summer sea-ice extent in Baffin Bay was close to the climatological average, with almost full ice cover in June 2023 (Fig. 2a), which is further consistent with the anomalously cool SSTs (see essay on *Sea Ice*).

The Arctic Ocean has experienced mean August SST warming trends from 1982 to 2023, with statistically significant (at the 95% confidence interval) linear warming trends in almost all regions (Fig. 3a). Mean August SSTs for the Arctic Ocean and marginal seas between 65° N and 80° N exhibit a linear warming trend of 0.05 ± 0.01°C/year (Fig. 3b; SSTs for 80° N-90° N are omitted since this region is largely perennially ice covered). Even while anomalously cool SSTs in Baffin Bay were prominent in August 2023 (Fig. 1c), SSTs show a linear warming trend over 1982-2023 of 0.07 ± 0.02°C/year (Fig. 3c) for this region, although with considerable interannual variability in mean August values.

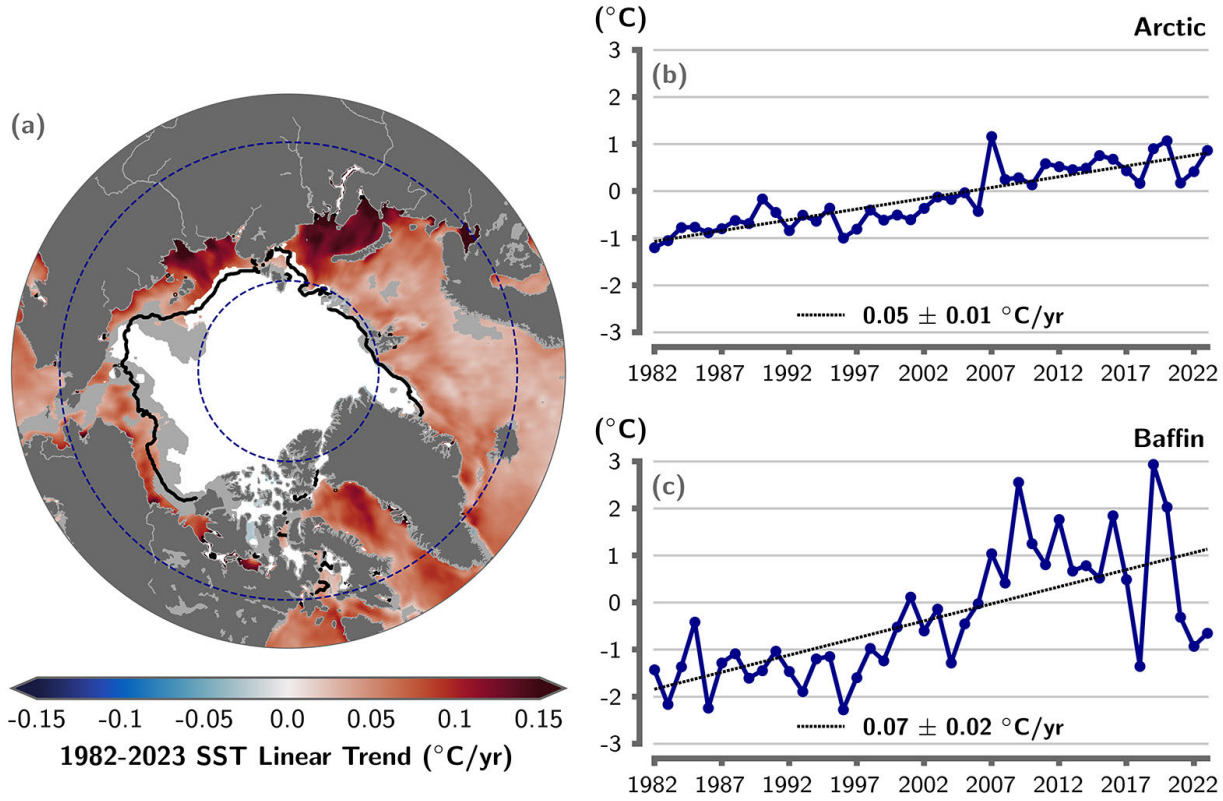

Fig. 3. (a) Linear SST trend (°C/yr) for August of each year from 1982 to 2023. The trend is only shown for values that are statistically significant at the 95% confidence interval; the region is shaded light gray otherwise. White shading is the August 2023 mean sea ice extent, and the black line indicates the August 1991-2020 median ice edge. (b,c) Area-averaged SST anomalies (°C) for August of each year (1982-2023) relative to the 1991-2020 August mean for (b) the Arctic Ocean between 65° N and 80° N (indicated by the dashed blue circles in (a)), and (b) Baffin Bay (see Fig. 1a). The dotted lines show the linear SST anomaly trends over the period shown and trends in °C/yr (with 95% confidence intervals) are indicated on the plots. See *Methods and data* for data-source information.

Methods and data

The SST data presented here are from the 0.25° × 0.25° NOAA Optimum Interpolation Sea Surface Temperature (OISST) Version 2.1 product, a blend of in situ and satellite measurements (Reynolds et al. 2002, 2007; Huang et al. 2021). Details are found here: https://psl.noaa.gov/data/gridded/data.noaa.oisst.v2.highres.html. The datafile "sst.mon.mean.nc" (comprising monthly means from the daily data) was retrieved from: https://downloads.psl.noaa.gov/Datasets/noaa.oisst.v2.highres/, [accessed 4 September 2023]. The period of analysis is June 1982 to August 2023, with 1991-2020 used as the climatological reference period for the June, July, and August means.

OISST Version 2.1 (v2.1) replaced the 1° × 1° NOAA OISST Version 2 (v2), which was discontinued in January 2023. Version 2.1 is the same as v2 (aside from the horizontal resolution difference) for the period prior to 1 January 2016. After 1 January 2016, v2.1 differs from v2 in multiple ways, including different correction methods and buoy datasets used (see Huang et al. 2021 for a full description). Notably for interpretation of Arctic Ocean SSTs, v2.1 employs a different method than v2 for setting a proxy SST in sea-ice covered regions. Version 2 uses a linear relationship with sea-ice concentration to

infer SST under sea ice (Reynolds et al. 2007), while v2.1 modifies this (following Banzon et al. 2020) to set SST equal to the freezing temperature (computed using a climatological sea-surface salinity) where ice concentrations are greater than 35%. We focus primarily on waters that are ice free in August, although the uncertainty in inferring SSTs (and SST trends) may be significant in the vicinity of the sea-ice edge, which varies in location each year.

For comparison with previous-year SST sections of the Arctic Report Card (e.g., Timmermans and Labe 2022), which used monthly-mean v2, we briefly note some important differences by way of example: comparison of the monthly mean August 2022 SST anomaly (relative to 1991-2020) between v2 (Fig. 4a) and v2.1 (Fig. 4b). The broad spatial patterns and their magnitudes are similar between the two products (e.g., generally cooler waters in the Norwegian Sea and the vicinity of Bering Strait, and warmer waters in the Barents and Laptev Seas). However, there are notable differences in the vicinity of the ice edge; for example, Beaufort Sea temperatures adjacent to the ice edge are ~2°C cooler in v2.1. This likely results from differences in the algorithm for proxy SST in the presence of sea-ice cover, and the differences in resolution between v2 and v2.1. Other notable areas are the marginal seas off the coast of Siberia where SSTs are warmer in v2.1. The source of these differences is unclear, although Huang et al. (2021) present a detailed analysis of differences in long-term averages between the two products. Nevertheless, the trends in August mean SSTs reported here (Fig. 3b,c) are statistically indistinguishable between v2 and v2.1, lending confidence to the conclusions and consistency with past Arctic Report Cards.

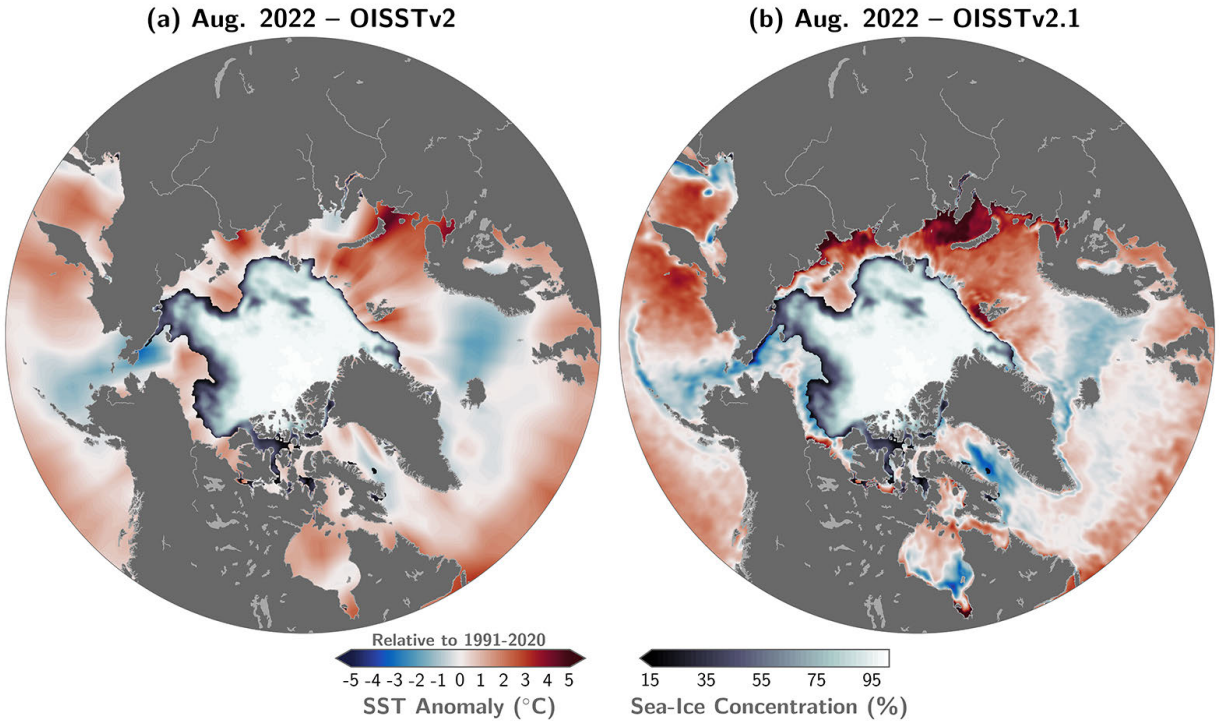

Fig. 4. August 2022 (monthly mean) SST (°C) anomaly (relative to the August 1991-2020 average) from OISST (a) Version 2 and (b) Version 2.1. White and grey shading indicates the mean sea-ice concentration for August 2022. See *Methods and data* for data-source information.

Sea ice concentration data are the NOAA/NSIDC Climate Data Record of Passive Microwave Sea Ice Concentration, Version 4 (https://nsidc.org/data/g02202) for the 1982-2022 period of record, and Near-Real-Time NOAA/NSIDC Climate Data Record of Passive Microwave Sea Ice Concentration, Version 2

(https://nsidc.org/data/g10016) (Peng et al. 2013; Meier et al. 2021a,b) is used for June-August 2023, where a threshold of 15% concentration is used to calculate sea ice extent.

Acknowledgments

M. -L. Timmermans acknowledges support from the National Science Foundation Office of Polar Programs and the Office of Naval Research. Z. Labe acknowledges support under award NA18OAR4320123 from the National Oceanic and Atmospheric Administration, U.S. Department of Commerce.

References

Banzon, V., T. M. Smith, M. Steele, B. Huang, and H. -M. Zhang, 2020: Improved estimation of proxy sea surface temperature in the Arctic. *J. Atmos. Ocean. Tech.*, **37**, 341-349, https://doi.org/10.1175/JTECH-D-19-0177.1.

Huang, B., C. Liu, V. Banzon, E. Freeman, G. Graham, B. Hankins, T. Smith, and H. Zhang, 2021: Improvements of the Daily Optimum Interpolation Sea Surface Temperature (DOISST) Version 2.1. *J. Climate*, **34**(8), 2923-2939, https://doi.org/10.1175/JCLI-D-20-0166.1.

Meier, W. N., F. Fetterer, A. K. Windnagel, and J. S. Stewart, 2021a: NOAA/NSIDC Climate Data Record of Passive Microwave Sea Ice Concentration, Version 4. [1982-2021]. NSIDC: National Snow and Ice Data Center, Boulder, CO, USA, accessed 10 September 2022, https://doi.org/10.7265/efmz-2t65.

Meier, W. N., F. Fetterer, A. K. Windnagel, and J. S. Stewart, 2021b: Near-Real-Time NOAA/NSIDC Climate Data Record of Passive Microwave Sea Ice Concentration, Version 2. [1982-2021], accessed 10 September 2022, https://doi.org/10.7265/tgam-yv28.

Peng, G., W. N. Meier, D. J. Scott, and M. H. Savoie, 2013: A long-term and reproducible passive microwave sea ice concentration data record for climate studies and monitoring. *Earth Syst. Sci. Data*, **5**, 311-318, https://doi.org/10.5194/essd-5-311-2013.

Reynolds, R. W., N. A. Rayner, T. M. Smith, D. C. Stokes, and W. Wang, 2002: An improved in situ and satellite SST analysis for climate. *J. Climate*, **15**, 1609-1625, https://doi.org/10.1175/1520-0442(2002)015<1609:AIISAS>2.0.CO;2.

Reynolds, R. W., T. M. Smith, C. Liu, D. B. Chelton, K. S. Casey, and M. G. Schlax, 2007: Daily high-resolution-blended analyses for sea surface temperature. *J. Climate*, **20**, 5473-5496, https://doi.org/10.1175/2007JCLI1824.1, and see http://www.esrl.noaa.gov/psd/data/gridded/data.noaa.oisst.v2.html.

Timmermans, M. -L., and Z. M. Labe, 2022: Sea surface temperature. *Arctic Report Card 2022*, M. L. Druckenmiller, R. L. Thoman, and T. A. Moon, Eds., https://doi.org/10.25923/p493-2548.

November 13, 2023

Arctic Ocean Primary Productivity: The Response of Marine Algae to Climate Warming and Sea Ice Decline

https://doi.org/10.25923/nb05-8w13

K. E. Frey[1], J. C. Comiso[2], L. W. Cooper[3], C. Garcia[4], J. M. Grebmeier[3], and L. V. Stock[2]

[1]Graduate School of Geography, Clark University, Worcester, MA, USA
[2]Cryospheric Sciences Laboratory, Goddard Space Flight Center, NASA, Greenbelt, MD, USA
[3]Chesapeake Biological Laboratory, University of Maryland Center for Environmental Science, University of Maryland, Solomons, MD, USA
[4]Arctic Research Program, Global Ocean Monitoring and Observing Program, NOAA, Silver Spring, MD, USA

Headlines

- Satellite estimates of ocean primary productivity (i.e., the rate at which marine algae transform dissolved inorganic carbon into organic material) show higher values for 2023 (relative to the 2003-22 mean) for five of nine regions assessed across the Arctic.
- All regions, except for the Amerasian Arctic (namely the Chukchi Sea, Beaufort Sea, and Canadian Archipelago), continue to exhibit positive trends in ocean primary productivity during 2003-23, with the largest percent change in the Eurasian Arctic (57.4% increase) and Barents Sea (20.7% increase).
- While positive decadal trends in annual ocean primary productivity continue to be dominant across the Arctic, large areas of lower-than-average values were observed during 2023 in the East Siberian Sea, Chukchi Sea, Greenland Sea, and Baffin Bay/Labrador Sea.

Introduction

A rapidly warming Arctic Ocean and peripheral seas (Rantanen et al. 2022) are undergoing shifts in marine primary productivity, largely driven by dynamic changes in sea ice extent, nutrient dynamics, and light regimes (Ardyna and Arrigo 2020; Terhaar et al. 2021; Frey et al. 2023). Understanding changes in Arctic marine primary productivity, the conversion of dissolved inorganic carbon into organic material, is vital as it forms the base of the marine ecosystem and plays a key role in carbon sequestration (Manizza 2023). In recent years, factors that include expanding sea-ice-free areas and thinning sea ice, enhanced wind mixing from storms, and efficient recycling of land-derived nutrients have regionally boosted ocean primary production (Fujiwara et al. 2018; Møller et al. 2023; Tank et al. 2023). In contrast, increased ocean stratification and a progressively cloudier Arctic atmosphere may curtail productivity by reducing nutrient and light availability to primary producers (Bélanger et al. 2013). Harmful algal blooms in warming Arctic waters have also become an emerging threat to human and ecosystem health (e.g., Anderson et al. 2022). The diverse marine sectors of the Arctic (from the nutrient-rich Barents Sea and shallow, productive northern Bering/Chukchi Seas to the low-productivity central deep Arctic basin) vary

widely in primary productivity patterns, as they are influenced by their unique hydrographic, atmospheric, and sea ice conditions. These regional variations are critical to understand, with each sector contributing differently to Arctic biodiversity, biogeochemical cycling, and global climate feedback mechanisms. Using satellite-derived Gross Primary Production data spanning more than two decades, nuanced changes in primary productivity across the pan-Arctic and within distinct Arctic sectors can be explored. Continued monitoring of Arctic marine primary productivity is vital, given its profound impacts on marine ecosystems across all trophic levels.

Chlorophyll-*a*

We present satellite-based estimates of algal chlorophyll-*a* (occurring in all species of phytoplankton) based on ocean color, and subsequently provide calculated primary production estimates (below). Observed patterns in chlorophyll-*a* concentrations (Fig. 1), which are spatially and temporally heterogeneous across the Arctic Ocean, are often associated with the timing of the seasonal break-up and retreat of the sea ice cover (Fig. 2) (see essay *Sea Ice*): high chlorophyll-*a* percentages tend to occur in regions where break-up is relatively early, while low percentages tend to occur in regions where break-up is delayed. During May 2023 (Fig. 1a), patterns in chlorophyll-*a* concentrations were heterogeneous with broad areas of lower-than-average values across most regions, interspersed with higher-than-average values in the Bering Sea and Barents Sea. During June 2023 (Fig. 1b), the heterogeneity continued with higher-than-average values interspersed within the Bering Sea, the Barents Sea, around the southern tip of Greenland, and near the North Water Polynya in northwest Greenland. During July 2023 (Fig. 1c), most areas showed lower-than-average values with the exception being a substantial swath (~2400 km long) of higher-than-average values in the Barents Sea, moving westward south of Svalbard and into the Greenland Sea. During August 2023 (Fig. 1d), most regions across the Arctic also exhibited lower-than-average values, except for notable higher-than-average values in the northern Bering Sea and southern Chukchi Sea.

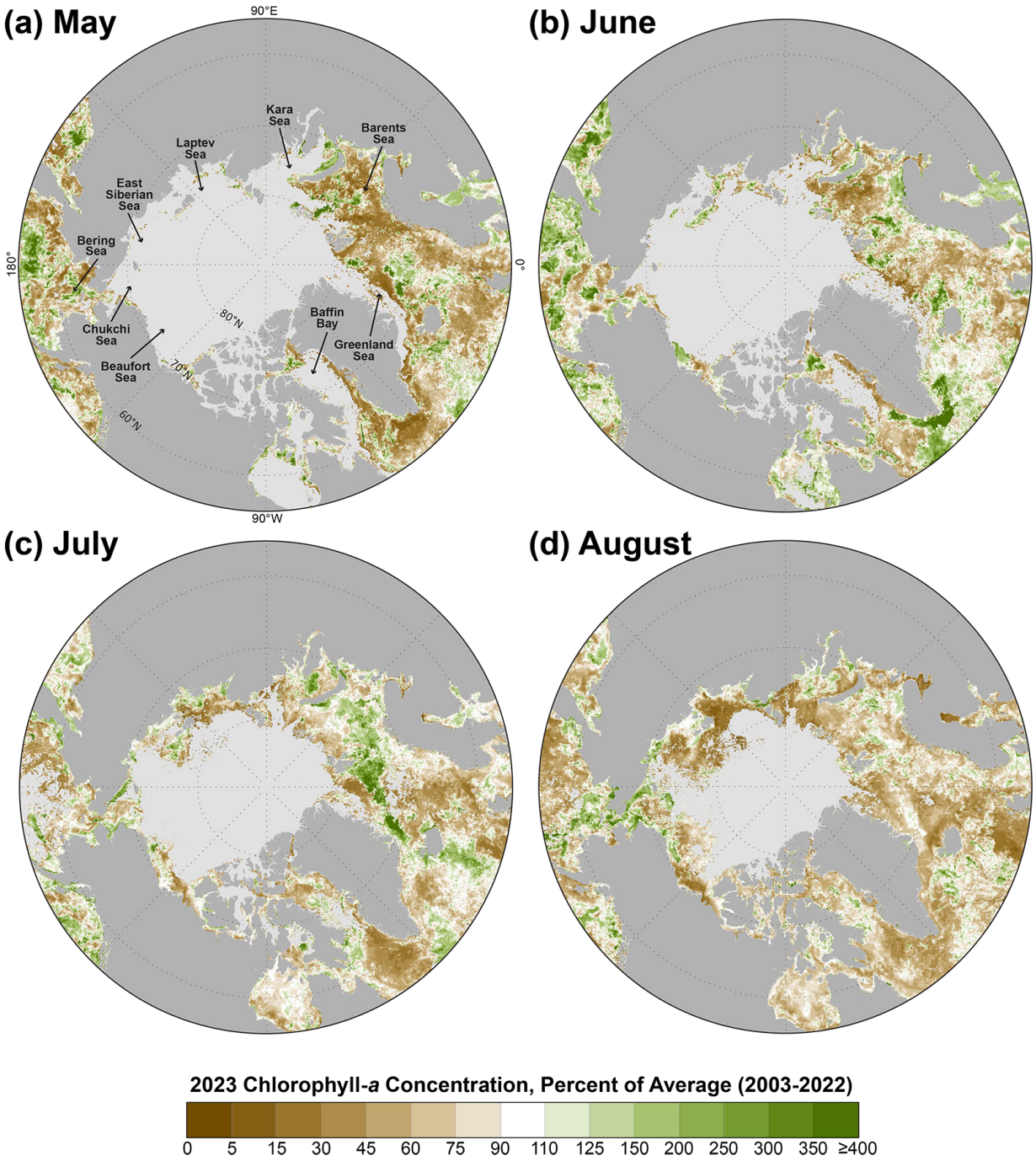

Fig. 1. Mean monthly chlorophyll-*a* concentrations during 2023, shown as a percent of the 2003-22 average for (a) May, (b) June, (c) July, and (d) August. The light gray regions represent areas where no data are available (owing to either the presence of sea ice or cloud cover). The color scale bar uses unequal intervals ranging from 5 to 50 percentage units, including the largest intervals for values greater than 125%. Data source: MODIS-Aqua Reprocessing 2022.0, chlor_a algorithm: https://oceancolor.gsfc.nasa.gov/.

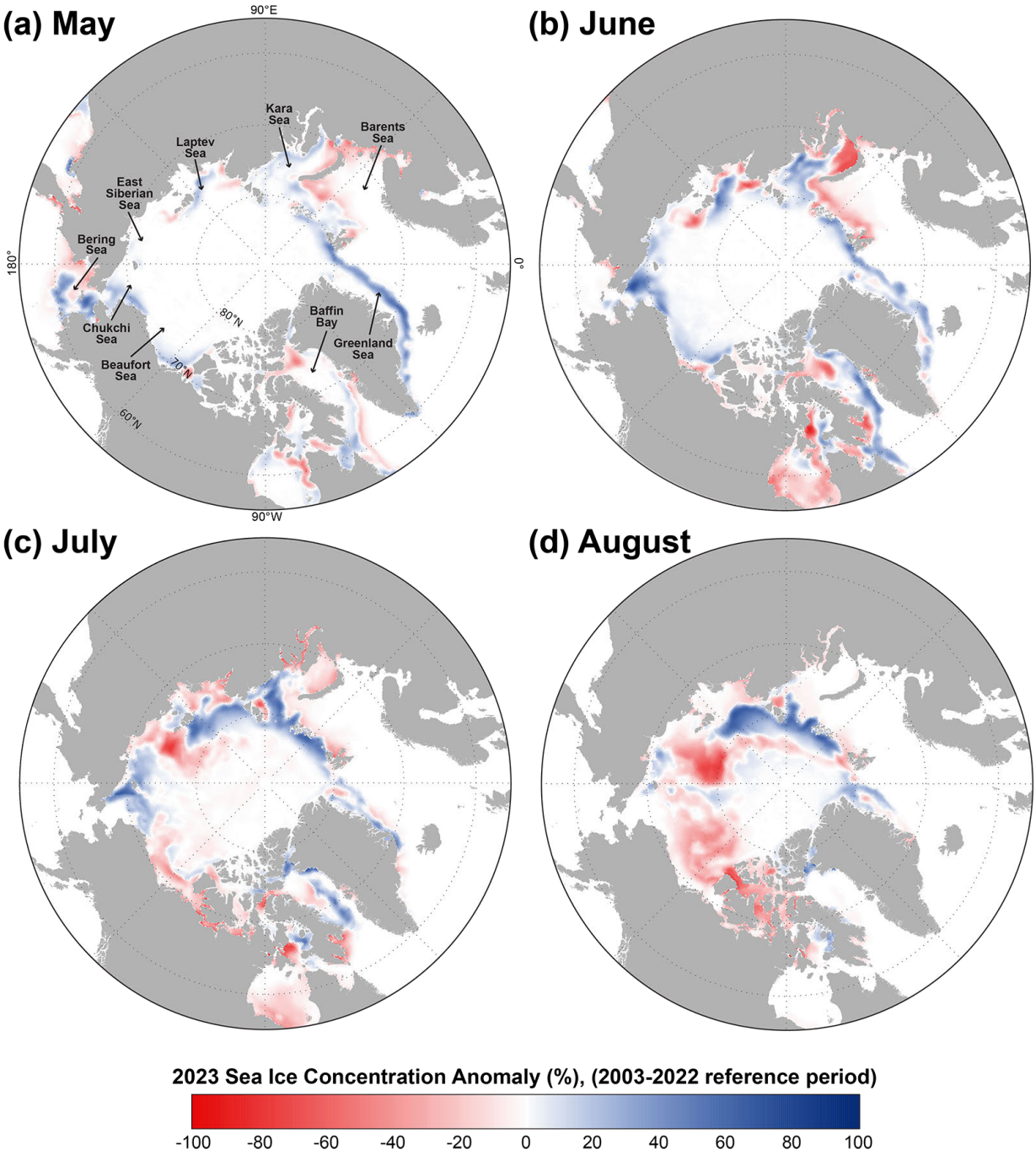

Fig. 2. Sea ice concentration anomalies (%) in 2023 (compared to a 2003-22 mean reference period) for (a) May, (b) June, (c) July, and (d) August. Data source: SSM/I and SSMIS passive microwave, calculated using the Goddard Bootstrap (SB2) algorithm (Comiso et al. 2017).

Primary production

While chlorophyll-*a* concentrations give an estimate of the total standing stock of algal biomass, rates of primary production (i.e., the production of organic carbon via photosynthesis) provide a different perspective since not all algae in the water column are necessarily actively producing. The mean annual (March through September) primary productivity across the Arctic shows important spatial patterns,

most notably the overall decreases moving northward as sea ice cover is present for a greater fraction of the year (Fig. 3a). Spatial trends in annual primary productivity (Fig. 3b) are a particularly useful tool for understanding hotspots of change. Statistically significant positive trends in primary productivity appear clustered in the southeastern Chukchi Sea, Barents Sea, and the Laptev Sea north of the New Siberian Islands (Fig. 3b). Positive trends adjacent to the Eurasian coastline may be associated with variability in river-derived chromophoric (light absorbing) dissolved organic matter (CDOM) as well (e.g., Lewis and Arrigo 2020). Using this primary productivity product, there is almost no evidence of significant negative trends in primary productivity across the Arctic (except for isolated locations in the southern Norwegian Sea; Fig. 3b). Investigations of 2023 annual primary productivity (Fig. 3c), as well as 2023 compared to the 2003-22 average (Fig. 3d), show greater-than-average annual productivity in the southern Beaufort Sea, northern Laptev Sea (east of the New Siberian Islands), western Kara Sea, and Barents Sea, but lower-than-average annual productivity in the Chukchi Sea, East Siberian Sea, Greenland Sea, and Baffin Bay.

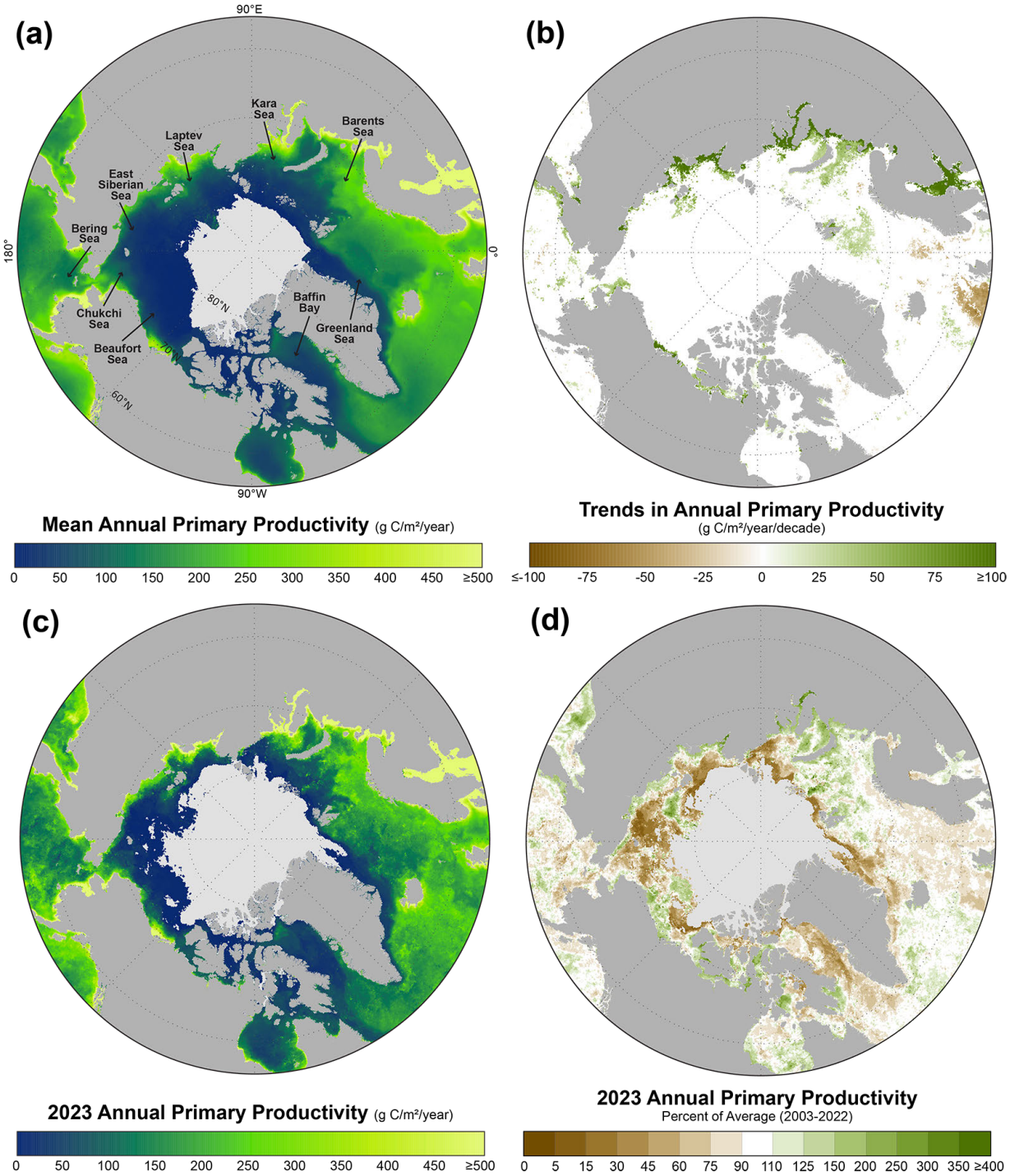

Fig. 3. For the pan-Arctic region: (a) mean annual (March-September only) primary productivity (2003-23); (b) trends in annual productivity (over 2003-23) where only those trends that are statistically significant (p<0.05) are shown; (c) annual primary productivity for 2023 only; and (d) 2023 annual primary productivity anomalies (shown as a percent of the 2003-22 average). In a, c, and d, light gray indicates no data owing to the presence of sea ice. Additional information regarding these data can be found in Table 1. See *Methods and data* section for details of how primary productivity was calculated.

Overall estimates of ocean primary productivity in 2023 for nine regions and across the Northern Hemisphere (relative to the 2003-22 reference period) were assessed (Fig. 4, Table 1). The Eurasian

Arctic region includes the Kara, Laptev, and East Siberian Seas. The Amerasian Arctic region includes the Chukchi Sea, Beaufort Sea, and Canadian Archipelago. The North Atlantic is categorized as south of 60° N and east of 45° W, which excludes the Labrador and Greenland Seas. Our results show above-average primary productivity for 2023 in five of the nine regions assessed, while the Amerasian Arctic, Greenland Sea, Baffin Bay/Labrador Sea, and North Atlantic exhibit lower-than-average values (Fig. 4, Table 1). While lower-than-average primary productivity percentages are geographically widespread within the Eurasian Arctic region for 2023 (Fig. 3d), those areas within the region that show higher-than-average percentages are disproportionately large enough to result in an overall higher-than-average 2023 regional primary productivity (Table 1). Across the whole time series, positive trends in primary productivity are continuing in all regions during the 2003-23 period, except for the Amerasian Arctic. The largest statistically significant positive trends occurred in the Eurasian Arctic and Barents Sea with 29.11 g C/m^2/yr/decade and 16.48 g C/m^2/yr/decade, respectively. Trends in primary production over 2003-23 show a ~57.4% increase in the Eurasian Arctic and a ~20.7% increase in the Barents Sea. Annual net primary production was also calculated for the Arctic region, defined as 60-90° N (Fig. 5), and shows a trend over 2003-23 of 15.5 Tg C/yr (Mann-Kendall significance $p<0.001$). The percent change estimated from the linear regression over the 21-year time series is 19.3%. In summary, while 2003-23 observations of primary productivity show complex interannual and spatial patterns, we continue to observe overall positive trends across most Arctic regions.

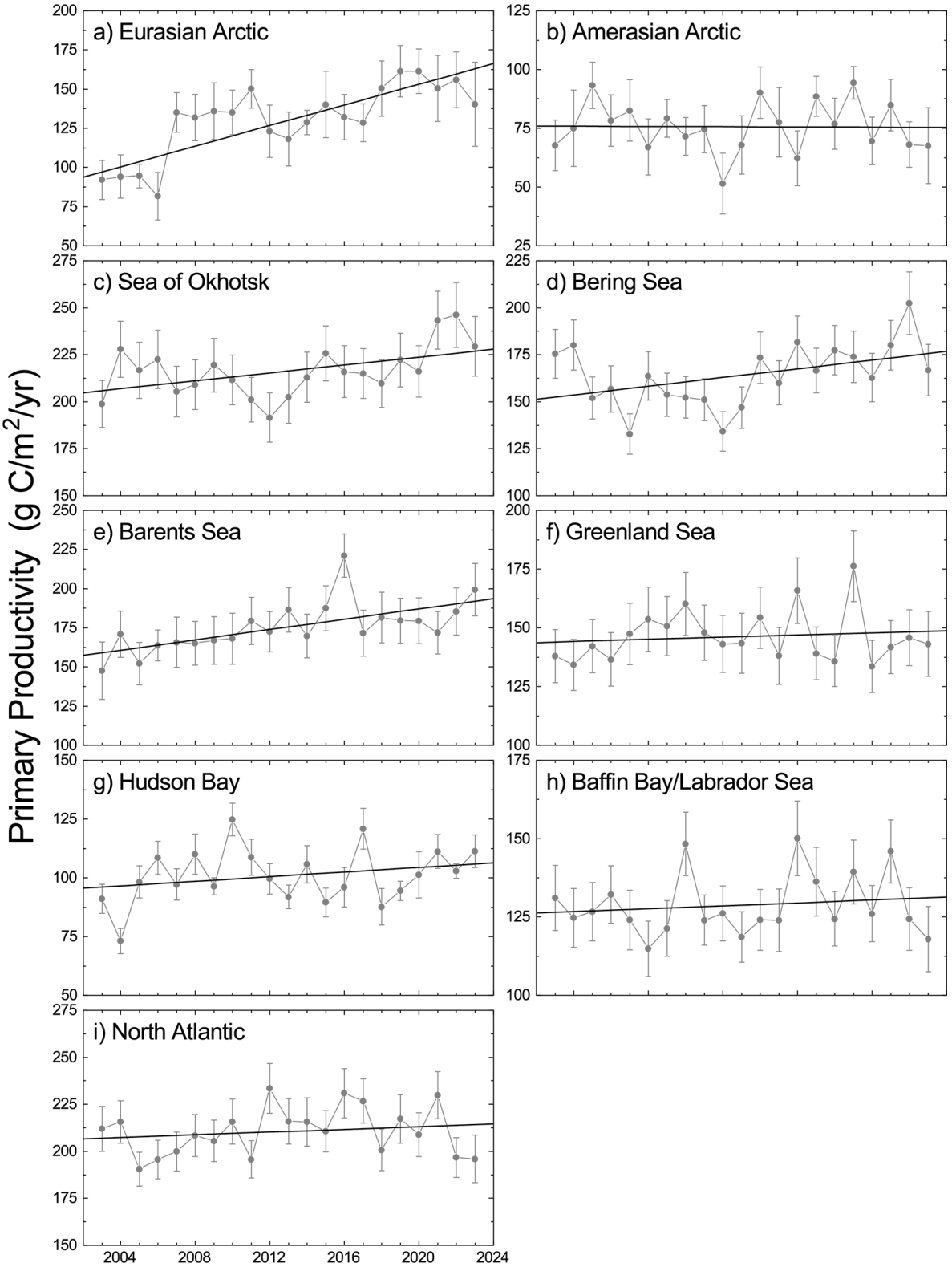

Fig. 4. Primary productivity (2003-23, March-September only) in nine different regions of the Northern Hemisphere (for a definition of the regions see Comiso (2015)). The statistical significance of the trends (based on the Mann-Kendall test), *p*-values, and additional information regarding these data can be found in Table 1. See *Methods and data* section for primary productivity calculation details.

Table 1. Linear trends, statistical significance, and percent change in primary productivity (2003-23) and primary productivity anomalies for 2023 (March-September) in the nine regions as shown in Fig. 4. Values in bold are statistically significant (p<0.05) using the Mann-Kendall test for trend. The percent change was estimated from the linear regression of the 21-year time series.

Region	**2003-23** Trend (g C/m^2/yr/ decade)	**2003-23** Mann-Kendall p-value	**2003-23** % Change	**2023** Anomaly (g C/m^2/yr) from the 2003-22 reference period	**2023** Primary Productivity (% of the 2003-22 average)
Eurasian Arctic	**29.11**	0.001	57.4	10.15	107.8
Amerasian Arctic	-0.23	0.833	-0.6	-8.48	88.8
Sea of Okhotsk	10.49	0.057	10.2	13.66	106.3
Bering Sea	11.59	0.075	15.2	2.94	101.8
Barents Sea	**16.48**	0.000	20.7	24.90	114.3
Greenland Sea	2.31	0.695	3.2	-3.25	97.8
Hudson Bay	4.89	0.319	10.2	10.94	110.9
Baffin Bay/Labrador Sea	2.33	0.928	3.7	-11.38	91.2
North Atlantic	3.69	0.349	3.6	-15.40	92.7

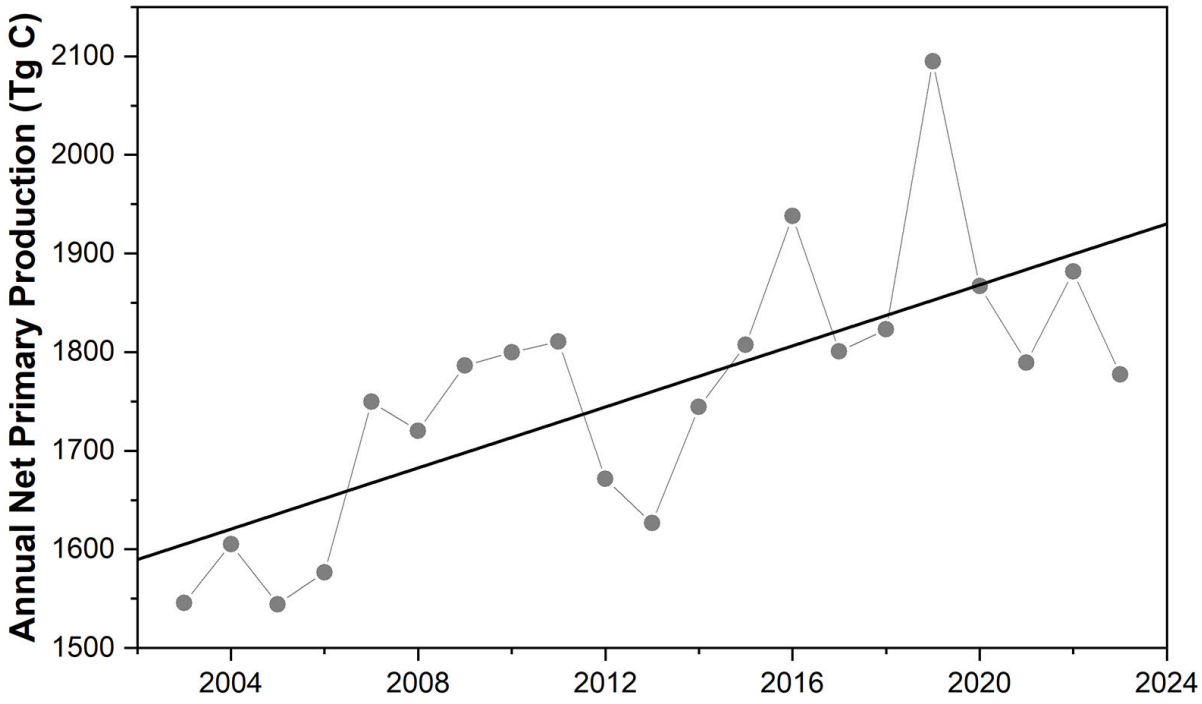

Fig. 5. Annual net primary production (2003-23, March-September only) for the Arctic region defined as 60-90° N. The trend over the 2003-23 time period is 15.5 Tg C/yr (Mann-Kendall significance p<0.001). The percent change estimated from the linear regression over the 21-year time series is 19.3%. See *Methods and data* section for primary productivity calculation details.

Methods and data

Measurements of the algal pigment chlorophyll (specifically, chlorophyll-*a*) serve as a proxy for algal biomass present in the ocean as well as overall plant health. The complete, updated Moderate Resolution Imaging Spectroradiometer (MODIS)-Aqua satellite record of chlorophyll-*a* concentrations within northern polar waters for the years 2003-23 serves as a time-series against which individual years can be compared. Satellite-based chlorophyll-*a* data across the pan-Arctic region were derived using the MODIS-Aqua Reprocessing 2022.0, chlor_a algorithm: https://oceancolor.gsfc.nasa.gov/. For this report, we show mean monthly chlorophyll-*a* concentrations calculated as a percentage of the 2003-22 average, which was chosen as the reference period to maximize the length of the satellite-based time series. Satellite-based sea ice concentrations were derived from the Special Sensor Microwave/Imager (SSM/I) and Special Sensor Microwave Imager/Sounder (SSMIS) passive microwave instruments, calculated using the Goddard Bootstrap (SB2) algorithm (Comiso et al. 2017). Monthly sea ice concentration anomalies were additionally calculated for 2023 (compared to the 2003-22 average) to streamline comparisons with the variability in monthly chlorophyll-*a* satellite data. Primary productivity data were derived using chlorophyll-*a* concentrations from MODIS-Aqua data (Reprocessing 2022.0, chlor_a algorithm), the NOAA 1/4° daily Optimum Interpolation Sea Surface Temperature dataset (or daily OISST) that uses satellite sea surface temperatures from AVHRR, incident solar irradiance, mixed layer depths, and additional parameters. Primary productivity values were calculated based on the Vertically Generalized Production Model (VGPM) algorithm described by Behrenfeld and Falkowski (1997) with further information provided by Frey et al. (2023). Chlorophyll-*a* and primary productivity data only incorporate pixels where sea ice is less than 10%, which is a compromise between potential pixel contamination with sea ice and an attempt to incorporate open water near the ice edge that typically exhibits high rates of primary production. The 2023 annual (March-September) primary productivity percent of average (compared to 2003-22) was calculated the same way as for chlorophyll-*a*, as described above. Lastly, Theil-Sen median trends were calculated spatially (Fig. 3b) and for the extracted time series for each geographic region (Table 1), where statistical significance of the trends ($p<0.05$) was determined using the Mann-Kendall trend test.

Because chlorophyll-*a* and primary productivity data are shown for ocean areas with less than 10% sea ice concentration, they do not include production by sea ice algae or under-ice phytoplankton blooms, which can be significant (e.g., Ardyna et al. 2020). Furthermore, it is well known that satellite observations can underestimate production under stratified ocean conditions when a deep chlorophyll maximum is present (Juranek et al. 2023). The variable distribution of sediments and CDOM (owing to riverine delivery, coastal erosion, and sea ice dynamics) can also affect the accuracy of satellite-based estimations of chlorophyll-*a* and primary productivity in Arctic waters (Lewis and Arrigo 2020). As such, in-situ observations continue to be important to provide overall context for changes to and drivers of primary productivity across Arctic marine ecosystems.

Acknowledgments

K. Frey acknowledges financial support from the National Science Foundation (NSF) Arctic Observing Network (AON) Program (Grant 1917434). Support for J. Grebmeier and L. Cooper was provided through NSF AON (Grant 1917469) and the NOAA Global Ocean Monitoring and Observing, Arctic Research Program (CINAR 22309.07_UMCES_Grebmeier).

References

Anderson, D. M., and Coauthors, 2022: Harmful algal blooms in the Alaskan Arctic: An emerging threat as the ocean warms. *Oceanography*, **35**(3/4), 130-139, https://doi.org/10.5670/oceanog.2022.121.

Ardyna, M., and K. R. Arrigo, 2020: Phytoplankton dynamics in a changing Arctic Ocean. *Nat. Climate Change*, **10**, 892-903 (2020), https://doi.org/10.1038/s41558-020-0905-y.

Ardyna, M., and Coauthors, 2020: Under-ice phytoplankton blooms: Shedding light on the "invisible" part of Arctic primary production. *Front. Mar. Sci.*, **7**, 608032, https://doi.org/10.3389/fmars.2020.608032.

Behrenfeld, M. J., and P. G. Falkowski, 1997: Photosynthetic rates derived from satellite-based chlorophyll concentration. *Limnol. Oceanogr.*, **42**(1), 1-20, https://doi.org/10.4319/lo.1997.42.1.0001.

Bélanger, S., M. Babin, and J. -É. Tremblay, 2013: Increasing cloudiness in Arctic damps the increase in phytoplankton primary production due to sea ice receding. *Biogeosciences*, **10**, 4087-4101, https://doi.org/10.5194/bg-10-4087-2013.

Comiso, J. C., 2015: Variability and trends of the global sea ice covers and sea level: Effects on physicochemical parameters. Climate Change and Marine and Freshwater Toxins, L. M. Botana, M. C. Lauzao, and N. Vilarino, Eds., De Gruyter, Berlin, Germany, https://doi.org/10.1515/9783110333596-003.

Comiso, J. C., W. N. Meier, and R. Gersten, 2017: Variability and trends in the Arctic Sea ice cover: Results from different techniques. *J. Geophys. Res.-Oceans*, **122**, 6883-6900, https://doi.org/10.1002/2017JC012768.

Frey, K. E., J. C. Comiso, L. V. Stock, L. N. C. Young, L. W. Cooper, and J. M. Grebmeier, 2023: A comprehensive satellite-based assessment across the Pacific Arctic Distributed Biological Observatory shows widespread late-season sea surface warming and sea ice declines with significant influences on primary productivity. *PLoS ONE*, **18**(7), e0287960, https://doi.org/10.1371/journal.pone.0287960.

Fujiwara, A., and Coauthors, 2018: Changes in phytoplankton community structure during wind-induced fall bloom on the central Chukchi shelf. *Polar Biol.*, **41**, 1279-1295, https://doi.org/10.1007/s00300-018-2284-7.

Juranek, L. W., B. Hales, N. L. Beaird, M. A. Goñi, E. Shroyer, J. G. Allen, and A. E. White, 2023: The importance of subsurface productivity in the Pacific Arctic gateway as revealed by high-resolution biogeochemical surveys. *J. Geophys. Res.-Oceans*, **128**, e2022JC019292, https://doi.org/10.1029/2022JC019292.

Lewis, K. M., and K. R. Arrigo, 2020: Ocean color algorithms for estimating chlorophyll *a*, CDOM absorption, and particle backscattering in the Arctic Ocean. *J. Geophys. Res.-Oceans*, **125,** e2019JC015706, https://doi.org/10.1029/2019JC015706.

Manizza, M., 2023: Carbon streams into the deep Arctic Ocean. *Nat. Geosci.*, **16**, 6-7, https://doi.org/10.1038/s41561-022-01102-1.

Møller, E. F., A. Christensen, J. Larsen, K. D. Mankoff, M. H. Ribergaard, M. Sejr, P. Wallhead, and M. Maar, 2023: The sensitivity of primary productivity in Disko Bay, a coastal Arctic ecosystem, to changes in freshwater discharge and sea ice cover. *Ocean Sci.*, **19**, 403-420, https://doi.org/10.5194/os-19-403-2023.

Rantanen, M., A. Y. Karpechko, A. Lipponen, K. Nordling, O. Hyvärinen, K. Ruosteenoja, T. Vihma, and A. Laaksonen, 2022: The Arctic has warmed nearly four times faster than the globe since 1979. *Commun. Earth Environ.*, **3**, 168, https://doi.org/10.1038/s43247-022-00498-3.

Tank, S. E., and Coauthors, 2023: Recent trends in the chemistry of major northern rivers signal widespread Arctic change. *Nat. Geosci.*, **16**, 789-796, https://doi.org/10.1038/s41561-023-01247-7.

Terhaar, J., R. Lauerwald, P. Regnier, N. Gruber, and L. Bopp, 2021: Around one third of current Arctic Ocean primary production sustained by rivers and coastal erosion. *Nat. Commun.*, **12**, 169, https://doi.org/10.1038/s41467-020-20470-z.

November 16, 2023

Tundra Greenness

https://doi.org/10.25923/s86a-jn24

G. V. Frost[1], M. J. Macander[1], U. S. Bhatt[2], L. T. Berner[3], J. W. Bjerke[4], H. E. Epstein[5], B. C. Forbes[6], M. J. Lara[7,8], R. Í. Magnússon[9], P. M. Montesano[10], G. K. Phoenix[11], S. P. Serbin[12], H. Tømmervik[4], C. Waigl[13], D. A. Walker[14], and D. Yang[12,15]

[1]Alaska Biological Research, Inc., Fairbanks, AK, USA
[2]Geophysical Institute, University of Alaska Fairbanks, Fairbanks, AK, USA
[3]School of Informatics, Computing and Cyber Systems, Northern Arizona University, Flagstaff, AZ, USA
[4]Norwegian Institute for Nature Research, FRAM - High North Research Centre for Climate and the Environment, Tromsø, Norway
[5]Department of Environmental Sciences, University of Virginia, Charlottesville, VA, USA
[6]Arctic Centre, University of Lapland, Rovaniemi, Finland
[7]Department of Plant Biology, University of Illinois, Urbana, IL, USA
[8]Department of Geography, University of Illinois, Urbana, IL, USA
[9]Plant Ecology and Nature Conservation Group, Wageningen University & Research, Wageningen, Netherlands
[10]Goddard Space Flight Center, NASA, Greenbelt, MD, USA
[11]School of Biosciences, University of Sheffield, Sheffield, UK
[12]Environmental and Climate Sciences Department, Brookhaven National Laboratory, Upton, NY, USA
[13]International Arctic Research Center, University of Alaska Fairbanks, Fairbanks, AK, USA
[14]Institute of Arctic Biology, University of Alaska Fairbanks, Fairbanks, AK, USA
[15]Department of Ecology and Evolution, Stony Brook University, Stony Brook, NY, USA

Headlines

- The circumpolar average peak tundra greenness value in 2023 was the third highest in the 24-year MODIS record, a slight increase from the previous year.
- Peak vegetation greenness in 2023 was much higher than usual in North American tundra, particularly in the Beaufort Sea region, while greenness was relatively low in the Eurasian Arctic, particularly in north-central Siberia and the Russian Far Northeast.
- The eight highest circumpolar tundra greenness values in the long-term satellite record (1982-2022) have all been recorded in the last 12 years, providing unequivocal evidence of Arctic greening.

Introduction

Earth's northernmost continental landmasses and island archipelagos are home to the Arctic tundra biome, a 5.1 million km^2 region that forms a "ring" of cold-adapted, treeless vegetation atop the globe, bordered by the Arctic Ocean to the north and the boreal forest biome to the south (Raynolds et al. 2019). The biological and physical conditions of Arctic tundra ecosystems are changing profoundly, as vegetation and underlying permafrost soils are strongly influenced by rising air temperatures and the

rapid decline of sea ice on the nearby Arctic Ocean (see essays *Surface Air Temperature* and *Sea Ice*). In the late 1990s, a sharp increase in the productivity of tundra vegetation became evident in global satellite observations, a phenomenon that soon became known as "the greening of the Arctic." Arctic greening is dynamically linked with Earth's changing climate, permafrost, seasonal snow, and sea-ice cover, and remains a focus of multi-disciplinary scientific research.

Spaceborne monitoring of Arctic tundra greenness

Global vegetation has been monitored from space for over four decades, beginning with the launch of the Advanced Very High Resolution Radiometer (AVHRR) sensor in late 1981. In 2000, the Moderate Resolution Imaging Spectroradiometer (MODIS) began providing a complementary record with higher spatial resolution and improved calibration. AVHRR and MODIS both monitor vegetation greenness using the Normalized Difference Vegetation Index (NDVI), a spectral metric that exploits the unique way in which vegetation absorbs and reflects light in the visible and infrared wavelengths, respectively.

Both AVHRR and MODIS have recorded increasing annual maximum tundra greenness (MaxNDVI) across most of the Arctic tundra biome during 1982-2022 and 2000-23, respectively (Figs. 1a,b). Although there is substantial regional variability in greenness trends, several areas of strong positive trend stand out in both records. In North America, greening has been strongest in northern Alaska, mainland Canada, and southern Baffin Island. In Eurasia, strong greening has occurred in Chukotka and portions of the Taymyr Peninsula. However, some Arctic tundra regions have experienced flat or negative (sometimes referred to as "browning") trends, including portions of southwestern Alaska, the Canadian High Arctic, and northeastern Siberia. Trends in northwestern Siberia and the European Arctic are mixed between the two satellite records, which may be partly attributable to their different observational periods. Regional contrasts in greening highlight the complexity of Arctic change, and the rich web of interactions that exist between tundra ecosystems and the local characteristics of sea ice, permafrost, seasonal snow (see essay *Terrestrial Snow Cover*), soil composition and moisture, disturbance processes, wildlife, and human activities (Bartsch et al. 2021; Heijmans et al. 2022). Parsing the underlying drivers of complex Arctic trends is important for improved monitoring and prediction of tundra ecosystem function and the consequences of Arctic change on the global carbon cycle (Rogers et al. 2022; see essay *Peatlands and Associated Boreal Forests of Finland Under Restoration*).

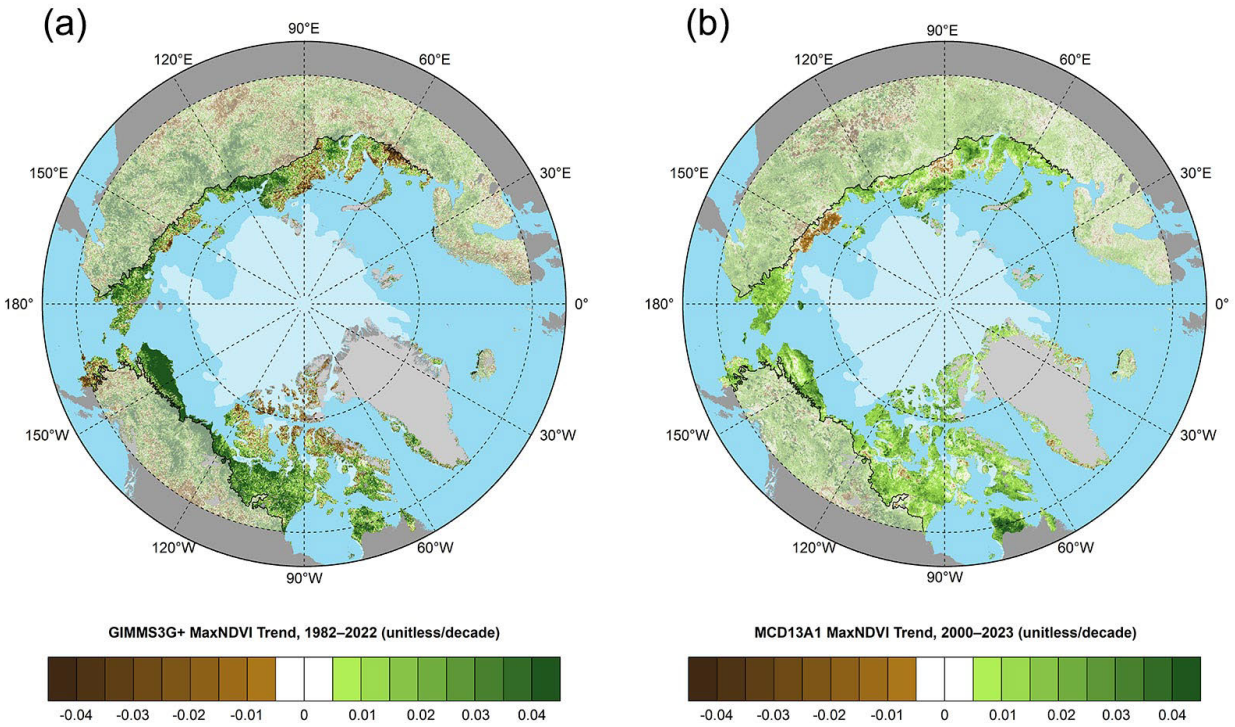

Fig. 1. Magnitude of the MaxNDVI trend calculated as the change per decade using ordinary least squares regression for Arctic tundra (solid colors), and boreal forest north of 60° latitude (muted colors) during (a) 1982-2022 based on the AVHRR GIMMS 3-g+ dataset, and (b) 2000-23 based on the MODIS MCD13A1 v6.1 dataset. In each panel, the circumpolar treeline is indicated by a black line, and the 15 August 2023 sea-ice extent is indicated by light shading.

The boreal forest biome (see Figs. 1a,b), which occupies large swaths of northern Eurasia and North America, has also emerged as a focal point of global environmental change. In this region, greening has generally prevailed along the forest-tundra ecotone in the north, whereas browning has been more frequent in the interior of the boreal forest biome (Berner and Goetz 2022). Patches of positive and negative greenness trends are widely interspersed, reflecting complex interactions among the biome's active wildfire regime, changing climate, extreme events, pathogens, and other factors (Foster et al. 2022).

In 2022—the most recent year with observations from both AVHRR and MODIS—circumpolar mean MaxNDVI for tundra regions was at or near record high values in both records. The AVHRR-observed MaxNDVI was the highest value on record (1982-2022), increasing 9.8% from 2021 (Fig. 2). Notably, the eight highest values in the 41-year AVHRR record have all been recorded within the last 12 years (i.e., 2011-22). The MODIS-observed circumpolar mean MaxNDVI value declined slightly (0.9%) from 2021 and was only 2.0% lower than the record high value observed in 2020. Circumpolar MaxNDVI trends derived from the two sensors are virtually identical for the period of overlap (2000-22), although the AVHRR record displays much higher variability, especially over the last 15 years. This is likely due in part to the lower spatial resolution and less advanced calibration of the AVHRR sensor compared to MODIS.

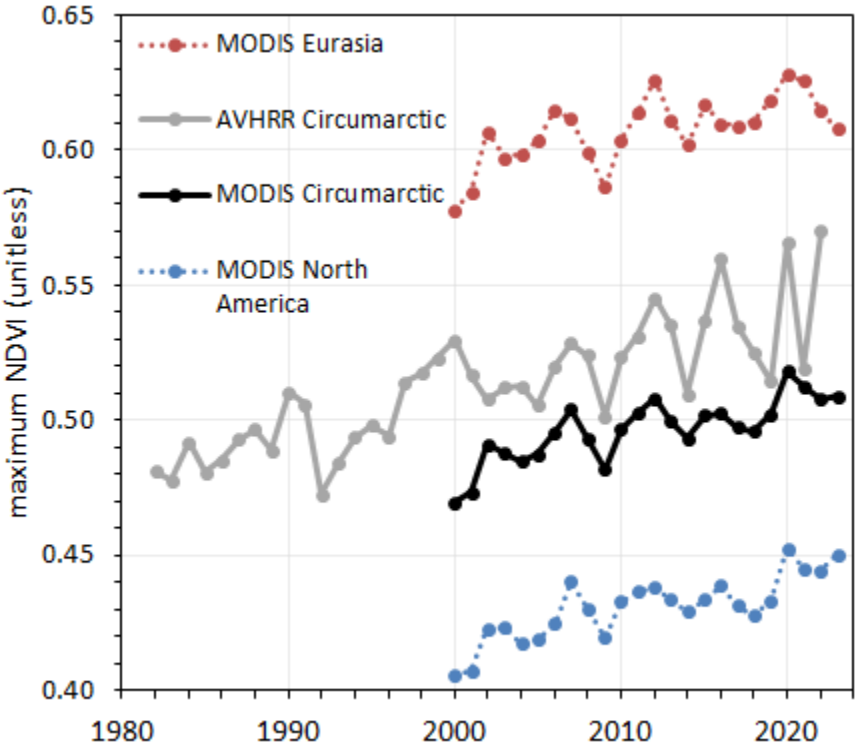

Fig. 2. Time-series of mean MaxNDVI for Arctic tundra from the MODIS MCD13A1 v6.1 (2000-23) dataset for the Eurasian Arctic (red), North American Arctic (blue), and the circumpolar Arctic (black), and from the long-term AVHRR GIMMS-3g+ dataset (1982-2022) for the circumpolar Arctic (gray).

In 2023, the circumpolar MODIS-observed MaxNDVI value increased slightly (0.3%) from the previous year and represents the third highest value in the 24-year MODIS record (Fig. 2). Tundra greenness was much higher than normal across most of the North American Arctic and especially in the Beaufort Sea region, but not in Eurasia, particularly in the East Siberian Sea region where sea ice persisted for much of the summer (Fig. 3). The overall trend in MODIS-observed circumpolar MaxNDVI remains strongly positive, with four of the five highest values in the 24-year record occurring in the last four years (Fig. 2).

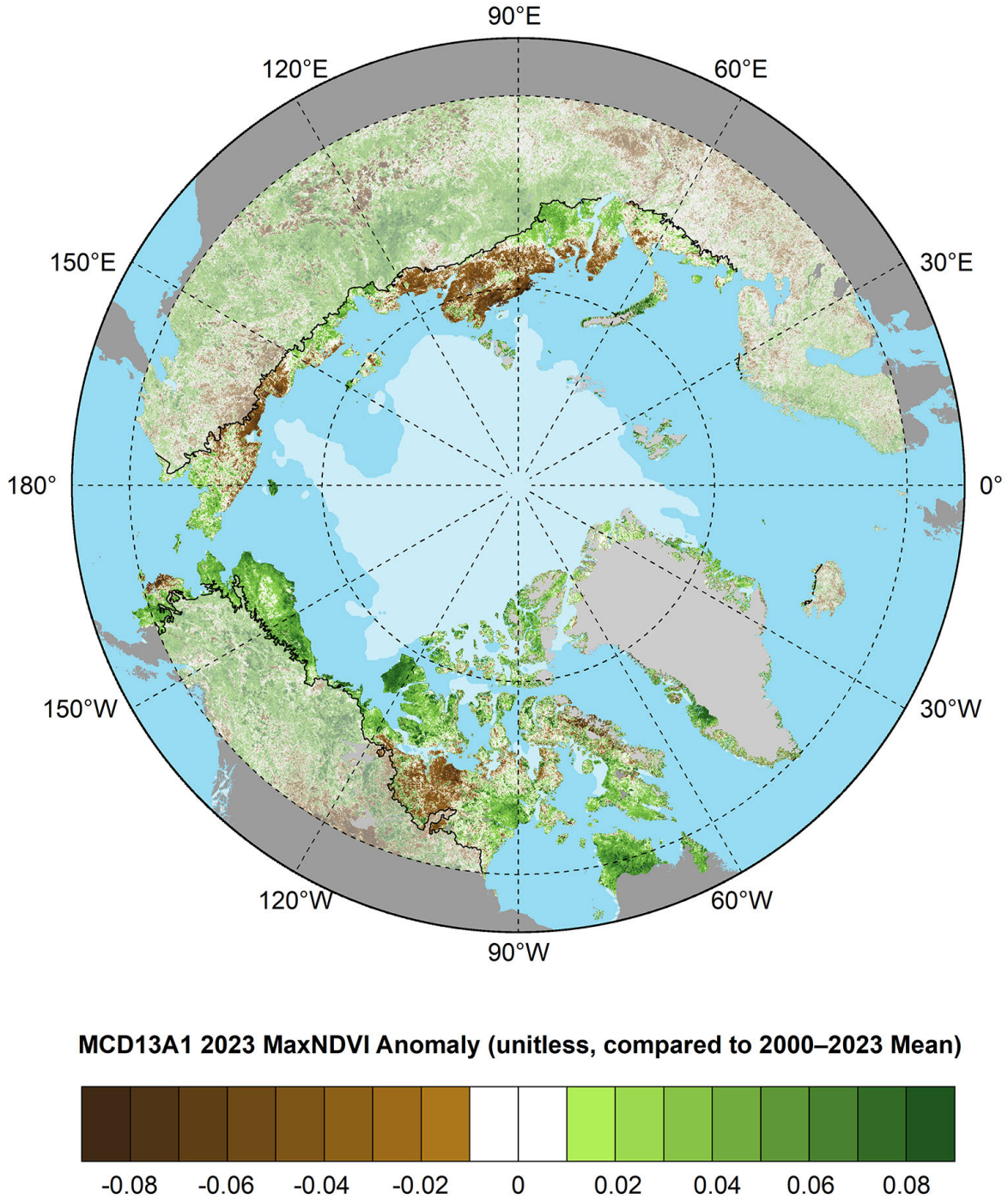

Fig. 3. Circumpolar MaxNDVI anomalies for Arctic tundra (solid colors), and boreal forest north of 60° latitude (muted colors) for the 2023 growing season relative to mean values (2000-23) from the MODIS MCD13A1 v6.1 dataset. The circumpolar treeline is indicated by a black line and the 15 August 2023 sea-ice extent is indicated by light shading.

Drivers and consequences of Arctic greening

Although the underlying drivers of Arctic greening vary from place to place, a growing body of observations brings into focus the types of change that an observer might see on the ground. One of the most widely studied manifestations of Arctic greening is *shrubification*—an increase in the cover, height, and biomass of tundra shrubs such as willows, birches, and alders (Fig. 4) (Mekonnen et al. 2021), largely at the expense of lichens and mosses, which have lower NDVI values (Erlandsson et al. 2023). Shrubification is also one of the most prevalent forms of change identified by Arctic residents, with consequences for wildlife abundance and human subsistence.

Fig. 4. Arctic landscapes present a complex mosaic of vegetation and waterbodies, which create variability in greenness trends across spatial scales (upper left; Seward Peninsula, Alaska). The expansion of shrubs, such as diamondleaf willow (*Salix pulchra*), is a key long-term driver of Arctic greening (upper right; Mulgrave Hills, Alaska), while ecological disturbances related to permafrost thaw (lower left; Noatak National Preserve, Alaska) and tundra wildfire (lower right; Kanuti River drainage, Alaska) can trigger abrupt declines in greenness at local scales. Photos by G. V. Frost (upper row and lower right) and M. J. Lara (lower left).

Although the satellite record provides unequivocal evidence of widespread tundra greening, there is substantial regional variability in trends that is likely driven by finer-scale, local patterns of vegetation cover and change. Some Arctic regions exhibit little or no trend, while a few, such as the East Siberian Sea sector, exhibit widespread declines, which are thought to reflect ground subsidence and increased surface water triggered by recent permafrost thaw and spring flood events (Magnússon et al. 2023).

Arctic animals can also influence vegetation greenness. For example, in northwestern Siberia, decadal evidence from MODIS and detailed ground-level migration data link herbivory by large semi-domesticated reindeer herds with lower coverage of deciduous shrubs (Spiegel et al. 2023).

While NDVI is typically observed from space, it can also be measured on the ground in tandem with detailed vegetation surveys, providing valuable local context for the trends observed by satellites. For example, Huemmrich et al. (2023) compared ground-based NDVI measurements from circa 2001 and 2022 along a transect near Utqiaġvik, Alaska. They found that field-measured NDVI trends largely mirrored greening trends detected by MODIS, and were accompanied by increases in leaf area, particularly in wet portions of the landscape.

Arctic greenness trends are influenced by a complex set of interacting climatic and environmental drivers. In the big picture, circumpolar tundra productivity has generally tracked climatic warming over multiple decades. However, the dynamics evident in satellite time-series also reflect many sources of interannual and decadal variability. For example, large-scale atmospheric patterns, such as the Arctic Oscillation and Arctic Dipole, have cascading effects on oceanic circulation, sea-ice extent, and surface air temperatures that influence tundra productivity (Polyakov et al. 2023). These cascading effects create complexity in Arctic greenness trends that operate against the backdrop of long-term climatic warming and sea-ice decline.

Methods and data

The satellite record of Arctic tundra greenness began in late 1981 using AVHRR, a sensor that collects daily observations and continues to operate onboard polar-orbiting satellites. As of September 2023, however, processed AVHRR data were only available through the 2022 growing season. Therefore, we also report observations from the Moderate Resolution Imaging Spectroradiometer (MODIS), a more modern sensor that became operational in 2000. The long-term AVHRR dataset analyzed here for 1982-2022 is the Global Inventory Modeling and Mapping Studies 3g V1.2 dataset (GIMMS-3g+), which is based on corrected and calibrated AVHRR data with a spatial resolution of about 8 km (Pinzon et al. 2023). For MODIS, we computed tundra greenness trends for 2000-23 at a much higher spatial resolution of 500 m, combining 16-day Vegetation Index products from Terra (MOD13A1, version 6.1) and Aqua (MYD13A1, version 6.1) (Didan 2021a,b), referred to here as MCD13A1. Circumpolar maps depicting greenness trends cover the Arctic tundra biome, as well as boreal forest and non-Arctic tundra above 60° N latitude. Time-series plots are based solely on tundra environments within the extent of the Circumpolar Arctic Vegetation Map (Raynolds et al. 2019). MODIS data were further masked to exclude permanent water based on the 2015 MODIS Terra Land Water Mask (MOD44W, version 6). We summarize the GIMMS-3g+ and MODIS records for Maximum NDVI (MaxNDVI), the peak yearly value that is typically observed during the months of July and August.

Acknowledgments

We thank J. Pinzon at the Biospheric Sciences Laboratory, NASA Goddard Space Flight Center for providing updates for the GIMMS-3g+ dataset.

References

Bartsch, A., and Coauthors, 2021: Expanding infrastructure and growing anthropogenic impacts along Arctic coasts. *Environ. Res. Lett.*, **16**, 115013, https://doi.org/10.1088/1748-9326/ac3176.

Berner, L. T., and S. J. Goetz, 2022: Satellite observations document trends consistent with a boreal forest biome shift. *Global Change Biol.*, **28**(10), 3275-3292, https://doi.org/10.1111/gcb.16121.

Didan, K., 2021a: MODIS/Terra Vegetation Indices 16-Day L3 Global 500m SIN Grid V061 [Data set]. NASA EOSDIS Land Processes Distributed Active Archive Center, https://doi.org/10.5067/MODIS/MOD13A1.061.

Didan, K., 2021b: MODIS/Aqua Vegetation Indices 16-Day L3 Global 500m SIN Grid V061 [Data set]. NASA EOSDIS Land Processes Distributed Active Archive Center, https://doi.org/10.5067/MODIS/MYD13A1.061.

Erlandsson, R., M. K. Arneberg, H. Tømmervik, E. A. Finne, L. Nilsen, and J. W. Bjerke, 2023: Feasibility of active handheld NDVI sensors for monitoring lichen ground cover. *Fungal Ecol.*, **63**, 101233, https://doi.org/10.1016/j.funeco.2023.101233.

Foster, A. C., and Coauthors, 2022: Disturbances in North American boreal forest and Arctic tundra: impacts, interactions, and responses. *Environ. Res. Lett.*, **17**, 113001, https://doi.org/10.1088/1748-9326/ac98d7.

Heijmans, M. M. P. D., and Coauthors, 2022: Tundra vegetation change and impacts on permafrost. *Nat. Rev. Earth Environ.*, **3**, 68-84, https://doi.org/10.1038/s43017-021-00233-0.

Huemmrich, K. F., J. Gamon, P. Campbell, M. Mora, S. Vargas Z, B. Almanza, and C. Tweedie, 2023: 20 years of change in tundra NDVI from coupled field and satellite observations. *Environ. Res. Lett.*, **18**, 094022, https://doi.org/10.1088/1748-9326/acee17.

Magnússon, R. Í., F. Groten, H. Bartholomeus, K. van Huissteden, and M. M. P. D. Heijmans, 2023: Tundra browning in the Indigirka Lowlands (north-eastern Siberia) explained by drought, floods and small-scale vegetation shifts. *J. Geophys. Res.-Biogeosci.*, **128**, e2022JG007330, https://doi.org/10.1029/2022JG007330.

Mekonnen, Z. A., and Coauthors, 2021: Arctic tundra shrubification: a review of mechanisms and impacts on ecosystem carbon balance. *Environ. Res. Lett.*, **16**, 053001, https://doi.org/10.1088/1748-9326/abf28b.

Pinzon, J. E., E. W. Pak, C. J. Tucker, U. S. Bhatt, G. V. Frost, and M. J. Macander, 2023: Global Vegetation Greenness (NDVI) from AVHRR GIMMS-3G+, 1981-2022 [Data set]. ORNL DAAC, Oak Ridge, TN, USA, https://doi.org/10.3334/ORNLDAAC/2187.

Polyakov, I. V., R. B. Ingvaldsen, A. V. Pnyushkov, U. S. Bhatt, J. A. Francis, M. Janout, R. Kwok, and Ø. Skagseth, 2023: Fluctuating Atlantic inflows modulate Arctic atlantification. *Science*, **381**, 972-979, https://doi.org/10.1126/science.adh5158.

Raynolds, M. K., and Coauthors, 2019: A raster version of the Circumpolar Arctic Vegetation Map (CAVM). *Remote Sens. Environ.*, **232**, 111297, https://doi.org/10.1016/j.rse.2019.111297.

Rogers, A., S. P. Serbin, and D. A. Way, 2022: Reducing model uncertainty of climate change impacts on high latitude carbon assimilation. *Global Change Biol.*, **28**, 1222-1247, https://doi.org/10.1111/gcb.15958.

Spiegel, M. P., A. Volkovitskiy, A. Terekhina, B. C. Forbes, T. Park, and M. Macias-Fauria, 2023: Top-down regulation by a reindeer herding system limits climate-driven Arctic vegetation change at a regional scale. *Earth's Future*, **11**, e2022EF003407, https://doi.org/10.1029/2022EF003407.

November 12, 2023

Permafrost Beneath Arctic Ocean Margins

https://doi.org/10.25923/fzwe-6432

P. P. Overduin[1], A. Portnov[2,3], and C. D. Ruppel[4]

[1]Permafrost Research Section, Alfred Wegener Institute, Helmholtz Centre for Polar and Marine Research, Potsdam, Germany
[2]Instituto Andaluz de Ciencias de la Tierra, CSIC-Universidad de Granada, Granada, Spain
[3]University of Texas Institute for Geophysics, Austin, TX, USA
[4]U.S. Geological Survey, Woods Hole, MA, USA

Headlines

- Since the end of the Last Glacial Maximum (~21,000 years ago), rising sea levels have inundated terrestrial permafrost surrounding the Arctic Ocean, resulting in subsea permafrost.
- An estimated 2.5 million km^2 of subsea permafrost remains today, but it continues to thaw due to the original ocean inundation event and more recent, rapid Arctic warming.
- Observations from the Beaufort and Kara Seas reveal that the remaining subsea permafrost is mostly distributed in coastal waters less than 30 m deep. Subsea permafrost distribution on the vast Siberian margin is comparatively poorly understood.
- International research collaboration is needed to address critical questions regarding the extent and current state of subsea permafrost and to estimate the potential release of greenhouse gases (carbon dioxide and methane) as it thaws.

Introduction

Even among scientists, it is not widely known that sediment beneath many continental shelves surrounding the Arctic Ocean is frozen. In areas that were exposed and not glaciated at the Last Glacial Maximum (LGM; approximately 21,000 years ago), prolonged subaerial exposure froze the ground down to hundreds of meters below the surface, creating permafrost. During deglaciation, sea levels rose and ocean water inundated coastal permafrost at low elevations, resulting in model estimates of 2.5 million km^2 of ice-bearing subsea permafrost today (Fig. 1, Overduin et al. 2019). Today, terrestrial permafrost extends from the boreal forests on the south to the Arctic Ocean coastline on the north. On some Arctic Ocean margins, subsea permafrost starts at the coastline and continues northward beneath the seabed, even reaching the edge of the continental shelf in some places.

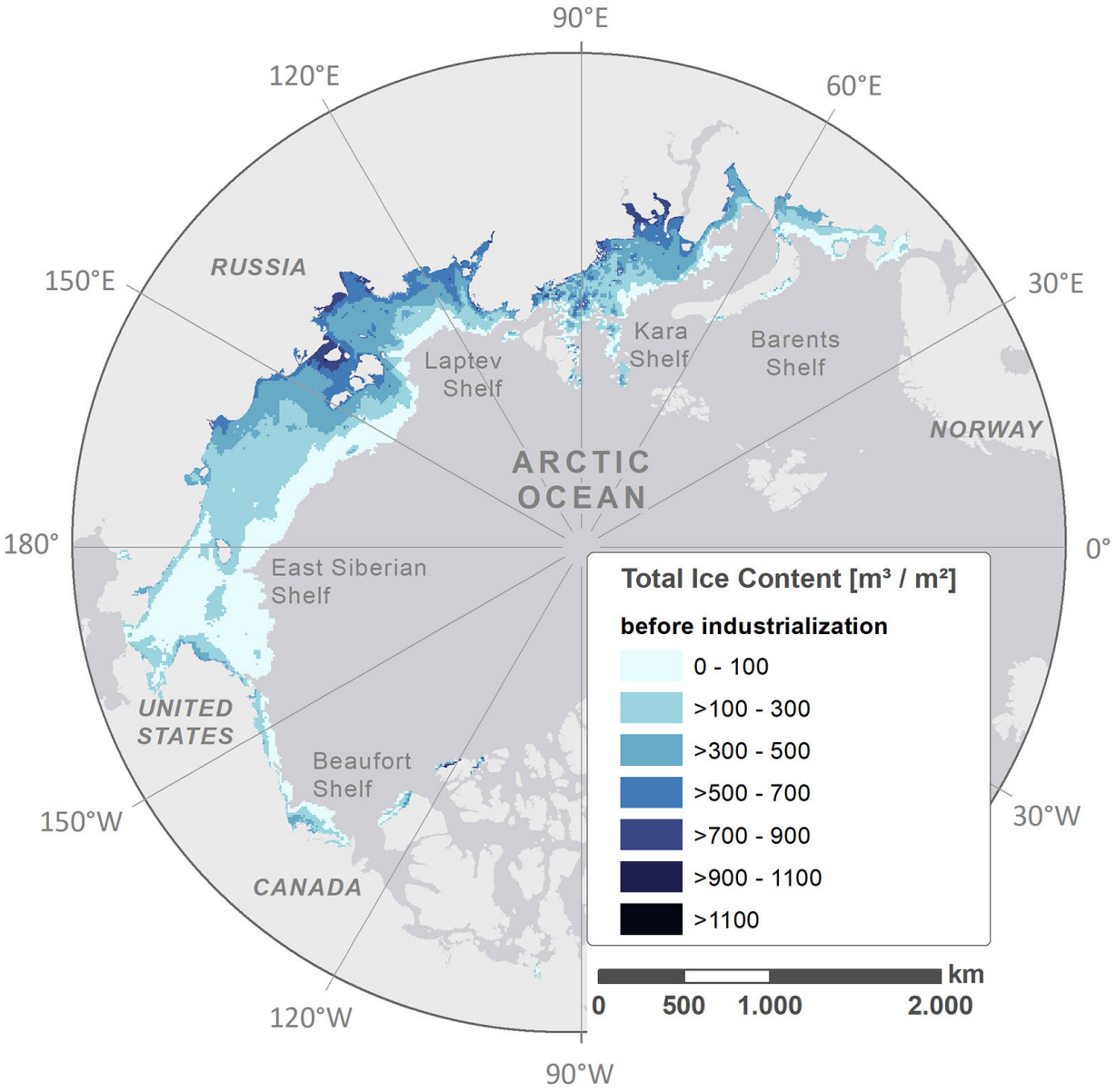

Fig. 1. Total ice content (in cubic meters per square meter) in the Arctic shelf sediment column based on modeled subsurface heat flow, accounting for glacial and sea level histories over the past 400,000 years (Overduin et al. 2019). The value shown is the estimated total amount of ice in the sediment column and represents total ice content "before industrialization", i.e., before human effects on the global climate, at ~1850.

Terrestrial permafrost is defined as earth material that remains below 0°C for at least two consecutive years. A key difference between terrestrial permafrost and permafrost below the seafloor on continental shelves is the presence of salt. Because salt depresses the freezing point of water, subsea sediment can remain unfrozen (containing no ice) even at temperatures <0°C. For this reason, delineation of subsea permafrost typically relies not on the temperature of the sediment, but rather on an observation or inference of ice being present. This essay reports on recent subsea permafrost studies and places them in a pan-Arctic context, thereby underscoring the need for far better data on many Arctic Ocean margins.

The sea level rise that inundated terrestrial permafrost (producing subsea permafrost) replaced the very low average annual air temperatures (-10 to -20°C) above the tundra with seawater close to or above freezing (-2 to 0°C) for most of the year. This significant increase in overlying temperatures has led to thawing at both the top and bottom of subsea permafrost (e.g., Taylor et al. 2013). The infiltration of saline waters affects thaw patterns, fluid flow, and gas migration within the subsea permafrost region. With thawing, organic carbon previously held in frozen sediments becomes more available for microbial decomposition, producing greenhouse gases such as methane that may migrate toward the seafloor, ultimately reaching the ocean and possibly the atmosphere. If released into the atmosphere, these gases could further enhance global warming. Thawing also reduces the effectiveness of subsea permafrost as a trap for gases rising from deep layers, which might contain oil and gas deposits.

The current state of subsea permafrost has been characterized in only a few locations around the Arctic Ocean. The next section reviews observations that constrain the distribution of subsea permafrost on two well-studied Arctic Ocean margins: the Beaufort Sea and the Kara Sea.

Beaufort Sea observations

In the past decade, direct observations from the Beaufort Sea offshore of Canada and Alaska have provided evidence about the extent of ice-bearing subsea permafrost for this part of the Arctic Ocean margin. In both settings, researchers have combined legacy borehole data and seismic data to estimate the seaward extent of subsea permafrost and certain characteristics of its vertical distribution. Beneath the U.S. Beaufort continental shelf, seismically-defined subsea permafrost extends at least 3 to 17 km offshore the coast from Smith Bay to Prudhoe Bay and is very close to the coastline from Prudhoe Bay to the U.S.-Canada border (Fig. 2; Brothers et al. 2016; Ruppel et al. 2016). The water depths coinciding with the minimum seaward extent of subsea permafrost are less than 20 m along this entire section. Permafrost thicknesses onshore adjacent to the coast range from approximately 300 to 600 m. On the Canadian shelf, subsea permafrost underlies a larger portion of the Beaufort Sea in shelf waters up to 100 m deep and extending more than 130 km offshore (Hu et al. 2013; Grob et al. 2023). The subsea permafrost is almost 700 m thick near the coastline and thins towards the edge of the continental shelf, where recent changes in seabed morphology may indicate seafloor subsidence and thawing of ice in the sediment (Paull et al. 2022), possibly in response to groundwater flow beneath the subsea permafrost. Ice-bearing seafloor mounds called pingo-like features (PLFs), some of which emit methane-rich gas, may be an indication of sediment warming (Paull et al. 2007) in the Canadian Beaufort Sea. In both U.S. and Canadian settings, subsea permafrost is inferred to be degrading simultaneously from the top and the bottom (Ruppel et al. 2016; Grob et al. 2023), consistent with models (Taylor et al. 2013; Farquharson et al. 2018). The differences between the subsea permafrost distributions on the U.S. and Canadian Beaufort shelves (Brothers et al. 2016) probably reflect several factors, including massive freshwater outflows from the Mackenzie River; varying glacial, inundation, and uplift/subsidence histories (Farquharson et al. 2018); and differences in tectonic regimes (a passive margin on the west and a more compressive margin with substantial faulting, folding, and deeper fluid migration on the east).

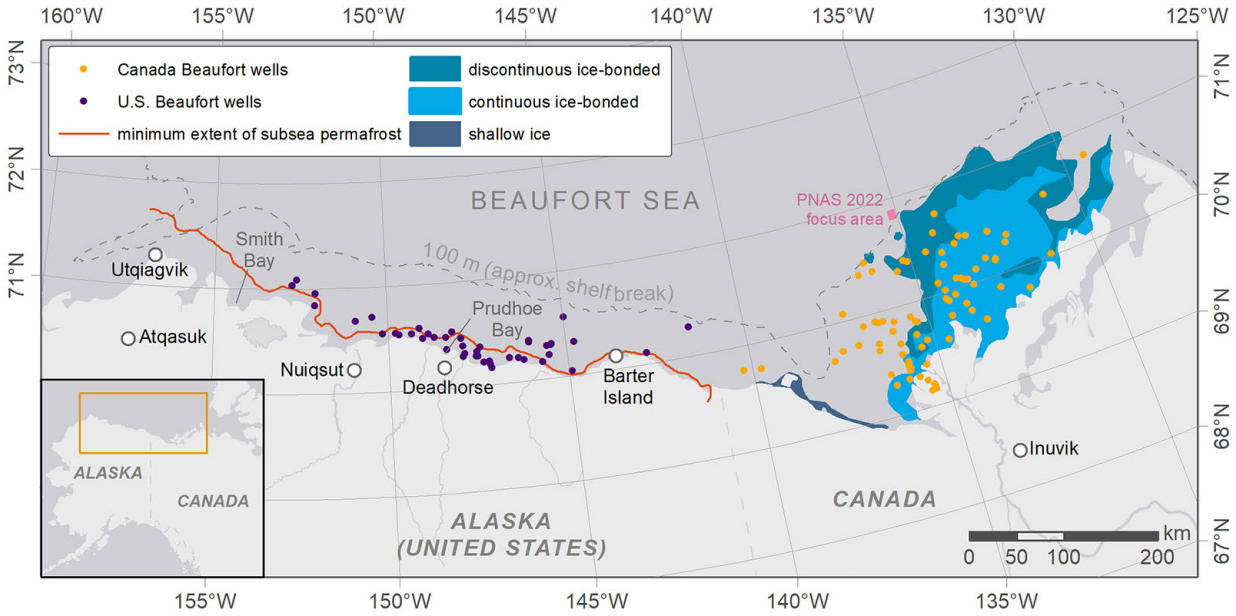

Fig. 2. Subsea permafrost extent on the Beaufort Sea margin. Purple and orange circles indicate logged boreholes on the U.S. (Ruppel et al. 2016) and Canadian margins, respectively. On the U.S. side, the red curve is the minimum offshore extent of subsea permafrost from Brothers et al. (2016) based on seismic velocity analysis. For the Canadian margin, light and medium blue indicate continuous and discontinuous ice-bonded permafrost, respectively. The dark blue shading west of the Mackenzie River along the Canadian coastline marks an area where shallow boreholes encountered ice. The Canadian margin compilation is after Grob et al. (2023). The pink square shows the location of the Paull et al. (2022) study.

Recent observations from the Kara Sea

The Beaufort shelf, while being the best studied for subsea permafrost, constitutes only 4% of the circum-Arctic Ocean shelf area, compared to 25% for the Siberian shelf. Most of the observational data analyzed so far for the Siberian shelf come from the Kara Sea, where high-resolution seismic data, limited borehole data, and water column observations were used to infer subsea permafrost distribution and thaw patterns. Unlike the Barents Sea, vast areas of the Kara Sea shelf remained unglaciated at the LGM (Nazarov et al. 2022) and therefore froze to hundreds of meters depth, as corroborated by sediment ice content modeled over four glacial cycles (Fig. 3a; Overduin et al. 2019). Seismic and water column records indicate extensive seafloor gas release, which indicates partial or complete permafrost thaw at water depths greater than 20 m (Fig. 3b; Portnov et al. 2013). Work in the Kara Sea has shown that floating ice scours the shallow seafloor (<26 m water depth; Ogorodov et al. 2013), affecting up to 100% of the seabed in some areas and potentially providing an alternative explanation for gas release. However, a combined modeling and observational approach suggests that continuous subsea permafrost thins from ~400 m near the coast to discontinuous or absent with increasing distance from the coastline, out to 20 m water depth (Portnov et al. 2014). Discontinuous subsea permafrost may extend further seaward in deeper waters, out to ~110 m water depth. Additional evidence for Kara Sea permafrost thawing comes from a study of PLFs (Serov et al. 2015); a PLF located at ~35 m water depth has very high methane concentrations and almost no remaining ice-bearing sediments near the seafloor. This suggests that the permafrost cap has degraded and that gas is freely migrating towards the seafloor.

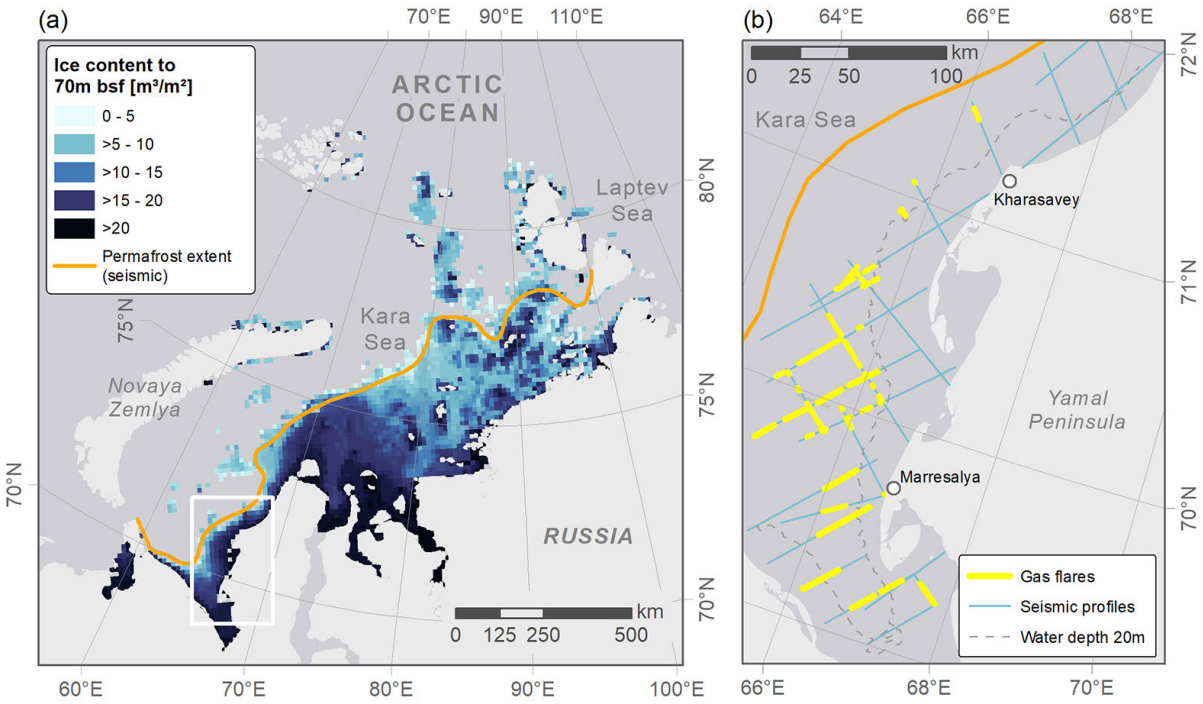

Fig. 3. Map of subsea permafrost indicators for the eastern Kara Sea. (a) The maximum seismically determined extent of discontinuous subsea permafrost (orange curve) is compared to modeled ice volume in the upper 70 m of sediment (Overduin et al. 2019; m bsf = meters below the sea floor). The white rectangle marks the extent of the map in (b). (b) The inferred maximum extent of discontinuous subsea permafrost (orange curve). The yellow segments of the light blue seismic lines show areas where gas flares were detected. The dashed line marks the 20 m isobath, which is the seaward extent of continuous permafrost based on seafloor gas releases.

Fewer observations for the rest of the Arctic shelf

More than 80% of Arctic subsea permafrost is likely to lie beneath the most areally-extensive shelves—those of the Laptev and East Siberian Seas. This shallow continental shelf region is the widest on Earth, extending 800 km poleward from coastline to shelf break, and the entire expanse was subaerial and almost completely unglaciated when ice caps were at their most extensive and sea levels at their lowest (around 21,000 years ago). The resulting deep freeze produced permafrost thicknesses that exceed 700 m at the coastline. Almost no data are available to constrain the distribution and characteristics of subsea permafrost on this margin. In particular, most boreholes described in the literature are less than 100 m deep and located within 20 km of the coast. Seismic data from the outer Laptev shelf suggest that permafrost extends from the coast to roughly 60 m water depth and reveal the presence of buried terrestrial permafrost landforms (Rekant et al. 2015; Bogoyavlensky et al. 2022). The lessons of the Beaufort margin imply that the even larger Eastern Siberian shelf margin is likely to have significant spatial variations in the offshore extent of subsea permafrost since the effects of the last glaciation were probably experienced at different times over such a large geographic area.

The longevity of subsea permafrost is dependent on bottom water temperatures and salinity in the overlying waters, as well as geothermal heat flow at the base of the permafrost. The longer the period of inundation, the deeper the top of ice-bearing permafrost thaws, but the slower its thaw rate. Thaw depths observed in boreholes in the Beaufort and Laptev Seas have reached less than 100 m below the seafloor after thousands of years of inundation (Angelopoulos et al. 2020). In the Laptev and East

Siberian Seas, annual sea ice formation is associated with sustained negative mean bottom water temperatures, which partially stabilize subsea permafrost against top-down thawing.

International collaborative research opportunity

The initial thawing of subsea permafrost was triggered by inundation during sea level rise following the end of the last glaciation. In the future, the rate of subsea permafrost thaw is expected to increase due to rapidly warming bottom water temperatures in an increasingly sea-ice-free Arctic Ocean (e.g., Wilkenskjeld et al. 2022), and new subsea permafrost will be added as low-lying coastal areas are covered by rising seas. The paucity of observational data about the extent of contemporary subsea permafrost on circum-Arctic Ocean shelves, especially on the vast Siberian margin, provides no baseline for comparing future subsea permafrost distributions nor for quantifying the rate of loss and implications of thawing. Critical questions are how much gas (particularly the greenhouse gases, carbon dioxide and methane) is trapped within and beneath subsea permafrost in bubbles or as frozen gas hydrates, and how rates of microbial methane production, gas hydrate dissociation, and gas migration may increase as sediments warm and ice thaws (Ruppel and Kessler 2017). Characterizing the extent and current state of subsea permafrost and estimating the potential gas release associated with its thaw could be productive areas for greater international and transboundary research cooperation.

Conclusions

Available observational data provide an incomplete picture of the circum-Arctic Ocean distribution of subsea permafrost, its current state (continuous vs. discontinuous; ice content) and its susceptibility to future warming. The perspective emerging from studies in the Beaufort and Kara Seas implies that substantial permafrost thaw has occurred under continental shelves over the last ~21,000 years since the onset of deglacial sea level rise. Lacking better constraints on the extent of subsea permafrost under the vast Siberian continental shelf, it is difficult to predict when future warming could lead to the complete disappearance of present-day subsea permafrost or to assess the likelihood and timing of enhanced seafloor releases of carbon dioxide and methane as a consequence of permafrost thaw.

Acknowledgments

P. Overduin received funding under the European Union's Horizon 2020 Research and Innovation Programme under grant agreement no. 773421. C. Ruppel's research was funded by the National Methane Hydrates R&D Program at the U.S. Dept. of Energy under agreements DE-FE0023495 and 89243320SFE000013. We thank Sebastian Laboor of AWI for producing the figures.

References

Angelopoulos, M., P. P. Overduin, F. Miesner, M. N. Grigoriev, and A. A. Vasiliev, 2020: Recent advances in the study of Arctic submarine permafrost. *Permafrost Periglacial Processes*, **31**, 442-453, https://doi.org/10.1002/ppp.2061.

Bogoyavlensky, V., A. Kishankov, A. Kazanin, and G. Kazanin, 2022: Distribution of permafrost and gas hydrates in relation to intensive gas emission in the central part of the Laptev Sea (Russian Arctic). *Mar. Petrol. Geol.*, **138**, 105527, https://doi.org/10.1016/j.marpetgeo.2022.105527.

Brothers, L. L., B. M. Herman, P. E. Hart, and C. D. Ruppel, 2016: Subsea ice-bearing permafrost on the US Beaufort margin: 1. Minimum seaward extent defined from multichannel seismic reflection data. *Geochem. Geophys. Geosyst.*, **17**, 4354-4365, https://doi.org/10.1002/2016GC006584.

Farquharson, L., D. Mann, T. Rittenour, P. Groves, G. Grosse, and B. Jones, 2018: Alaskan marine transgressions record out-of-phase Arctic Ocean glaciation during the last interglacial. *Geology*, **46**, 783-786, https://doi.org/10.1130/g40345.1.

Grob, H., M. Riedel, M. J. Duchesne, S. Krastel, J. Bustamante, G. Fabien-Ouellet, Y. K. Jin, and J. K. Hong, 2023: Revealing the extent of submarine permafrost and gas hydrates in the Canadian Arctic Beaufort Sea using seismic reflection indicators. *Geochem. Geophys. Geosyst.*, **24**, e2023GC010884, https://doi.org/10.1029/2023GC010884.

Hu, K., D. R. Issler, Z. Chen, and T. A. Brent, 2013: Permafrost investigation by well logs, and seismic velocity and repeated shallow temperature surveys, Beaufort-Mackenzie Basin. Natural Resources Canada/CMSS/Information Management, Open File 6956, https://doi.org/10.4095/293120.

Nazarov, D. V., O. A. Nikolskaia, I. V. Zhigmanovskiy, M. V. Ruchkin, and A. A. Cherezova, 2022: Lake Yamal, an ice-dammed megalake in the West Siberian Arctic during the Late Pleistocene, ~60-35 ka. *Quat. Sci. Rev.*, **289**, 107614, https://doi.org/10.1016/j.quascirev.2022.107614.

Ogorodov, S., V. Arkhipov, O. Kokin, A. Marchenko, P. Overduin, and D. Forbes, 2013: Ice effect on coast and seabed in Baydaratskaya Bay, Kara Sea. *Geogr. Environ. Sustain.*, **6**, 21-37, https://doi.org/10.24057/2071-9388-2013-6-3-21-37.

Overduin, P. P., and Coauthors, 2019: Submarine permafrost map in the Arctic modeled using 1-D transient heat flux (SuPerMAP). *J. Geophys. Res.-Oceans*, **124**, 3490-3507, https://doi.org/10.1029/2018jc014675.

Paull, C. K., and Coauthors, 2007: Origin of pingo-like features on the Beaufort Sea shelf and their possible relationship to decomposing methane gas hydrates. *Geophys. Res. Lett.*, **34**, L01603, https://doi.org/10.1029/2006gl027977.

Paull, C. K., S. R. Dallimore, Y. K. Jin, and H. Melling, 2022: Rapid seafloor changes associated with the degradation of Arctic submarine permafrost. *Proc. Natl. Acad. Sci.*, **119**, e2119105119, https://doi.org/10.1073/pnas.2119105119.

Portnov, A., A. J. Smith, J. Mienert, G. Cherkashov, P. Rekant, P. Semenov, P. Serov, and B. Vanshtein, 2013: Offshore permafrost decay and massive seabed methane escape in water depths >20 m at the South Kara Sea shelf. *Geophys. Res. Lett.*, **40**, 3962-3967, https://doi.org/10.1002/grl.50735.

Portnov, A., J. Mienert, and P. Serov, 2014: Modeling the evolution of climate-sensitive Arctic subsea permafrost in regions of extensive gas expulsion at the West Yamal shelf. *J. Geophys. Res.-Biogeosci.*, **119**, 2082-2094, https://doi.org/10.1002/2014jg002685.

Rekant, P., H. A. Bauch, T. Schwenk, A. Portnov, E. Gusev, V. Spiess, G. Cherkashov, and H. Kassens, 2015: Evolution of subsea permafrost landscapes in Arctic Siberia since the Late Pleistocene: a synoptic insight from acoustic data of the Laptev Sea. *Arktos*, **1**, 11, https://doi.org/10.1007/s41063-015-0011-y.

Ruppel, C. D., B. M. Herman, L. L. Brothers, and P. E. Hart, 2016: Subsea ice-bearing permafrost on the U.S. Beaufort margin: 2. Borehole constraints. *Geochem. Geophys. Geosyst.*, **17**, 4333-4353, https://doi.org/10.1002/2016GC006582.

Ruppel, C. D., and J. D. Kessler, 2017: The interaction of climate change and methane hydrates. *Rev. Geophys.*, **55**, 126-168, https://doi.org/10.1002/2016RG000534.

Serov, P., A. Portnov, J. Mienert, P. Semenov, and P. Ilatovskaya, 2015: Methane release from pingo-like features across the South Kara Sea shelf, an area of thawing offshore permafrost. *J. Geophys. Res.-Earth*, **120**, 1515-1529, https://doi.org/10.1002/2015jf003467.

Taylor, A. E., S. R. Dallimore, P. R. Hill, D. R. Issler, S. Blasco, and F. Wright, 2013: Numerical model of the geothermal regime on the Beaufort Shelf, arctic Canada since the Last Interglacial. *J. Geophys. Res.-Earth*, **118**, 2365-2379, https://doi.org/10.1002/2013jf002859.

Wilkenskjeld, S., F. Miesner, P. P. Overduin, M. Puglini, and V. Brovkin, 2022: Strong increase in thawing of subsea permafrost in the 22nd century caused by anthropogenic climate change. *Cryosphere*, **16**, 1057-1069, https://doi.org/10.5194/tc-16-1057-2022.

November 14, 2023

Nunaaqqit Savaqatigivlugich: Working with Communities to Observe the Arctic

https://doi.org/10.25923/2sx6-kx89

R. T. Glenn-Borade[1,2], B. Adams[3], R. Schaeffer[4], C. SimsKayotuk[5], G. Omnik[6], J. M. Leavitt[3], and D. D. W. Hauser[1,2]

[1]International Arctic Research Center, University of Alaska Fairbanks, Fairbanks, AK, USA
[2]Alaska Arctic Observatory and Knowledge Hub, Fairbanks, AK, USA
[3]Alaska Arctic Observatory and Knowledge Hub, Utqiaġvik, AK, USA
[4]Alaska Arctic Observatory and Knowledge Hub, Kotzebue, AK, USA
[5]Alaska Arctic Observatory and Knowledge Hub, Kaktovik, AK, USA
[6]Alaska Arctic Observatory and Knowledge Hub, Point Hope, AK, USA

Headlines

- The Alaska Arctic Observatory and Knowledge Hub (AAOKH) works with a network of coastal Indigenous observers to document long-term and holistic observations of environmental change and impacts in northern Alaska.
- Recently, Indigenous observers have noted sea ice loss, warmer air and ocean temperatures, changing wind patterns, and increased intensity and frequency of coastal storms that contribute to flooding and erosion.
- Indigenous observers also document local-scale impacts of environmental changes to community and cultural infrastructure, traditional harvests and activities, and travel safety across the land and sea.
- Applying and centering Indigenous perspectives and observations of Arctic change in decision-making can lead to more inclusive, equitable, and community-led responses.

Introduction

> *"What is a key environmental change in your community that you want people to know about?" "The sea ice and permafrost are melting too fast."*
>
> – Joe Mello Leavitt [Iñupiat], Utqiaġvik (AAOKH 2023).

Numerous lines of evidence indicate how climate change is unfolding in the Arctic (see essay *Executive Summary*). Understanding and responding to these changes, many of which impact coastal Indigenous communities, can be strengthened by the inclusion of community-based observations. Community-based observations provide a local perspective not available through conventional scientific methods alone and can fill existing spatial or temporal knowledge gaps (Danielsen et al. 2020; Eicken et al. 2021).

The Alaska Arctic Observatory and Knowledge Hub (AAOKH) is a collaboration between university scientists and a network of Iñupiaq observers in northern Alaska coastal communities (Fig. 1). AAOKH (pronounced "A-OK") provides long-term documentation of weather, ocean, sea ice, and landscape

conditions and context to wildlife, harvesting, and cultural and community activities (e.g., Fig. 2) by creating space for Indigenous Knowledge holders to share their expertise and observations of environmental change. The primary objectives of AAOKH, determined by the observers, are to sustain Arctic Indigenous observing, support Indigenous scholarship, and apply observations to inform decision-making in response to environmental change (Hauser et al. 2023). Here, we describe themes in environmental changes observed across the AAOKH network. We also describe our overall efforts to increase knowledge exchange, leveraging our experiences combining scientific measurements with observations to create relevant data products that can directly support community priorities (Hauser et al. 2023).

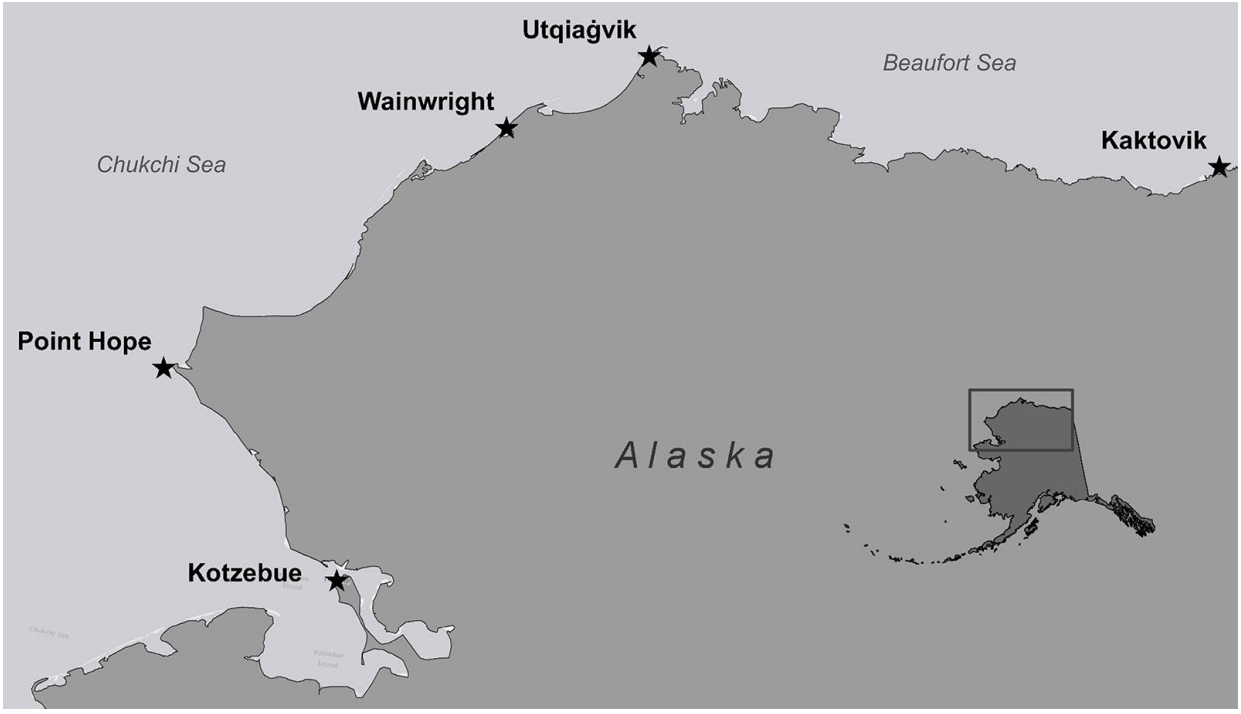

Fig. 1. Map of AAOKH communities included in this synthesis of recent observing themes.

Fig. 2. Under clear skies with blowing winds, crews in Point Hope, Alaska are at the shorefast sea ice edge for the spring whaling season. On 7 April 2023, Guy Norman Omnik reported "*-11°F, mostly cloudy, north winds 10 mph. Poyuaqpanguu! – first [bowhead] whale sighting.*" Photo credit: Guy Norman Omnik

Observations are the foundation of the AAOKH Network

> *"Global warming is happening. It is affecting different villages in different ways. I collect observations…this is an important tool for the future"… "We can look back on these observations in years to come…[and] compare if there are any dramatic changes."*
>
> – Guy Norman Omnik [Iñupiat], Point Hope, shared December 2020 (quoted in Hauser et al. 2023)

Arctic coastal communities have long recognized that sea ice conditions are changing. The ocean is freezing later in fall and melting earlier in spring, shorefast sea ice is less stable, and thick multiyear sea ice is harder to find (see essay *Sea Ice*). Overall, conditions are considered less predictable (Hauser et al. 2021). Several themes of physical environmental changes have been reported by AAOKH observers, including warmer air and ocean temperatures, shifts in prevailing wind direction and intensity, and increasing frequency of coastal storms, all of which affect community subsistence calendars and infrastructure (Glenn et al. 2022).

Fall storms were a key observing theme among AAOKH communities in 2022-23. Lack of sea ice makes coastal communities more vulnerable to storm impacts, as noted by Bobby Schaeffer in Kotzebue and Billy Adams in Utqiaġvik:

> *"We had three strong storms. The July 18 storm had the strongest winds. Southwest winds to 50 mph brought in a storm surge that set the record… Wind, huge surf and a lot of rain. The second storm hit us on July 28 and Merbok on September 14 [to 18]… I think we lost more earth to the ocean than ever before."*
>
> – Bobby Schaeffer [Iñupiat], Kotzebue, September 2022 (AAOKH 2023, see Fig. 3).

Fig. 3. Flooding in the low-lying areas in Kotzebue in October 2022, as described in observations by Bobby Schaeffer. Photo credit: Isabelle Mendenhall

> *"The storm like this reminds us the true power of nature! Erosion, west winds, waves and high water levels were key factors in this storm. The winds were not as high as we thought they were predicted to be but all the other factors were in line to cause significant damage. We hope to be much more prepared as we should take notes and learn from this."*
>
> – Billy Adams [Iñupiat], Utqiaġvik, 10 October 2022 (AAOKH 2023).

Storms, and associated flooding or erosion, impact roads and buildings and also cultural infrastructure, such as community ice cellars, which are critical to Indigenous food security (Fig. 4).

Fig. 4. Coastal erosion in Utqiaġvik, including the loss of an ice cellar in July 2023, as observed by Billy Adams, *"erosion continues to wash away our coasts and important historical landmarks and where family members [have] cellars and ancient dwellings."* Photo credit: Billy Adams

Weather and temperature changes in turn affect the animals and their ecosystem, as noted by Carla SimsKayotuk and Billy Adams. This includes temporal shifts in location and abundance of various subsistence resources, including fish, waterfowl, caribou, and marine mammals (Glenn et al. 2022).

> *"Wind, fog, rain and sun today. Still a bit too rough to go whaling. Bears are keeping the community busy. Feels like 28. Winds are down to 10 NE." "Very strong winds out of the east. Gusting to 45, making it feel like 22. Lagoon and ocean are both very rough and whitecaps. High count of polar bears is 48 around our area."*
>
> – Carla SimsKayotuk [Iñupiat], Kaktovik, 14-17 September 2022 (Fig. 5).

Fig. 5. Carla SimsKayotuk emphasizes that an increased abundance of polar bears near Kaktovik is a recent change. After a week of rough waters for local whalers and a spike in polar bear numbers, she reports: "*What a beautiful day, hardly any wind, the waves died down, sun was shining, the whalers went out! Feels like 41. No ice mirage but water mirage and rollers in the ocean.*"- Carla SimsKayotuk [Iñupiat] Kaktovik, September 2022. Photo credit: Carla SimsKayotuk

> *"The westerly winds have been consistent since late January, this has brought in the pack ice up against the shorefast ice. The east side of Pt. Barrow has been the area of open water making it a productive area for animals."*
>
> – Billy Adams [Iñupiat], Utqiaġvik, 11 March 2023 (Fig. 6)

Fig. 6. *"We had lots of west winds that changed a lot of things that came in January all the way to March. It opened up the Beaufort side of the ocean and many of the bears were using that side… I responded to about 40 polar bears calls. We had lots of animals. Very hefty animals. Especially the ringed seals, the polar bears, I hunt a lot on the ice and that's what I saw. Lots of healthy young animals. Also lots of young bearded seals showed up. The hunting was very good, despite the conditions we had, the storms and different winds and sustained west winds for a long time. But animals figure out what they need to do."* – Billy Adams [Iñupiat] Utqiaġvik, shared August 2023. Photo credit: Billy Adams

Observations can inform decision-making

> *"I think it is really important that our observations are being used by tribes for planning purposes. What about documenting storms or supporting food security? We are documenting these observations for the first time. How can tribes use our observations for planning?"*
>
> – Bobby Schaeffer [Iñupiat], Kotzebue, shared 30 November 2022

An increasing emphasis of AAOKH is to build connections across regional, national, and international scales, with entities such as wildlife co-management organizations, tribal governments, and federal agencies that could use observations to support decision-making. Through long-term community-based observing, local knowledge and observations can be applied to decision-making regarding Indigenous peoples, communities, and the land and resources on which they depend and thrive, leading to more

sustainable and effective approaches to resource management and climate change adaptation (e.g., Carothers et al. 2021). For example, regular sea ice and weather observations help improve remotely-sensed data interpretation, which can lead to better forecasts and climate models (e.g., Fox et al. 2020; Simonee et al. 2021). Observer reports also inform hunters or travelers going out on the ocean or sea ice (e.g., Druckenmiller et al. 2013). Similarly, observations of fish or wildlife presence, abundance, location, body condition, and other information can be used to elevate the use of Indigenous data in wildlife co-management decision-making about how and when Indigenous people can legally harvest their traditional foods (e.g., Breton-Honeyman et al. 2021).

Collaboration to achieve a shared vision moving forward

> *"I think the most important thing is that we've fostered a level of trust among our community members and the scientific community… So if we could keep it going, if we have the funding to do it, and keep the trust of our communities with them. Otherwise we'll start over again and they'll have to gain their trust again, and that could be another hurdle, and that could take away from valuable time that we could be doing towards research."*
>
> – Noah Naylor [Iñupiat], Kotzebue, AAOKH Steering Group member (quoted in Hauser et al. 2023)

Complementing Indigenous Knowledge and observations with scientific research enhances our understanding of Arctic environmental change, promotes holistic approaches to observing, and helps to identify strategies for adaptation that are rooted in local priorities. AAOKH's network and organizational structure intentionally creates space for knowledge exchange and feedback on program activities and research products. This dialogue between university researchers and Indigenous Knowledge holders helps to establish shared understandings about Arctic environmental change and particularly impacts to Indigenous communities. These shared understandings are the foundation on which AAOKH will move forward, sustaining long-term observations while also addressing priorities and research questions advanced by community and regional partners.

Despite well-documented literature on Arctic environmental change, efforts to understand and respond to these changes are often led by outside researchers and do not address the perspectives and priorities of local Indigenous Peoples (Ellam Yua et al. 2022; Knapp and Trainor 2015). Lack of engagement to understand and respond to local priorities perpetuates further colonialism and inequity in Arctic research, disregarding pre-existing knowledge systems and oral histories that can inform and lead scientific research (Inuit Circumpolar Council 2022). Research done in Indigenous communities, without inclusion of and credit to the people living there, further disenfranchises Indigenous people, their knowledge systems, and their histories on the land. We recognize the importance of collaborative research approaches that honor and uplift Indigenous Knowledge holders and their connections to the land and sea. By amplifying Indigenous Knowledge and observations, AAOKH aims to challenge the power imbalances inherent in conventional scientific practices and contribute to the transformation of Arctic observing protocols to better serve Indigenous Peoples and communities.

Methods and data

AAOKH's five current observers are residents of four predominantly Iñupiaq communities along northern coastal Alaska (Kotzebue, Point Hope, Utqiaġvik, and Kaktovik). Observers lead traditional

Iñupiaq ways of life based on the land and sea and contribute regular observations that are significant to the observers, as described in Hauser et al. (2023). Over 10,000 observations, dating back to 2006, are archived and accessible in an online database, upon acceptance of data use agreements (Observers of Coastal Arctic Alaska 2022).

This essay is authored by Iñupiaq (R. G-B., R. S., B. A., C. S., G. O., J. M. L.) and non-Indigenous (D. D. W. H.) scholars to share research and activities from an interdisciplinary and cross-cultural team, each bringing unique knowledge, identities, experiences, and perspectives to the AAOKH project. We acknowledge that AAOKH communities have been stewarded as part of Iñupiaq homelands since time immemorial. Here, we identify cultural identities of our contributors to uplift and amplify the contributions of Indigenous researchers in the Arctic. We include direct quotations and text provided directly from community members and observers without edits to retain the intentions and perspectives shared by each individual. English is not always the first language of the contributor, and any edits or clarifications by the authors are included as [brackets].

References

Alaska Arctic Observatory and Knowledge Hub, 2023: AAOKH News. Issue 8, Winter 2023, https://arctic-aok.org/2023/02/21/hot-off-the-press-check-out-our-winter-2023-newsletter.

Breton-Honeyman, K., and Coauthors, 2021: Beluga whale stewardship and collaborative research practices among Indigenous peoples in the Arctic. *Polar Res.*, **40**(S1), https://doi.org/10.33265/polar.v40.5522.

Carothers, C., and Coauthors, 2021: Indigenous peoples and salmon stewardship: a critical relationship. *Ecol. Soc.*, **26**(1), 16, https://doi.org/10.5751/ES-11972-260116.

Danielsen, F., and Coauthors, 2020: Community-based monitoring in the Arctic. University Press of Colorado, Denver, CO, https://upcolorado.com/university-of-alaska-press/item/6022-community-based-monitoring-in-the-arctic.

Druckenmiller, M. L., H. Eicken, J. C. George, and L. Brower, 2013: Trails to the whale: reflections of change and choice on an Iñupiat icescape at Barrow, Alaska. *Polar Geogr.*, **36**, 5-29, https://doi.org/10.1080/1088937X.2012.724459.

Eicken, H., and Coauthors, 2021: Connecting top-down and bottom-up approaches in environmental observing. *BioScience*, **71**, 467-483, https://doi.org/10.1093/biosci/biab018.

Ellam Yua, J. Raymond-Yakoubian, R. A. Daniel, and C. Behe, 2022: A framework for co-production of knowledge in the context of Arctic research. *Ecol. Soc.*, **27**(1), 34, https://doi.org/10.5751/ES-12960-270134.

Fox, S., E. Qillaq, I. Angutikjuak, D. J. Tigullaraq, R. Kautuk, H. Huntington, G. E. Liston, and K. Elder, 2020: Connecting understandings of weather and climate: steps towards co-production of knowledge and collaborative environmental management in Inuit Nunangat. *Arct. Sci.*, **6**, 267-278, https://doi.org/10.1139/as-2019-0010.

Glenn, R. G., D. D. W. Hauser, M. DeLue, B. Adams, J. Leavitt, G. Omnik, S. Patkotak, R. Schaeffer, and C. SimsKayotuk, 2022: Insights from Coastal Arctic Indigenous Observers, ArcGIS StoryMap available online, https://storymaps.arcgis.com/stories/30d30ab062ea4aadb39b3734dd7770ae.

Hauser, D. D. W., and Coauthors, 2021: Co-production of knowledge reveals loss of Indigenous hunting opportunities in the face of accelerating Arctic climate change. *Environ. Res. Lett.*, **16**, 095003, https://doi.org/10.1088/1748-9326/ac1a36.

Hauser, D. D. W., and Coauthors, 2023: Nunaaqqit Savaqatigivlugich—working with communities: evolving collaborations around an Alaska Arctic observatory and knowledge hub. *Arct. Sci.*, **9**, 635-656, https://doi.org/10.1139/as-2022-0044.

Inuit Circumpolar Council, 2022: Circumpolar Inuit Protocols for Equitable and Ethical Engagement, Technical report available online, https://www.inuitcircumpolar.com/project/circumpolar-inuit-protocols-for-equitable-and-ethical-engagement/.

Knapp, C. N., and S. F. Trainor, 2015: Alaskan stakeholder-defined research needs in the context of climate change. *Polar Geogr.*, **38**, 42-69, https://doi.org/10.1080/1088937X.2014.999844.

Observers of Coastal Arctic Alaska, 2022: Local Observations from the Seasonal Ice Zone Observing Network (SIZONet) and Alaska Arctic Observatory and Knowledge Hub (AAOKH), Version 2. Edited by the AAOKH Team, National Snow and Ice Data Center, Boulder, CO, https://doi.org/10.7265/jhws-b380.

Simonee, N., J. Alooloo, N. A. Carter, G. Ljubicic, and J. Dawson, 2021: Sila Qanuippa? (How's the weather?): integrating Inuit Qaujimajatuqangit and environmental forecasting products to support travel safety around Pond Inlet, Nunavut, in a changing climate. *Wea. Climate Soc.*, **13**, 933-962, https://doi.org/10.1175/WCAS-D-20-0174.1.

November 13, 2023

Peatlands and Associated Boreal Forests of Finland Under Restoration

https://doi.org/10.25923/dxxd-ef53

T. Mustonen

Snowchange Cooperative, Lehtoi, Finland

Headlines

- The scale of peatland degradation in Finland has been severe, with negative influences on culture, traditional livelihoods, ecosystems, and carbon storage.
- The scale of peatland restoration and rewilding (here discussed at 52,000 hectares) demonstrates a globally relevant climate solution of carbon sinks and points to a need of replication across impacted sites.
- Rewilding requires partnership, recognition of Indigenous and community rights, and the use of Indigenous knowledge alongside science to succeed and avoid replication of past inequities.

Rewilding peatlands and forests – Context for Finland and Northern Europe

The European North (Norway, Sweden, Finland, and NW Russia)—also called Fennoscandia—contains the largest wilderness areas of Europe and is the traditional home of many peoples, including the Sámi, Europe's only recognized Indigenous people. Many other Finno-Ugric groups such as Karelians, Komi, Nenets, Livonians, and residents of Finnish rural villages have also co-habited this region for centuries, developing their traditional knowledge of habitats and sustainable use of resources.

The linguistic and cultural links across the region provide for a unique cultural patchwork reaching from Western Siberia to Norway (Fig. 1). Despite their long establishment in the region, the traditional communities across Fennoscandia are experiencing various stages of cultural and economic homogenization due to significant industrialization over the past 100 years.

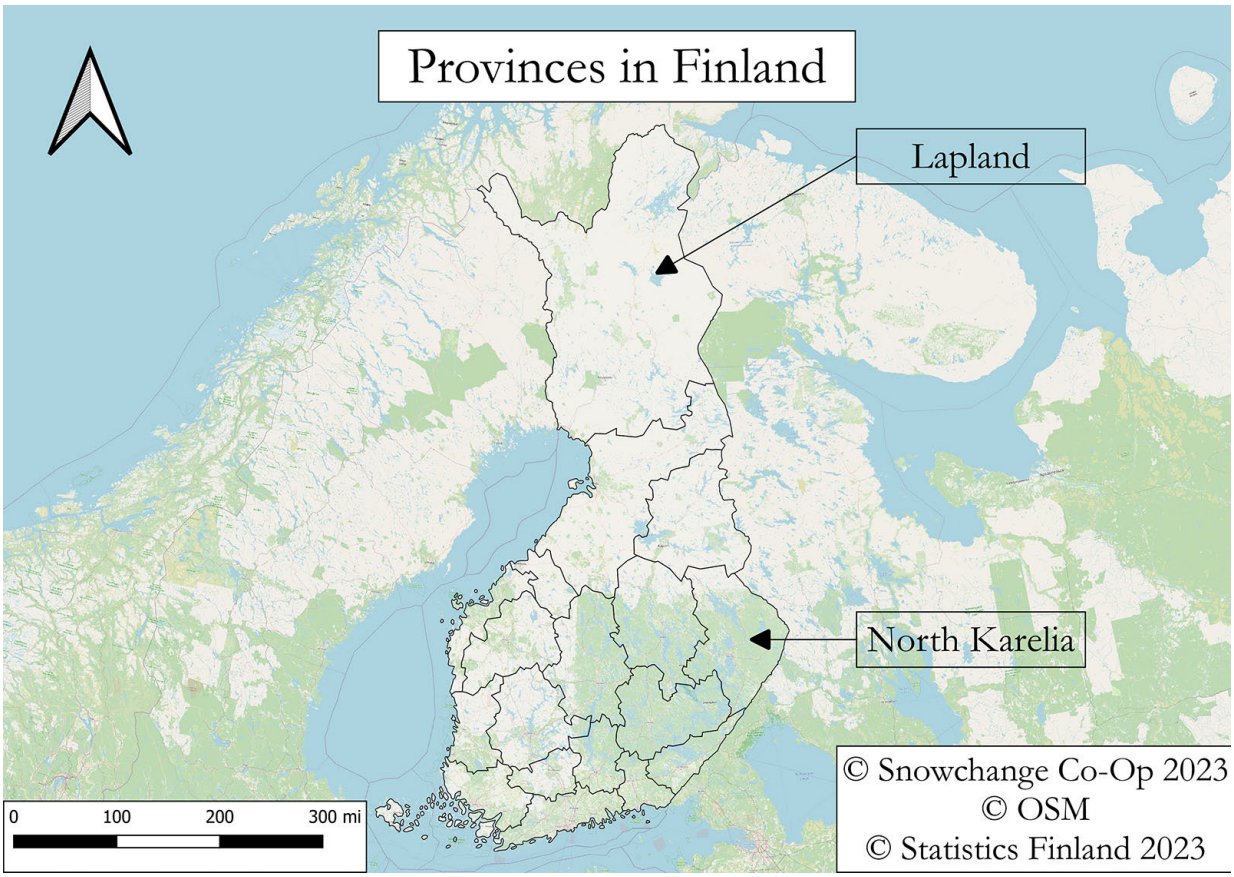

Fig. 1. Regions relevant to the rewilding work in Finland, indicating the Lapland and North Karelia Provinces.

Since 2000, the Finnish non-profit organization Snowchange Cooperative has piloted far-reaching rewilding (Perino et al. 2019) and ecosystem restoration actions in North Karelia and Sámi areas that combine Indigenous and local-traditional knowledge of the Finno-Ugric peoples with the latest science. Rewilding is seen often as a part of nature-based solutions, where the emphasis is placed on restarting the natural functions of a site and limiting human interventions. (*Note that in this essay the concept of Indigenous knowledge is associated with the Sámi, the only Indigenous peoples of mainland Europe. Local-traditional knowledge is associated with national minorities and villages that are designated by the society as cultural heritage areas or otherwise maintain lifeways that provide a cultural context for knowledge. Indigenous knowledge has been defined in the North American context in some cases differently than in the European context.*)

In 2017, Snowchange initiated the Landscape Rewilding Program (LRP) with the European Investment Bank (EIB) and other actors to develop landscape rewilding actions built on community rights of Indigenous and traditional peoples as a novel vehicle to address the challenges of simultaneous climate and biodiversity crises. Landscape rewilding refers to restorative actions that enable the comeback of natural processes to alleviate peatland damages and restart carbon storage (Haapalehto et al. 2011; Mustonen and Kontkanen 2019). In this work, the first year often requires blocking ditches to enable the water table to recover. Occasionally wetlands need to be formed artificially to restart succession. As a result, autonomous proliferation of a variety of sphagnum moss species provides the ‘engine’ required to restart the natural processes that constitute a functioning peatland.

This essay explores Snowchange's work in Finland with a specific focus on Indigenous Sámi-led and community-led rewilding projects.

Landscape rewilding of Sámi forests to enable resilience and Indigenous management

Finland is a central location for boreal and Arctic peatlands, with over 10 million hectares of peatlands within its borders (~30% of the land area). Globally, peatlands store more than 30% of the remaining soil-based carbon in the world today (IPCC 2022). Since the 1940s, the proliferation of industrial forestry and peat mining has degraded more than 5 million hectares of Finnish peatlands through "ditching"—a process of draining peatlands through removing vegetation and digging water canals so that the peat dries prior to industrial processing (Fig. 2). In addition to site-specific loss of habitat and species that require stable wetland environments, these changes also have downstream water quality impacts.

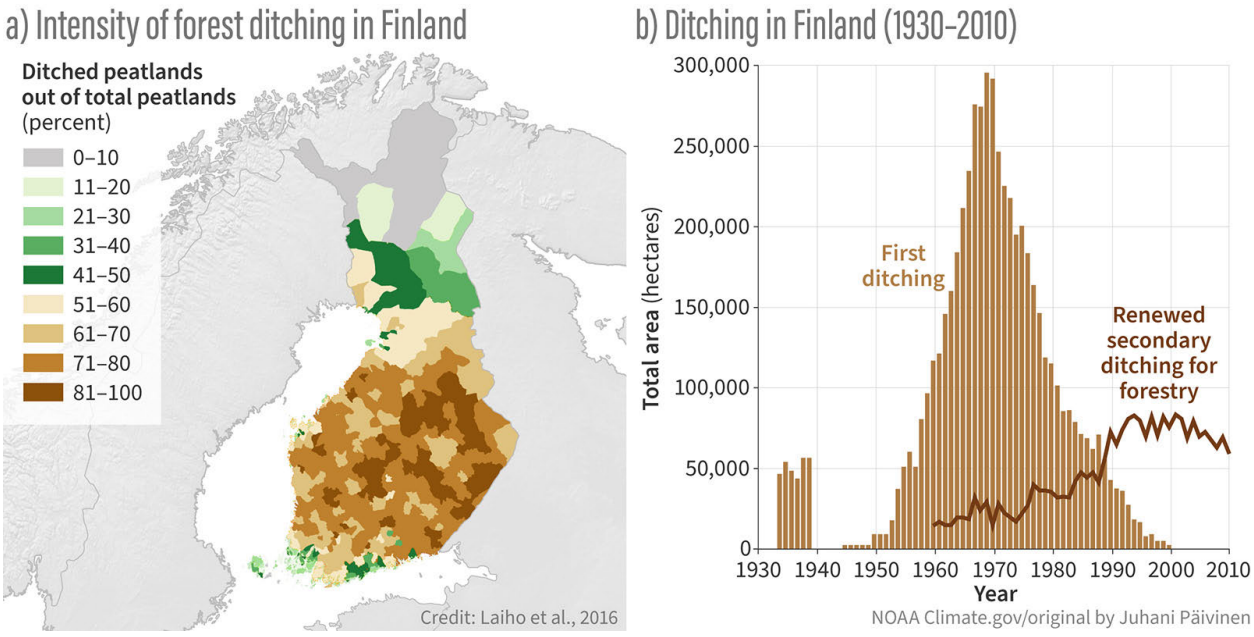

Fig. 2. (a) Intensity of ditching across Finland showing ditched peatlands as percent of total peatlands for each province (Laiho et al. 2016; Korhonen et al. 2021, creative commons) and (b) the temporal scale of peatland ditching 1930-2010 (NOAA Climate.gov modified from Juhani Päivinen/University of Helsinki, used with permission).

The first wave of commercial exploitation in what are now Finland's forests started with the international tar trade in the 1600s, when tar, which is produced from wood, became the territory's primary export. A second wave of commercial forestry emerged in the 1800s after the invention of steam powered sawmill equipment, increasing sawmill productivity. The third and most environmentally-destructive wave was the large-scale clear-felling of timber forests for the pulp and paper industries starting in 1945. This wave resulted in the loss of 95% of Finland's natural boreal forest ecosystems south of the Arctic Circle over just 80 years. A large driver of this industrial push was the war repatriations Finland was obligated to pay to the Soviet Union in the years following World War II. This resulted in a rapid, single-generation technological, economic, and cultural transition in Finnish society. Historically, the interlinked Finnish and Sámi communities maintained lifeways built on fishing, hunting, small-scale slash and burn farming, and reindeer herding, resulting in multi-age and multi-species forests. The period from 1945 to the 1990s (and in some ways to the present day) was a time of

interconnected, top-down, massive shifts that altered these large wilderness ecosystems. Forest degradation was intrinsically linked to the transformation of traditional Sámi wilderness economies and communities, resulting in the loss of rights and subsequently direct assimilation into the cultural, linguistic, and economic norms and practices of dominant western European societies.

Large-scale logging, the establishment of major hydropower stations on rivers, and road construction altered the fabric of life from 1960s onwards, especially in the southern portions of the Sámi homeland. The proliferation of snowmobiles also altered the dynamics of reindeer herding, creating an additional dependency on the cash economy. Many semi-nomadic herders were living in houses by the 1960s. The Sámi navigated these changes by adjusting and maintaining their reindeer herding, and since the 1990s, there has been an accelerating linguistic and cultural revitalization and reclamation of cultural histories and practices. Rewilding efforts can be seen as a part of this process.

It is against this background of ecological and cultural degradation that Snowchange Cooperative founded the LRP with the specific goal of empowering and realizing Indigenous and community rights (Huntington et al. 2017). This includes having the community always guide our work through collaborative management, having Indigenous women lead the decision-making process when projects are on their territory, and never making decisions without the consent of the affected Indigenous community or traditional owners. Similar North American approaches have been implemented for example in Canada under the Indigenous Guardians Secretariat (Drever et al. 2021). LRP stands out as a mechanism for the European North where similar community-driven efforts have not taken place to the same extent before.

Landscape rewilding of peatlands as an answer to the climate challenge

In the first six years of the LRP, Snowchange has rewilded and restored 52,000 hectares over dozens of catchments and peatland systems. To make this work possible, Snowchange has purchased some sites while others are managed through land use agreements (Snowchange and private landowners agree on restoration and management actions that will take place on their property). To date, over 85 sites Snowchange works in have been identified as Indigenous and Community Conserved Areas (ICCAs), with the largest site (Kivisuo peatland) being the same size as some Finnish national parks.

Landscape rewilding was piloted at a former peat mining area in North Karelia, Linnunsuo (“Marsh of Birds”), which was mined between 1982 and 2010. Traditional Finnish fisherman in the area identified several massive fish die-offs in the Jukajoki River downstream of Linnunsuo, resulting from mud and acidic peat runoff from peat mining operations. Working with village leaders in the town of Selkie in the Jukajoki watershed, the fishermen were successful in suspending peat mining. Once mining was suspended, residents of Selkie and Alavi initiated a community-led restoration of Linnunsuo, and Snowchange included the site in the LRP in 2017. Since 2017, the villages have expanded their work throughout the Jukajoki watershed, working with dozens of landowners, companies, cities, and municipalities.

To date, restoration actions include building nine large wetlands spanning 180 hectares that capture peat sediment and heavy metals and prevent more carbon dioxide from leaving the peat soils. As a result of restoration, the area has become an important bird habitat with 215 species recorded (Mustonen and Kontkanen 2019; Jarma 2022; Tiira 2023), including regionally rare species such as the

long-billed dowitcher (*Limnodromus scolopaceus*) and terek sandpiper (*Xenus cinereus*). Before these actions, only 4-6 species were observed (Tiira 2023). Additionally, having been considered an ecologically severely impacted river (according to the national ELY authority) just a decade before, in 2023 Jukajoki is once again a trout river with a spawning population of critically endangered Vuoksi brown trout (*Salmo trutta*) (Järvitaimentyöryhmä 2018; Koljonen et al. 2022).

Linnunsuo is an example of a traditional Finnish village using local ecological knowledge and science to address large-scale extractive damages and lead a path to recovery. Rewilding peatlands serves several central functions in the European boreal and Sub-Arctic—it keeps carbon in the ground, provides for important habitat and natural flood controls and may start carbon sinks, enabling the drawdown of carbon dioxide in large quantities (Fig. 3). Restoration of peatlands is also a mechanism to address almost a century of top-down natural resources governance by slowly moving towards village-led co-management and locally shared joint benefits (Mustonen et al. 2022).

Fig. 3. Makkaralatva-aapa, an Arctic peatland in the Landscape Rewilding Programme.

In 2022, a Sámi reindeer community reached out to Snowchange to strategically restore partially logged boreal forests, which are slow to regenerate with cycles of 100-200 years for a natural comeback. Restoration and rewilding were seen by the Sámi as an answer to the quickly proliferating clear-cuts. These Sub-Arctic boreal forests are key post-Ice Age forest ecosystems that, together with adjacent peatlands, store large amounts of carbon (Bradshaw and Warkentin 2015).

A 70-hectare Altto-oja forest (Fig. 4), which was partially logged in 1990s but that also contains remaining old-growth forests, was added to the Landscape Rewilding Programme in 2023 with joint management. This protects the remaining primary forest segments. Using oral histories, Indigenous knowledge (cultural indicators of good ecological quality and maintenance of key species such as aspen),

and science, Snowchange and the Sámi inventoried the logged areas and developed targets for forest comeback, guided by the Sámi use of the landscape for reindeer herding and non-timber forest products (Fig. 5). By creating baselines from Indigenous memory and knowledge, establishing culturally appropriate fenced areas for monitoring the comeback of Scots Pine, inventorying the site's habitats and stream quality, identifying areas for traditional burns and other sites of high priority to be restored in the following summers, and controlling the reindeer pasture uses in the area, this Altto-oja forest is emerging as a valuable example for how affected Sámi forests can be restored using science and Indigenous knowledge.

Fig. 4. Altto-oja Sámi forest site. Photo: Snowchange.

Fig. 5. Altto-oja restoration work during summer 2023.

Rewilding has risen to the challenge of responding to widespread environmental degradation and acknowledging and realizing community rights. Rewilding, restoration, and Indigenous partnerships are a powerful vehicle of solutions for the most pressing issues in the North. Importantly, these partnerships need to be equitable and fully recognize Indigenous rights in conservation to be relevant and valuable to all parties.

Acknowledgments

Tero Mustonen was supported by the Biodiversa NARROW and Swedish PostCode Foundation Indigenous and Traditional Knowledge Rewilding of Boreal Forests in Finland-22A910 projects.

References

Bradshaw, C. J., and I. G. Warkentin, 2015: Global estimates of boreal forest carbon stocks and flux. *Global Planet. Change*, **128**, 24-30, https://doi.org/10.1016/j.gloplacha.2015.02.004.

Drever, C. R., and Coauthors, 2021: Natural climate solutions for Canada. *Sci. Adv.*, **7**, eabd6034, https://doi.org/10.1126/sciadv.abd6034.

Haapalehto, T. O., H. Vasander, S. Jauhiainen, T. Tahvanainen, and J. S. Kotiaho, 2011: The effects of peatland restoration on water-table depth, elemental concentrations, and vegetation: 10 years of changes. *Restor. Ecol.*, **19**, 587-598, https://doi.org/10.1111/j.1526-100X.2010.00704.x.

Huntington, H. P., and Coauthors, 2017: How small communities respond to environmental change: patterns from tropical to polar ecosystems. *Ecol. Soc.*, **22**(3), 9, https://doi.org/10.5751/ES-09171-220309.

IPCC, 2022: Climate Change 2022: Impacts, Adaptation and Vulnerability. Contribution of Working Group II to the Sixth Assessment Report of the Intergovernmental Panel on Climate Change [H. -O. Pörtner, D. C. Roberts, M. Tignor, E. S. Poloczanska, K. Mintenbeck, A. Alegría, M. Craig, S. Langsdorf, S. Löschke, V. Möller, A. Okem, and B. Rama (eds.)]. Cambridge University Press. Cambridge University Press, Cambridge, UK and New York, NY, USA, 3056 pp., https://doi.org/10.1017/9781009325844.

Jarma, A., 2022: Biodiversity in Linnunsuo's Area. Ecological Monitoring Report, available on request from Snowchange Cooperative, www.snowchange.org.

Järvitaimentyöryhmä, 2018: Vuoksen vesistöalueen järvitaimenkantojen toimenpideohjelma: Pohjois-Savon elinkeino-, liikenne- ja ympäristökeskus (Management Programme for the Brown Trout in Vuoksi Water Area, in Finnish).

Koljonen, M. -L., and Coauthors, 2022: Genetic structure of landlocked salmon, brown trout and European grayling in the River Vuoksi catchment (FIN-RUS). Natural resources and bioeconomy studies 77/2022, Natural Resources Institute Finland, Helsinki, 47 p.

Korhonen, K. T., and Coauthors, 2021: Forests of Finland 2014-2018 and their development 1921-2018. *Silva Fenn.*, **55**(5), 10662, https://doi.org/10.14214/sf.10662.

Laiho, R., S. Tuominen, S. Kojola, T. Penttilä, M. Saarinen, and A. Ihalainen, 2016: Heikkotuottoiset ojitetut suometsät – missä ja paljonko niitä on? Metsätieteen aikakauskirja (Yearbook of Forest Sciences – in Finnish).

Mustonen, T., and H. Kontkanen, 2019: Safe places: Increasing Finnish waterfowl resilience through human-made wetlands. *Polar Sci.*, **21**, 75-84, https://doi.org/10.1016/j.polar.2019.05.007.

Mustonen, T., A. Scherer, and J. Kelleher, 2022: We belong to the land: review of two northern rewilding sites as a vehicle for equity in conservation. *Humanit. Soc. Sci. Commun.*, **9**, 402, https://doi.org/10.1057/s41599-022-01424-w.

Perino, A., and Coauthors, 2019: Rewilding complex ecosystems. *Science*, **364**(6438), eaav5570, https://doi.org/10.1126/science.aav5570.

Tiira, 2023: National Bird Monitoring Database, Birdlife Finland, available at www.tiira.fi, accessed 10 November, 2023.

November 20, 2023

Divergent Responses of Western Alaska Salmon to a Changing Climate

https://doi.org/10.25923/f2hv-5581

E. R. Schoen[1], K. G. Howard[2], J. M. Murphy[3], D. E. Schindler[4], P. A. H. Westley[5], and V. R. von Biela[6]

[1]International Arctic Research Center, University of Alaska Fairbanks, Fairbanks, AK, USA
[2]Division of Commercial Fisheries, Alaska Department of Fish and Game, Anchorage, AK, USA
[3]Auke Bay Laboratories, Alaska Fisheries Science Center, NOAA, Juneau, AK, USA
[4]School of Aquatic and Fishery Sciences, University of Washington, Seattle, WA, USA
[5]College of Fisheries and Ocean Sciences, University of Alaska Fairbanks, Fairbanks, AK, USA
[6]Alaska Science Center, U.S. Geological Survey, Anchorage, AK, USA

Headlines

- Western Alaska salmon abundance reached historic extremes during 2021-22, with record lows for Chinook and chum salmon (81% and 92% below the 30-year mean, respectively) and record highs for sockeye salmon (98% above the 30-year mean).
- Salmon are maturing at smaller sizes. Since the 1970s, for example, Yukon River Chinook salmon have decreased an estimated 6% in mean adult body length and 15% in fecundity, likely exacerbating population declines.
- Salmon population declines have led to fishery closures, worsened user conflicts, and had profound cultural and food security impacts in Indigenous communities that have been tied to salmon for millennia.
- Changes in abundance and size are associated with climatic changes in freshwater and marine ecosystems and competition in the ocean. Changes in predators, food supply, and disease are also likely important drivers.

Introduction

Pacific salmon populations in western Alaska have responded differently to recent climatic changes, with Chinook salmon (*Oncorhynchus tshawytscha*) and chum salmon (*O. keta*) reaching record low abundance levels, while sockeye salmon (*O. nerka*) have attained record high abundance levels since 2020 (Fig. 1). Why these species have responded differently has important implications for the future of Pacific salmon in a warming Arctic. Here, we refer to “western Alaska” salmon as those spawning in watersheds that drain into the eastern Bering Sea. Indigenous Peoples in this region, including First Nations communities residing along Canadian tributaries to the Yukon River, have been tied to salmon for at least 12,000 years, while commercial fisheries have been economic mainstays since the late 1800s (Carothers et al. 2021). Salmon populations in this region have global significance, producing over half of the world’s commercial catch of sockeye salmon from Bristol Bay and have historically supported the world’s largest subsistence fisheries for Chinook and chum salmon in the Yukon and Kuskokwim watersheds. These species, and to a lesser extent, pink (*O. gorbuscha*) and coho (*O. kisutch*) salmon, remain a critical source of food, employment and cash income, and cultural practices essential for

communities' well-being and traditional ways of life (Brown and Godduhn et al. 2015). We report evidence of these changes primarily through the lens of western science, focusing on a few well-studied stocks, and we acknowledge this essay does not convey the breadth of perspectives or the complexity of ecological changes across the region.

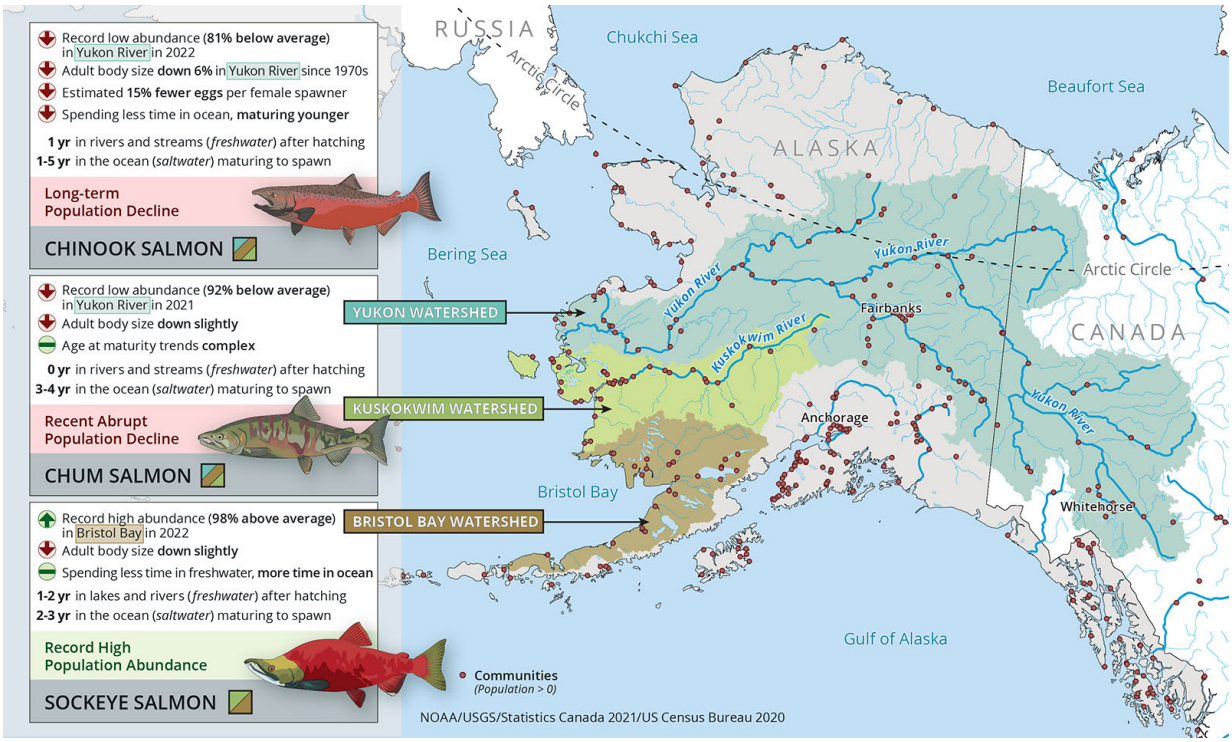

Fig. 1. Contrasting trends in abundance and demographics of key salmon stocks in western Alaska. Dots represent communities in the US and Canada. Map and infographic credit: NOAA/Sarah Battle. Salmon illustrations credit: Katie Kobayashi.

Changes in salmon abundance

Chinook salmon abundance has declined in western Alaska over several decades, culminating with the lowest adult returns on record in the Yukon River in 2022 at 81% below the recent 30-yr mean (1991-2020; Fig. 2). Adult returns reflect the numbers of maturing salmon that return to inshore waters each year, including those that return to freshwater to spawn and those that are harvested in fisheries. Chinook salmon abundance also reached record lows in other Bering Sea drainages, including the Unalakleet, Kuskokwim, and Nushagak Rivers during the last five years, mirroring recent declines of this species throughout its range in the North Pacific Ocean. Chum salmon abundance was above average during most of the 2010s, then declined abruptly in the last five years across the region, falling to a record low in 2021 at 92% below the recent 30-yr mean in the Yukon River, for example. Preliminary data indicate Chinook and chum abundance rebounded slightly in 2023 but remained well below average.

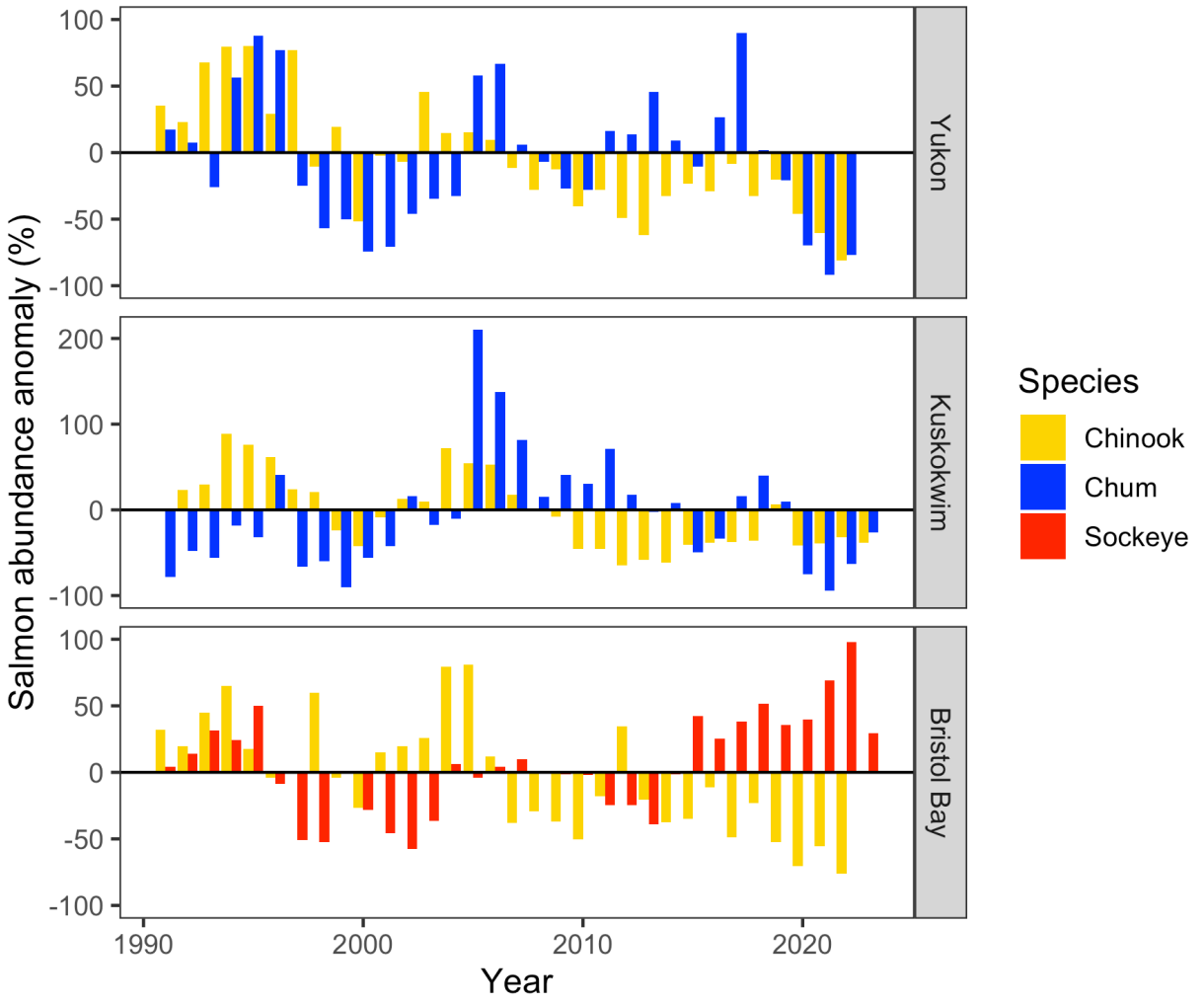

Fig. 2. Abundance of key salmon stocks in the Yukon and Kuskokwim Rivers and Bristol Bay. Abundance includes spawning abundance and fisheries harvest, estimated with run reconstruction models (see *Methods and data*). Anomalies are shown relative to their 1991-2020 means. 2023 data are preliminary and only available for some stocks. Source: Alaska Department of Fish and Game (ADF&G).

In contrast, sockeye salmon abundance has increased in western Alaska during the last decade, including a record high return to Bristol Bay in 2022 at 98% above the 30-yr mean. These record high runs have supported record harvests in fisheries while also surpassing management targets for spawner abundances. Substantial increases in sockeye salmon abundance have also been documented in the Kuskokwim River to the north of Bristol Bay.

Declines of Chinook salmon in the Yukon River have received particular attention, revealing associations with climatic and biological changes in freshwater and marine ecosystems. Most of the year-to-year variation in adult returns is correlated with the abundance of juveniles at the end of their first summer in the Bering Sea (Murphy et al. 2021). This has led researchers to focus on the early marine stage and preceding life stages in freshwater (adult spawner, embryo, and juvenile) as most influential for understanding the population declines, but no single explanation has emerged. Reduced abundance of Yukon River Chinook salmon is correlated with warmer water temperatures and lower river discharge during adult spawner migrations (Howard and von Biela 2023) and higher precipitation during juvenile

rearing (Murdoch et al. 2023). These patterns suggest Chinook salmon may face increasing challenges in a warmer and rainier climate (see essays *Surface Air Temperature* and *Precipitation*). Conversely, increased abundance is correlated with warmer winter temperatures during embryo incubation and early marine residence and earlier river ice breakup during the year juveniles migrate to the ocean (Cunningham et al. 2018, Murdoch et al. 2023), suggesting potential benefits from warming trends in some cases. Traditional knowledge and western science indicate species interactions including competition, predation, food supply, and disease also influence salmon abundance (e.g., Feddern et al. 2023; Ruggerone et al. 2023). Bycatch of Chinook and chum salmon in Bering Sea trawl fisheries is also a known source of mortality, although it explains only a small fraction of historic Chinook salmon declines (Cunningham et al. 2018). Drivers of abundance of other western Alaska salmon species and populations remain less understood.

Changes in salmon size and life history

Salmon from western Alaska are returning to spawn at smaller sizes than in the past, reducing their reproductive capacity and the value of each fish to humans and ecosystems (Ohlberger et al. 2020, 2023; Oke et al. 2020). The average length of adult Chinook salmon in the Yukon River has declined by 5-7% since the 1970s, contributing to estimated losses of 13-20% in fecundity and 24-35% in total egg mass and likely reinforcing long-term population declines (Ohlberger et al. 2020; Fig. 3). Western Alaska chum and sockeye salmon have shown smaller declines in body size.

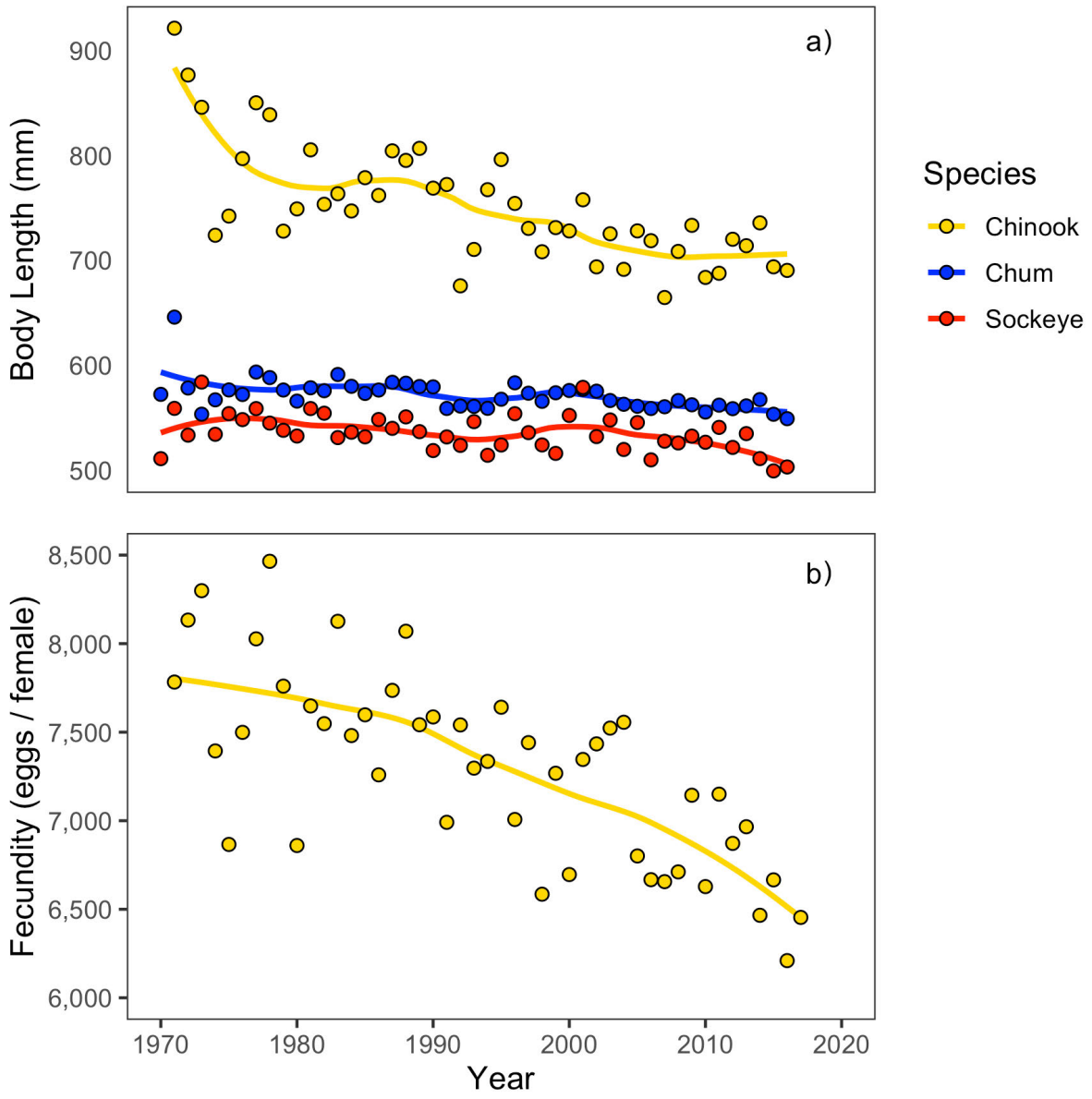

Fig. 3. (a) Trends in body length of three species of salmon in western Alaska and (b) estimated fecundity of Yukon River Chinook salmon. Points represent annual mean estimates, and curves represent non-linear trends fit using loess regression. Sources: ADF&G, Oke et al. (2020), and Ohlberger et al. (2020). See *Methods and data* for details.

Changes in the size of spawning salmon are explained by earlier maturation and reduced growth rates. After hatching, Chinook salmon in western Alaska typically spend one year rearing in streams and rivers before migrating to the ocean, where they spend 1-5 years maturing before returning to spawn in fresh water. Chinook salmon are smaller at a given age and are maturing at younger ages than in the past (Ohlberger et al. 2020). Chum salmon swim to the ocean immediately after emerging from the gravel, and trends in age at maturity are less clear. Sockeye salmon spend 1-2 years rearing in fresh water (mostly in lakes, but sometimes in rivers). In Bristol Bay, the warming climate has led to a decline in the number of sockeye salmon that rear for two years in lakes, with most fish now leaving fresh water after one year. This shift in freshwater age and declining growth rates in the ocean have led to more fish

spending three rather than two years in the ocean and returning to spawn at smaller average sizes (Cline et al. 2019; Ohlberger et al. 2023).

Changes in growth and age of maturity of western Alaska Chinook salmon have been linked to changes in ocean climate (Siegel et al. 2017), and selective predation of larger individuals may also be contributing to accelerated maturation (e.g., Manishin et al. 2021). Though these trends are observed throughout the North American range of Chinook salmon, they are particularly marked in western Alaska stocks (Ohlberger et al. 2018). Changes in growth and energy allocation in juvenile chum salmon are associated with a marked loss of sea ice and decline in prey energy density during a recent (2014-2019) warm period with marine heatwaves in the Bering Sea (Farley et al. In press). Declining body sizes of sockeye salmon in Bristol Bay are most strongly associated with their own increasing abundance, and secondarily with increasing abundance of chum and pink salmon in the North Pacific Ocean and warming sea surface temperatures (see essay *Sea Surface Temperature*). These patterns have been associated with intra- and inter-specific competition for food in the ocean, possibly exacerbated by climate warming (Ohlberger et al. 2023; Ruggerone et al. 2023).

Implications for fisheries and people

Depressed abundances of salmon create problems for fisheries and the people that depend on them. Low returns of Chinook and chum salmon to the Yukon and Kuskokwim Rivers have resulted in closed or heavily restricted subsistence, commercial, and sport fisheries, including unprecedented complete closures of salmon-directed fisheries on the Yukon River during 2021-22 and very limited openings during 2023 (JTC 2023; Fig. 4). Tribal and local leaders are raising their voices to communicate how the synchronous collapse of multiple salmon populations and species has created a region-wide crisis in communities reliant on salmon for food security, culture, mental health, and a way of life (Brown and Godduhn 2015; Feddern et al. 2023). Fish camps sit empty, fishing gear is not maintained, and younger generations are not able to learn the fishing and processing techniques that have been refined over thousands of years when there are no fish to be caught (Brown and Godduhn 2015; Sakati 2023). Harvests of alternative wild foods including fish, birds, and moose have increased where possible, but have also added concerns about the sustainability of those resources. The need to protect Chinook and chum salmon limits the harvest of other fish species that co-occur in fishing areas. Commercial salmon fishery restrictions and closures curtail a source of otherwise scarce jobs and economic development in the region. Federal Fishery Disaster Determinations were granted for the 2020 and 2021 salmon fisheries in the Yukon and Kuskokwim Rivers and Norton Sound and the 2022 salmon fishery in the Yukon River, among other Alaska fisheries (NOAA 2023).

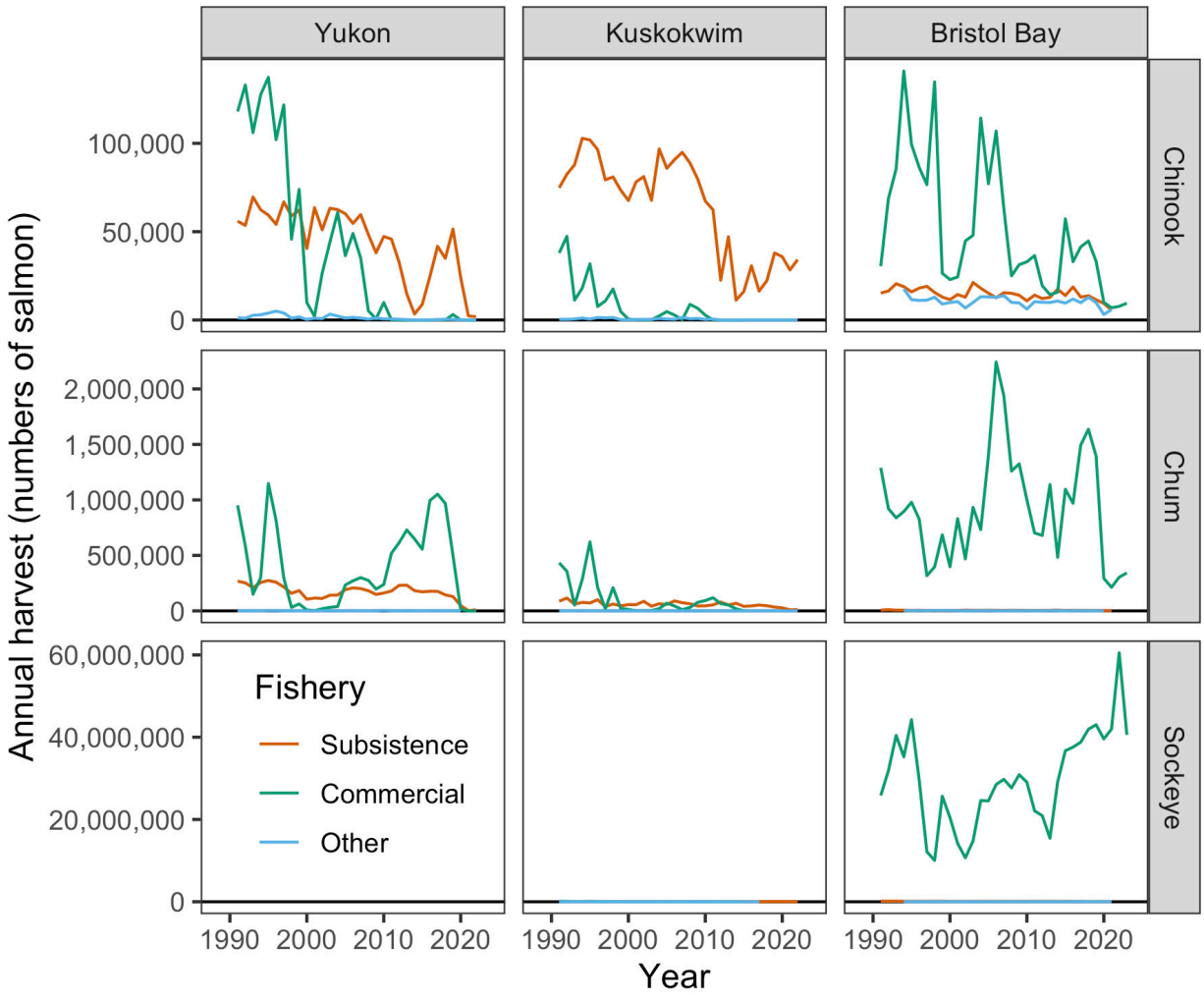

Fig. 4. Annual harvest of major western Alaska salmon stocks by fishery sector. Subsistence harvest in the Yukon watershed includes First Nations and aboriginal fisheries in Canada. Other fisheries include recreational hook-and-line and personal-use fisheries in Alaska and domestic net fisheries on the Yukon in Canada. 2023 data are preliminary and only available for some fisheries. Source: ADF&G (see *Methods and data* for details).

At the other extreme, historically high sockeye salmon returns in Bristol Bay have boosted economic opportunities, but also introduced sources of conflict. The Bristol Bay commercial harvest of 60 million sockeye salmon in 2022 was a record high in a fishery dating back to 1883, exceeding the previous record set in 1995 by 36% (Fig. 4). However, extremely high sockeye harvests in consecutive years, in concert with record catches of pink salmon globally, have outpaced global demand for salmon products, leading to severe reductions in prices paid to commercial fishers. Low prices can drive western Alaska fishers to sell their commercial permits to those outside the region, with lasting implications for local economies (Carothers et al. 2021). Mixed-stock fisheries along the coast of the Alaska Peninsula targeting abundant sockeye salmon also harvest chum salmon bound for western Alaska (Dann et al. 2023). This introduces conflict in how chum salmon are prioritized between subsistence and commercial fisheries and has the potential to impact their recovery and the human communities that depend on them.

Many organizations are working to restore salmon abundance and habitat in watersheds impacted by human activity, including 125 years of placer mining (e.g., BLM 2023). Community-based monitoring programs are incorporating local and traditional knowledge into research and management decisions (Feddern et al. 2023), as has proven successful in northern Alaska (see essay *Nunaaqqit Savaqatigivlugich: Working with Communities to Observe the Arctic*). Other proposed actions include limiting chum salmon bycatch in marine fisheries, limiting harvest of western Alaska salmon in coastal mixed stock fisheries, establishing hatcheries in western Alaska, and limiting hatchery enhancement of pink and chum salmon stocks in other parts of Alaska and the North Pacific that may compete with western Alaska salmon in the ocean (AFN 2022; Feddern et al. 2023; Herz 2023; Ruggerone et al. 2023). All of these proposed actions involve trade-offs and are hotly debated. While the rapidly changing climate appears to be an important driver of salmon abundance, more work is needed to understand the causal mechanisms and to develop policy actions that are responsive to changing salmon abundance and demographics. Actionable research at the science-policy interface is needed to understand how decisions at local, regional, and global levels can most effectively support salmon recovery, sustainable fisheries, and the well-being of people in a warming world.

Methods and data

Salmon abundance was estimated using run reconstruction models by the Alaska Department of Fish and Game (ADF&G) and the Joint Technical Committee of the US/Canada Yukon River Panel (e.g., JTC 2023). These models use information on harvest in mixed-stock and terminal fisheries, stock composition data, and estimates of spawning abundance to determine the total numbers of maturing salmon that returned to in-shore waters. Body length measurements were compiled by Oke et al. (2020) from ADF&G data. We filtered these data to include only salmon captured in western Alaska using minimally size-selective gear (weirs, seines, and carcass surveys). Fecundity of Chinook salmon was estimated from body length using an empirical length-fecundity relationship from the Yukon River by Ohlberger et al. (2020). Fisheries harvest data were provided by ADF&G. All data and code are available at https://github.com/eschoen/ArcticReportCard-Salmon.

Acknowledgments

We are grateful to the many knowledge holders, managers, and scientists who contributed to the long-term datasets and understanding included in this report. We especially thank ADF&G staff for compiling and sharing the salmon abundance and harvest data. Any use of trade, firm, or product names is for descriptive purposes only and does not imply endorsement by the U.S. Government.

References

AFN (Alaska Federation of Natives), 2022 AFN Resolutions. https://www.nativefederation.org/wp-content/uploads/2023/04/Final-2022-Resolutions.2.pdf (Accessed 2 October 2023).

BLM (Bureau of Land Management), 2023: Gravel to Gravel Keystone Initiative. https://www.blm.gov/programs/aquatic-resources/alaska/gravel-gravel-keystone-initiative (Accessed 1 September 2023).

Brown, C. L., and A. R. Godduhn (Eds.), 2015: Socioeconomic effects of declining salmon runs on the Yukon River (Technical Paper No. 398). Alaska Department of Fish and Game, Division of Subsistence, http://www.adfg.alaska.gov/techpap/TP398.pdf.

Carothers, C., and Coauthors, 2021: Indigenous peoples and salmon stewardship: a critical relationship. *Ecol. Soc.*, **26**, 16, https://doi.org/10.5751/es-11972-260116.

Cline, T. J., J. Ohlberger, and D. E. Schindler, 2019: Effects of warming climate and competition in the ocean for life-histories of Pacific salmon. *Nat. Ecol. Evol.*, **3**, 935-942, https://doi.org/10.1038/s41559-019-0901-7.

Cunningham, C. J., P. A. H. Westley, and M. D. Adkison, 2018: Signals of large scale climate drivers, hatchery enhancement, and marine factors in Yukon River Chinook salmon survival revealed with a Bayesian life history model. *Global Change Biol.*, **24**, 4399-4416, https://doi.org/10.1111/gcb.14315.

Dann, T. H., H. A. Hoyt, E. M. Lee, E. K. C. Fox, and M. B. Foster, 2023: Genetic stock composition of chum salmon harvested in commercial salmon fisheries of the South Alaska Peninsula, 2022. Alaska Department of Fish and Game, Special Publication No. 23-07, Anchorage, https://www.adfg.alaska.gov/FedAidPDFs/SP23-07.pdf.

Farley, E. V., E. M. Yasumiishi, J. M. Murphy, W. Strasburger, F. Sewall, K. Howard, S. Garcia, and J. H. Moss, In press: Juvenile western Alaska chum salmon and critical periods during their marine life history in a changing climate. *Mar. Ecol. Prog. Ser.*, https://doi.org/10.3354/meps14491.

Feddern, M. L., and Coauthors, 2023: Kings of the north: Bridging disciplines to understand the effects of changing climate on Chinook salmon in the Arctic-Yukon-Kuskokwim region. *Fisheries*, **48**, 331-343, https://doi.org/10.1002/fsh.10923.

Herz, N., 2023: Fish hatcheries, long seen as a last resort, get a new look amid Yukon River salmon crisis. Northern Journal, 7 April 2023. https://northernjournal.substack.com/p/fish-hatcheries-long-seen-as-a-last?utm_source=post-email-title&publication_id=1057678&post_id=113385992&isFreemail=true&utm_medium=email.

Howard, K. G., and V. von Biela, 2023: Adult spawners: A critical period for subarctic Chinook salmon in a changing climate. *Global Change Biol.*, **29**, 1759-1773, https://doi.org/10.1111/gcb.16610.

JTC (Joint Technical Committee of the Yukon River U.S./Canada Panel), 2023: Yukon River salmon 2022 season summary and 2023 season outlook. Alaska Department of Fish and Game, https://www.yukonriverpanel.com/download/13/joint-technical-committee-reports/3775/yukon-jtc-23-01-2022-season-review-2023-outlook.pdf.

Manishin, K. A., C. J. Cunningham, P. A. H. Westley, and A. C. Seitz, 2021: Can late stage marine mortality explain observed shifts in age structure of Chinook salmon? *PLoS One*, **16**, e0247370, https://doi.org/10.1371/journal.pone.0247370.

Murdoch, A. D., B. M. Connors, N. W. R. Lapointe, J. Mills Flemming, S. J. Cooke, and C. Mantyka-Pringle, 2023: Multiple environmental drivers across life-stages influence Yukon River Chinook salmon productivity. *Can. J. Fish. Aquat. Sci.*, https://doi.org/10.1139/cjfas-2022-0254.

Murphy, J., and Coauthors, 2021: Northern Bering Sea surface trawl and ecosystem survey cruise report, 2019. U.S. Department of Commerce, NOAA Tech. Memo, NMFS-AFSC-423, 124 p., https://repository.library.noaa.gov/view/noaa/32075.

NOAA (National Oceanic and Atmospheric Administration), 2023: Fishery Disaster Determinations. https://www.fisheries.noaa.gov/national/funding-and-financial-services/fishery-disaster-determinations (Accessed 29 September 2023).

Ohlberger, J., E. J. Ward, D. E. Schindler, and B. Lewis, 2018: Demographic changes in Chinook salmon across the Northeast Pacific Ocean. *Fish Fish.*, **19**, 533-546, https://doi.org/10.1111/faf.12272.

Ohlberger, J., D. E. Schindler, R. J. Brown, J. M. S. Harding, M. D. Adkison, A. R. Munro, L. Horstmann, and J. Spaeder, 2020: The reproductive value of large females: consequences of shifts in demographic structure for population reproductive potential in Chinook salmon. *Can. J. Fish. Aquat. Sci.*, **77**(8), 1292-1301, https://doi.org/10.1139/cjfas-2020-0012.

Ohlberger, J., T. J. Cline, D. E. Schindler, and B. Lewis, 2023: Declines in body size of sockeye salmon associated with increased competition in the ocean. *Proc. Roy. Soc. B.-Biol. Sci.*, **290**, 20222248, https://doi.org/10.1098/rspb.2022.2248.

Oke, K. B., and Coauthors, 2020: Recent declines in salmon body size impact ecosystems and fisheries. *Nat. Commun.*, **11**, 4155, https://doi.org/10.1038/s41467-020-17726-z.

Ruggerone, G. T., A. M. Springer, G. B. van Vliet, B. Connors, J. R. Irvine, L. D. Shaul, M. R. Sloat, and W. I. Atlas, 2023: From diatoms to killer whales: impacts of pink salmon on North Pacific ecosystems. *Mar. Ecol. Prog. Ser.*, **719**, 1-40, https://doi.org/10.3354/meps14402.

Sakati, C., 2023: Fishing in the desert: Modernizing Alaskan salmon management to protect fisheries and preserve fishers' livelihoods. *Alaska Law Review*, **40**, 137-169, https://scholarship.law.duke.edu/alr/vol40/iss1/6/.

Siegel, J. E., M. V. McPhee, and M. D. Adkison, 2017: Evidence that marine temperatures influence growth and maturation of western Alaskan Chinook salmon. *Mar. Coast. Fish.*, **9**, 441-456, https://doi.org/10.1080/19425120.2017.1353563.

November 22, 2023

Authors and Affiliations

B. Adams, Alaska Arctic Observatory and Knowledge Hub, Utqiaġvik, AK, USA

T. J. Ballinger, International Arctic Research Center, University of Alaska Fairbanks, Fairbanks, AK, USA

L. T. Berner, School of Informatics, Computing and Cyber Systems, Northern Arizona University, Flagstaff, AZ, USA

U. S. Bhatt, Geophysical Institute, University of Alaska Fairbanks, Fairbanks, AK, USA

S. Bigaalke, Department of Geography, Portland State University, Portland, OR, USA

J. W. Bjerke, Norwegian Institute for Nature Research, FRAM – High North Research Centre for Climate and the Environment, Tromsø, Norway

J. E. Box, Geological Survey of Denmark and Greenland, Copenhagen, Denmark

B. Brettschneider, National Weather Service Alaska Region, NOAA, Anchorage, AK, USA

J. C. Comiso, Cryospheric Sciences Laboratory, Goddard Space Flight Center, NASA, Greenbelt, MD, USA

L. W. Cooper, Chesapeake Biological Laboratory, University of Maryland Center for Environmental Science, University of Maryland, Solomons, MD, USA

B. Decharme, Centre National de Recherches Météorologiques, Météo-France, Toulouse, France

C. Derksen, Climate Research Division, Environment and Climate Change Canada, Toronto, ON, Canada

D. Divine, Norwegian Polar Institute, Fram Centre, Tromsø, Norway

M. L. Druckenmiller, National Snow and Ice Data Center, Cooperative Institute for Research in Environmental Sciences, University of Colorado Boulder, Boulder, CO, USA

A. Elias Chereque, Department of Physics, University of Toronto, Toronto, ON, Canada

H. E. Epstein, Department of Environmental Sciences, University of Virginia, Charlottesville, VA, USA

S. Farrell, Department of Geographical Sciences, University of Maryland, College Park, MD, USA

R. S. Fausto, Geological Survey of Denmark and Greenland, Copenhagen, Denmark

X. Fettweis, SPHERES Research Unit, University of Liège, Liège, Belgium

B. C. Forbes, Arctic Centre, University of Lapland, Rovaniemi, Finland

K. E. Frey, Graduate School of Geography, Clark University, Worcester, MA, USA

G. V. Frost, Alaska Biological Research, Inc., Fairbanks, AK, USA

C. Garcia, Arctic Research Program, Global Ocean Monitoring and Observing Program, NOAA, Silver Spring, MD, USA

S. Gerland, Norwegian Polar Institute, Fram Centre, Tromsø, Norway

R. T. Glenn-Borade, International Arctic Research Center, University of Alaska Fairbanks, Fairbanks, AK, USA; Alaska Arctic Observatory and Knowledge Hub, Fairbanks, AK, USA

J. M. Grebmeier, Chesapeake Biological Laboratory, University of Maryland Center for Environmental Science, University of Maryland, Solomons, MD, USA

E. Hanna, Department of Geography and Lincoln Climate Research Group, Lincoln, UK

I. Hanssen-Bauer, Norwegian Meteorological Institute, Oslo, Norway

D. D. W. Hauser, International Arctic Research Center, University of Alaska Fairbanks, Fairbanks, AK, USA; Alaska Arctic Observatory and Knowledge Hub, Fairbanks, AK, USA

S. Hendricks, Alfred Wegener Institute, Helmholtz Centre for Polar and Marine Research, Bremerhaven, Germany

K. G. Howard, Division of Commercial Fisheries, Alaska Department of Fish and Game, Anchorage, AK, USA

C. D. Jensen, Danish Meteorological Institute, Copenhagen, Denmark

L. Kaleschke, Alfred Wegener Institute, Helmholtz Centre for Polar and Marine Research, Bremerhaven, Germany

S. -J. Kim, Korea Polar Research Institute, Incheon, Republic of Korea

Z. Labe, Atmospheric and Oceanic Sciences Program, Princeton University, Princeton, NJ, USA

R. Lader, International Arctic Research Center, University of Alaska Fairbanks, Fairbanks, AK, USA

M. J. Lara, Department of Plant Biology, University of Illinois, Urbana, IL, USA; Department of Geography, University of Illinois, Urbana, IL, USA

J. M. Leavitt, Alaska Arctic Observatory and Knowledge Hub, Utqiaġvik, AK, USA

B. D. Loomis, Goddard Space Flight Center, NASA, Greenbelt, MD, USA

K. Luojus, Arctic Research Centre, Finnish Meteorological Institute, Helsinki, Finland

M. J. Macander, Alaska Biological Research, Inc., Fairbanks, AK, USA

R. Í. Magnússon, Plant Ecology and Nature Conservation Group, Wageningen University & Research, Wageningen, Netherlands

K. D. Mankoff, Goddard Institute of Space Studies, NASA, New York, NY, USA; Autonomic Integra, New York, NY, USA

S. A. McAfee, Department of Geography, University of Nevada Reno, Reno, NV, USA

W. N. Meier, National Snow and Ice Data Center, Cooperative Institute for Research in Environmental Sciences, University of Colorado Boulder, Boulder, CO, USA

P. M. Montesano, Goddard Space Flight Center, NASA, Greenbelt, MD, USA

T. A. Moon, National Snow and Ice Data Center, Cooperative Institute for Research in Environmental Sciences, University of Colorado Boulder, Boulder, CO, USA

T. L. Mote, Department of Geography, University of Georgia, Athens, GA, USA

L. R. Mudryk, Climate Research Division, Environment and Climate Change Canada, Toronto, ON, Canada

J. M. Murphy, Auke Bay Laboratories, Alaska Fisheries Science Center, NOAA, Juneau, AK, USA

T. Mustonen, Snowchange Cooperative, Lehtoi, Finland

G. Omnik, Alaska Arctic Observatory and Knowledge Hub, Point Hope, AK, USA

P. P. Overduin, Permafrost Research Section, Alfred Wegener Institute, Helmholtz Centre for Polar and Marine Research, Potsdam, Germany

J. E. Overland, Pacific Marine Environmental Laboratory, NOAA, Seattle, WA, USA

D. Perovich, Thayer School of Engineering, Dartmouth College, Hanover, NH, USA

A. Petty, Earth System Science Interdisciplinary Center, University of Maryland, College Park, MD, USA

G. K. Phoenix, School of Biosciences, University of Sheffield, Sheffield, UK

K. Poinar, University at Buffalo, Buffalo, NY, USA

A. Portnov, Instituto Andaluz de Ciencias de la Tierra, CSIC-Universidad de Granada, Granada, Spain; University of Texas Institute for Geophysics, Austin, TX, USA

R. Ricker, NORCE Norwegian Research Centre, Tromsø, Norway

C. D. Ruppel, U.S. Geological Survey, Woods Hole, MA, USA

R. Schaeffer, Alaska Arctic Observatory and Knowledge Hub, Kotzebue, AK, USA

D. E. Schindler, School of Aquatic and Fishery Sciences, University of Washington, Seattle, WA, USA

E. R. Schoen, International Arctic Research Center, University of Alaska Fairbanks, Fairbanks, AK, USA

S. P. Serbin, Environmental and Climate Sciences Department, Brookhaven National Laboratory, Upton, NY, USA

M. C. Serreze, National Snow and Ice Data Center, Cooperative Institute for Research in Environmental Sciences, University of Colorado Boulder, Boulder, CO, USA

C. SimsKayotuk, Alaska Arctic Observatory and Knowledge Hub, Kaktovik, AK, USA

L. V. Stock, Cryospheric Sciences Laboratory, Goddard Space Flight Center, NASA, Greenbelt, MD, USA

M. Tedesco, Lamont-Doherty Earth Observatory, Columbia Climate School, Columbia University, Palisades, NY, USA

R. L. Thoman, Alaska Center for Climate Assessment and Policy, University of Alaska Fairbanks, Fairbanks, AK, USA; International Arctic Research Center, University of Alaska Fairbanks, Fairbanks, AK, USA

X. Tian-Kunze, Alfred Wegener Institute, Helmholtz Centre for Polar and Marine Research, Bremerhaven, Germany

M. -L. Timmermans, Yale University, New Haven, CT, USA

H. Tømmervik, Norwegian Institute for Nature Research, FRAM – High North Research Centre for Climate and the Environment, Tromsø, Norway

V. R. von Biela, Alaska Science Center, U.S. Geological Survey, Anchorage, AK, USA

C. Waigl, International Arctic Research Center, University of Alaska Fairbanks, Fairbanks, AK, USA

D. A. Walker, Institute of Arctic Biology, University of Alaska Fairbanks, Fairbanks, AK, USA

J. E. Walsh, Alaska Center for Climate Assessment and Policy, University of Alaska Fairbanks, Fairbanks, AK, USA; International Arctic Research Center, University of Alaska Fairbanks, Fairbanks, AK, USA

M. Wang, Cooperative Institute for Climate, Ocean, and Ecosystem Studies, University of Washington, Seattle, WA, USA; Pacific Marine Environmental Laboratory, NOAA, Seattle, WA, USA

M. Webster, Polar Science Center, Applied Physics Laboratory, University of Washington, Seattle, WA, USA

A. Wehrlé, Department of Geography, University of Zurich, Zurich, Switzerland

P. A. H. Westley, College of Fisheries and Ocean Sciences, University of Alaska Fairbanks, Fairbanks, AK, USA

D. Yang, Environmental and Climate Sciences Department, Brookhaven National Laboratory, Upton, NY, USA; Department of Ecology and Evolution, Stony Brook University, Stony Brook, NY, USA